Order Number 1346697

In-situ flow testing of borehole plugs

Crouthamel, David Roger, M.S.

The University of Arizona, 1991

U·M·I
300 N. Zeeb Rd.
Ann Arbor, MI 48106

IN-SITU FLOW TESTING OF BOREHOLE PLUGS

by

David Roger Crouthamel

A Thesis Submitted to the Faculty of the

DEPARTMENT OF MINING AND GEOLOGICAL ENGINEERING

In Partial Fulfillment of the Requirements
For the Degree of

MASTER OF SCIENCE
WITH A MAJOR IN GEOLOGICAL ENGINEERING

In the Graduate College

THE UNIVERSITY OF ARIZONA

1 9 9 1

STATEMENT BY AUTHOR

This thesis has been submitted in partial fulfillment of requirements for an advanced degree at The University of Arizona and is deposited in the University Library to be made available to borrowers under rules of the Library.

Brief quotations from this thesis are allowable without special permission, provided that accurate acknowledgement of source is made. Requests for permission for extended quotation from or reproduction of this manuscrip in whole or in part may be granted by the head of the major department or the Dean of the Graduate College when in his or her judgement the proposed use of the material is in the interests of scholarship. In all other instances, however, permission must be obtained from the author.

SIGNED: David R. Coulthard

APPROVAL BY THESIS DIRECTOR

This thesis has been approved on the date shown below:

Kulatilake

Pinnaduwa H.S.W. Kulatilake
Associate Professor of Mining
and Geological Engineering

Dec. 11th 1991
Date

ACKNOWLEDGMENTS

This work was performed at the Department of Mining and Geological Engineering, University of Arizona for the U.S. Nuclear Regulatory Commission, Division of Engineering under Contract No. NRC-04-86-113 and No. NRC-04-90-077 during the period of April 1988 to May 1991.

The accomplishment of this work was through a combined effort of talented people. Dr. K. Fuenkajorn who assisted and supervised a great deal of the field work, got this project started and on its feet. Bill Greer provided valuable suggestions based upon his experiences in the field. In addition, the following hard-working people contributed much of their time and skills (often as volunteers) to this project both in the field and lab, they are Oleg Lysyj, Jim Wilson, Bob Moulton, David Pelitier, Robert Armstrong, Robert Morgan, Shoung Ouyang, David Smith, Issac Jeng, C. Ran, Colin Sharpe, John Stormont, Arif Cetintas, J.J. Hunter, Carl Crouthamel and Kyle Griffith who would always work no matter what the conditions.

The Magma Mining Company of the Magma Mine in Superior Az. permitted the use of their land for the field site and access way. The Magma Mining Company of the San Manuel Mine graciously supported this work through the loaning of their equipment. Dowell-Schlumberger, Houston Texas donated the cement and additives for the cement plug, and American Colloid Company supplied C/S Granular Bentonite for the mixture plug.

This work would not have been possible without the support and patient guidance of Dr. Jaak Daemen and support of my thesis director Dr. P.H.S.W. Kulatilake.

TABLE OF CONTENTS

LIST OF FIGURES..... 7

LIST OF TABLES..... 10

ABSTRACT..... 11

CHAPTER ONE: INTRODUCTION..... 12

1.1 Introduction..... 12
1.1.1 Objective of Study..... 13
1.1.2 Scope and Limitations of Study..... 13
1.1.3 Organization..... 14
1.2 Previous In-Situ Tests of Seals Applied Toward Nuclear Waste Isolation..... 17
1.2.1 University of Arizona..... 17
1.2.2 Dowell Schlumberger Corporation..... 18
1.2.3 Sandia National Laboratories..... 19
1.2.4 Stripa Project..... 21
1.3 Other Uses of Borehole Seals..... 22
1.4 Emplacement Methods of Seals..... 22

CHAPTER TWO: TEST DESCRIPTIONS..... 24

2.1 Introduction..... 24
2.2 Steady Constant-Head Injection Tests and Falling Head Tests For Determination of Rock Mass Permeability..... 24
2.2.1 Rock Mass Permeability..... 24
2.2.2 Measurement of Bottom Borehole Seal Permeability. 29
2.3 Fluid Flow Through a Porous-Medium Borehole Seal..... 32
2.3.1 One Dimensional Flow Through A Borehole Seal..... 32
2.3.2 Head-Buildup Test..... 37
2.3.3 Transient Constant Head Test..... 41

CHAPTER THREE: SITE SELECTION AND CHARACTERIZATION..... 48

3.1 Introduction..... 48
3.2 Regional Geological Setting and General Setting..... 48
3.3 Drilling of Inclined Access Holes..... 51
3.4 Drilling of 150 mm Diameter Vertical Holes..... 53
3.5 Joint Orientation Measurement..... 55
3.5.1 Method of Measurement..... 55
3.5.2 Results of Joint Orientation..... 58
3.6 Video Logging of Vertical Holes..... 60
3.7 Fracture Detection Using Ground Penetrating Radar..... 61
3.7.1 Method of Investigation..... 61
3.7.2 Results of the GPR..... 62
3.8 Hydraulic Characterization of Inclined Holes..... 64
3.8.1 Test Method..... 64

TABLE OF CONTENTS--Continued

3.8.2 Test Results..... 65
3.8.3 Long Term Straddle Packer Test of Inclined Hole C 67
3.9 Hydraulic Characterization of the Vertical Boreholes.... 69
3.9.1 Steady State Flow Test with Straddle Packer System..... 69
3.9.2 Results of Packer Flow Testing at Site C..... 70
3.9.3 Results of Packer Flow Testing at Site A..... 74

CHAPTER FOUR: LABORATORY SIMULATION OF FIELD EMPLACEMENT..... 76

4.1 Introduction..... 76
4.2 Laboratory Model of Cementitious Plugs..... 76
4.2.1 Results of Pouring With Water Present..... 77
4.2.2 Results of Pouring Without Water Present..... 79
4.2.3 Conclusions and Recommendations..... 83
4.3 Laboratory Model of Crushed Tuff and Bentonite Seals Simulating In-Situ Conditions..... 84
4.3.1 Trial 1..... 86
4.3.2 Trial 2..... 89
4.3.3 Trial 3..... 91
4.3.4 Conclusions and Recommendations..... 94

CHAPTER FIVE: INSITU TESTING OF CEMENT BOREHOLE PLUGS..... 97

5.1 Introduction..... 97
5.2 Preparation of Vertical Borehole..... 98
5.3 Steady-State Flow Testing of the Rock and Bottom Borehole Seal..... 100
5.4 Installation of Cement Borehole Plug..... 106
5.5 Steady-State Flow Tests..... 106
5.5.1 Trial 1..... 108
5.5.2 Trial 2..... 117
5.5.3 Trial 3..... 120
5.5.4 Summary of Steady-State Injection Beneath the Plug..... 122
5.6 Head Buildup Test (Recovery Variation)..... 125
5.6.1 Results of Test..... 125
5.6.2 Analysis..... 126
5.7 Transient Constant Head Test..... 128
5.7.1 Results of Test..... 129
5.7.2 Analysis..... 129

CHAPTER SIX: FIELD TESTING OF CRUSHED TUFF/BENTONITE PLUG..... 132

6.1 Introduction..... 132
6.2 Preparation of Site A for Crushed Tuff/Bentonite Plug Tests..... 133
6.2.1 Instrumentation Configuration..... 133

TABLE OF CONTENTS--Continued

6.2.2 Hydraulic Characterization of Rock & Bottom Seal. 138
6.3 Installation of Crushed Tuff/Bentonite Plug..... 140
6.4 Flow Tests of Crushed Tuff/Bentonite Plug..... 142

CHAPTER SEVEN: SUMMARY, CONCLUSIONS AND RECOMMENDATIONS FOR FURTHER RESEARCH..... 149

7.1 Summary..... 149
7.1.1 Objectives..... 149
7.1.2 Approach of Study..... 149
7.1.3 Expansive Cement Plug, Site C..... 151
7.1.3.1 Steady-State Constant Head Test..... 151
7.1.3.2 Head-Buildup Test..... 153
7.1.3.3 Transient Constant Head Test..... 153
7.1.4 Crushed Tuff/Bentonite Mixture Plug, Site A..... 154
7.1.4.1 Falling Head Injection Flow Test..... 154
7.2 Conclusions..... 155
7.2.1 Characterization of the Field Sites Prior To Plug Installation..... 155
7.2.2 Expansive Cement Seal Installation..... 156
7.2.3 Crushed Tuff/Bentonite Mixture Plug Installation. 157
7.2.4 Configuration..... 159
7.2.5 Sealing Performance of Expansive Cement Plug..... 160
7.2.6 Sealing Performance of Crushed Tuff/Bentonite Plug..... 161
7.2.7 Equipment Performance..... 162
7.3 Recommendations..... 163
7.3.1 Cement Seal..... 163
7.3.2 Crushed Tuff/Bentonite Seals..... 164

APPENDIX A: JOINT ORIENTATION MEASUREMENTS..... 166

APPENDIX B: PRESSURIZED GROUTING OF SITE A..... 168

REFERENCES..... 189

LIST OF FIGURES

Figure		Page
1.1	Schematic of the field testing investigation.....	16
2.1	Assumed flow patterns in analysis of straddle packer tests.	26
2.2	Significance of radius influence.....	28
2.3	Single packer flow test for determination of rock and bottom borehole seal permeability.....	30
2.4	One-dimensional flow through a borehole seal.....	33
2.5	Flow components associated with the borehole seal test performed in this study.....	36
2.6	Generalized schematic of head buildup test.....	38
2.7	Dimensionless plots describing the buildup of head in a collection zone.....	42
2.8	Generalized schematic of the transient constant head test..	44
2.9	Collection and injection type curves for transient constant head test.....	47
3.1	Location of field sites near Superior Arizona.....	52
3.2	Dimensions of holes at sites A, B, and C.....	56
3.3	Location of survey lines L1-L5 for joint orientation measurements near sites A and B.....	57
3.4	Contour plot of the poles of the joint planes.....	59
3.5	Facsimile printout of the radar returns obtained at the original location of inclined hole C.....	63
3.6	Hydraulic conductivity as a function of hole depth of locations A, B and C respectively.....	66
3.7	Long term straddle packer flow test, inclined hole C.....	68
3.8	Results of the falling head tests conducted in hole C.....	71
3.9	Results of the steady-state constant head test, vertical hole C, 342-531 cm hole depth.....	72

LIST OF FIGURES--Continued

3.10 Extended steady-state constant head test performed for 19 hours at interval 16..... 73

4.1 First trial of laboratory simulation of field cement pouring..... 78

4.2 Second plug pouring trial..... 80

4.3 Third trial of cement pouring..... 81

4.4 Fourth trial of cement pouring..... 82

4.5 Trial 1 of the laboratory crushed tuff/bentonite plugs..... 87

4.6 Falling head flow tests performed on laboratory plug..... 88

4.7 Second trial of the crushed tuff/bentonite plug..... 90

4.8 Results of falling head tests on the third trial..... 92

4.9 Third installation trial..... 93

5.1 Injection stand installed at site C..... 101

5.2 Injection stand installed at the bottom of the test zone... 102

5.3 Configuration for steady-state flow testing of bottom seal. 103

5.4 Flow rates as a function of time; results of bottom hole flow test..... 105

5.5 Schematic of cement plug installed at site C..... 107

5.6 a) Injection flow rate as a function of time, first trial
b) cumulative change of fluid volume injected beneath the borehole plug..... 109

5.7 a) Collection outflow rate as a function of time, first steady-state injection trial
b) Cumulative change in collection fluid volume..... 111

5.8 Injection & collection flow rates..... 113

5.9 Packer and collection outflow..... 116

5.10 Injection and collection flow rates as a function of time trial 2..... 118

LIST OF FIGURES--Continued

5.11 Cumulative change in collected fluid volume, trial 2..... 119

5.12 Cumulative change in injected fluid volumes, trial 2..... 121

5.13 Injection and collection flow rates as a function of time for the third trial..... 123

5.14 Results of head-buildup test, site C..... 127

5.15 Results of transient-constant head test..... 130

6.1 General schematic of the vertical and intersecting inclined borehole of site A..... 134

6.2 Inclined hole access with two pressure transducers to measure piezometric head in the inclined borehole..... 136

6.3 Instrumentation shelter for site A..... 137

6.4 Results of injection flow tests to characterize both the host grouted rock mass, and bottom borehole seal..... 139

6.5 Schematic of the installed crushed tuff/bentonite plug in the vertical hole of site A..... 141

6.6 Results of the falling head flow test on the crushed tuff/ bentonite plug at site A..... 143

6.7 Readings of the lower piezometer during the flow test period..... 145

6.8 Readings of the upper piezometer taken during the flow test period..... 147

LIST OF TABLES

Table		Page
2.1	Flow Components of Borehole Seal Test.....	37
3.1	Orientation and Spacing of the Four Recognized Joint Sets in Quadrant Format.....	60
4.1	Physical and Hydraulic Characteristics of Laboratory Trials.....	85
5.1	Potential Causes for Excessive Outflow.....	114
5.2	Summary of Trials 1-3 of Steady-State Injection Tests.....	125
5.3	Hydraulic Conductivity and Specific Storage for Site C Based on Results of Head Build-up Test.....	128

ABSTRACT

A cement borehole plug and a crushed tuff/bentonite clay mixture borehole plug were tested insitu in highly welded tuff. The hydraulic performance of the cement plug was evaluated through steady-state and transient hydraulic tests with a hydraulic conductivity in the range of 10^{-10} cm/s. A crushed tuff/bentonite mixture plug was tested through a steady-state flow test with a measured hydraulic conductivity of 10^{-9} cm/s. The plug was installed in a fractured borehole which was grouted to reduce the overall rockmass permeability.

Installation procedures were evaluated in the laboratory prior to field installation. Installation of the cement seal with a bailer indicated seal degradation with water present in the borehole. Degradation appeared as piping, both internal and along the interface, and mixing of the cement with the water. Tests on the mixture seal indicated the need for homogeneous placement and adequate compaction to resist internal water piping and channelling.

CHAPTER ONE

INTRODUCTION

1.1 Introduction

Boreholes, shafts and tunnels drilled or excavated prior to or during the construction of a subsurface nuclear repository may create direct passages for radionuclide transport to the biosphere. It is therefore essential to seal them. Current U.S. Federal Regulations require that relevant boreholes be sealed "so that following permanent closure, (of the repository), they do not become pathways that compromise the repository's ability to meet performance objectives." (10CFR60, Section 60.134, 1981).

Few documented test results are available concerning the hydraulic performance of borehole seals. Test results, method of seal performance evaluation and installation procedures are lacking. Case histories are the common vehicle for presentation of information. Many laboratory investigations have been made into the fluid flow and mechanical properties of seal materials, host-rock and seal-rock systems (e.g., Sutherland and Cave, 1984; Gulick et al., 1980; South and Daemen, 1986; Lingle et.al., 1981; Holcomb and Hannum, 1982). While results obtained in the laboratory are important and worthwhile, their inherent shortcomings make in situ testing imperative. Primarily, in situ conditions

cannot be duplicated in the laboratory. One of the most significant obstacles in the laboratory are size limitations in laboratory tests that may have significant size effects. Also, emplacement techniques in the field may vary substantially from those in the laboratory and noticeably impact seal performance. Thus, in situ testing of seal system performance is essential.

1.1.1 Objective of Study

The objective of this research is to provide an experimental assessment of existing seal materials for sealing boreholes, in particular, in highly welded tuff. This assessment will provide a valuable data base on the effectivness of presently used materials to reduce fluid migration through boreholes or any other man made penetrations in or near a High Level Waste (HLW) repository. The study will also will provide information regarding methods of installation and performance monitoring of seals.

1.1.2 Scope and Limitations of Study

The tests and analysis techniques presented in this study are applicable to seal material and surrounding rock masses which can be treated as homogeneous, isotropic porous media. Two types of seal materials are primarily considered. The first seal material is chiefly

composed of Type II portland cement grout with admixtures to enhance its performance. The material is a product of the Dowell-Schlumberger Company with the name Self-Stress II. The second seal material consists of a bentonite/crushed tuff mixture plug designed by Ouyang and Daemen, (1991). The seals are installed in a rock mass selectively composed of Apache Leap Tuff from the densely welded brown unit near Superior Arizona. All the tests and analysis methods presented are limited to water or any other only slightly compressible fluid as the permeant.

This study concentrates on the installation and evaluation of seals in open and uncased boreholes. Seals in cased boreholes with the seal installed inside the hole and in the annulus between the casing and the borehole wall are not considered.

1.1.3 Organization

The first chapter presents the purpose of this study, a brief review of past field tests of seal performance, and an overview of the approach to seal testing presented in succeeding chapters. The second chapter presents test descriptions for measuring rock mass permeability, and three one-dimensional analytical hydraulic models for describing fluid flow through a porous-medium borehole seal. The third chapter describes the parameters used for site selection, drilling of the test

and access holes at each site, and the physical and hydraulic characterization of each site. The fourth chapter describes the laboratory simulations of field emplacement of both the cementitous and crushed tuff/bentonite plugs. In particular, chapter four examines the effects of field installation procedures on the sealing performance of these two plug materials types. Chapter five describes the in-situ testing of the neat cement plug material. Results and comparisons of the tests described in chapter two are given and recommendations for further testing are presented. Chapter six describes the in-situ testing of the crushed tuff/bentonite plug material. Comparisons to laboratory test results are made and recommendations for changes in installation procedures and expanded flow testing are made. The study is summarized and conclusions and recommendations for future work are presented in the seventh chapter.

An overview of the execution of the investigation is described in Figure 1.1. The investigation is divided into three main categories. The first one is the site selection and hydraulic characterization. The second category is the laboratory simulation of seal emplacement and evaluation of installation procedures, and the third category is the in-situ evaluation of the seals.

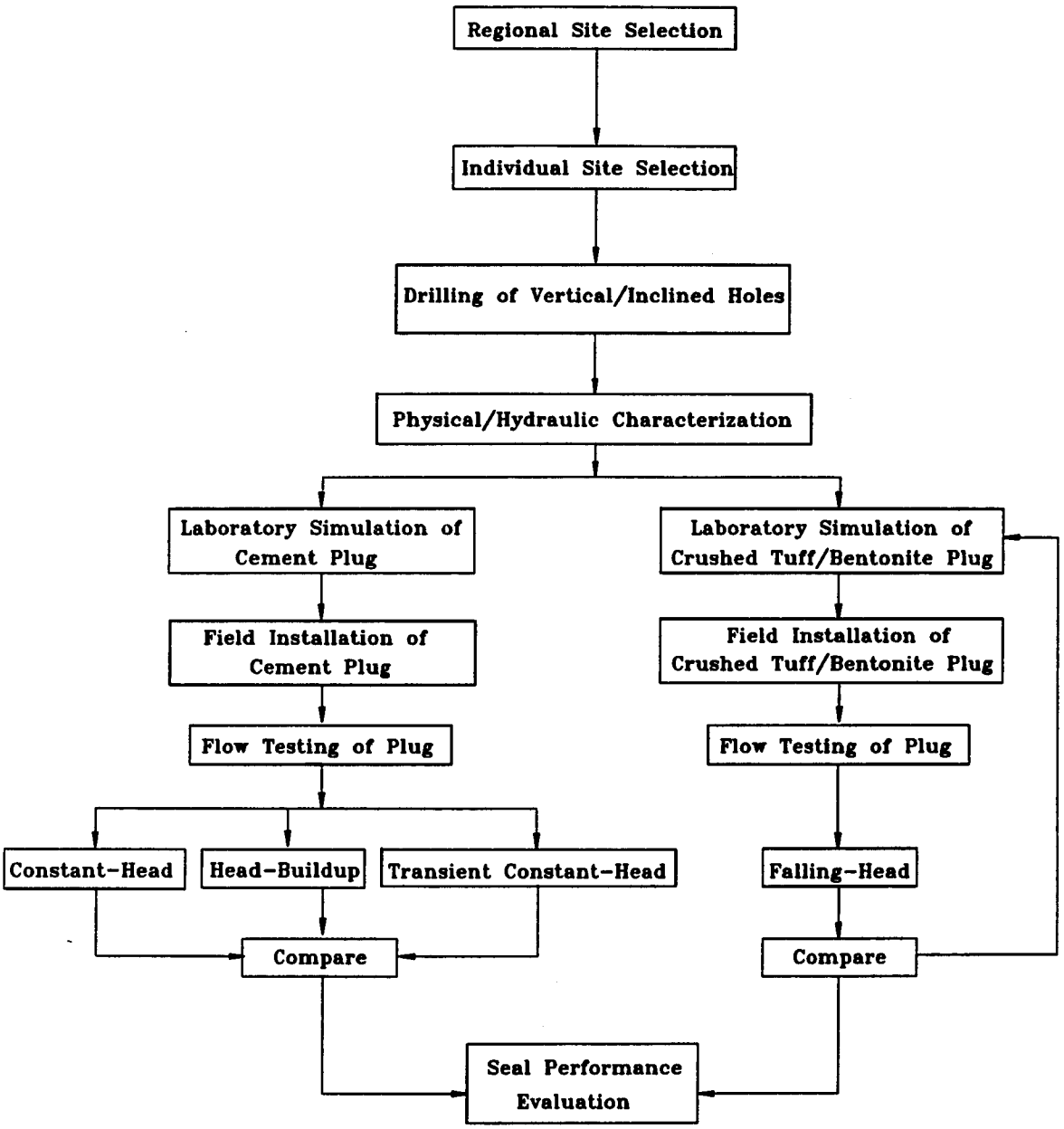

Figure 1.1 Schematic of the field testing investigation.

1.2 Previous In-Situ Tests of Seals Applied Toward Nuclear Waste Isolation

1.2.1 University of Arizona

In addition to the testing reported here, the University of Arizona has performed field tests on cement grout seals and bentonite seals in granite by Kimbrell, Avery, and Daemen, (1987) and cement grout seals in dense basalt and a recrystallized limestone by Greer and Daemen, (1991).

Greer and Daemen, (1991) proposed three tests for determining the hydraulic properties of in-situ borehole seals. Two of the tests consist of monitoring the rate of injection of water at constant pressure into an injection zone at one end of a seal and monitoring the collection rate of flow out of a free-draining collection zone at the other end. The third proposed test is performed by shutting in the collection zone and monitoring the buildup in hydraulic head. The test results were analyzed through both one-dimensional and axisymmetric three-dimensional flow models. Closed-form solutions were made for the analysis of tests using the one-dimensional models. The axisymmetric models used a finite element analysis for ground-water flow. This analysis included the effects of variations in hydraulic parameters of the flow tests and a comparison of the one-dimensional and axisymmetric models. A fourth test involved a tracer travel-time analysis for detecting the existence of a high-velocity (preferential) flow path through or around the seal. The in-situ tests were performed on cement

seals ranging 10-36 cm in length and 10 cm in diameter. Results of the seal tests indicate a mesured hydraulic conductivity of the seals to range from 10^{-9}-10^{-10} cm/s.

Kimbrell, Avery, and Daemen, (1987) performed seal testing in shallow, vertical boreholes, 16 cm in diameter. Two types of flow tests were conducted. Transient pulse tests were performed on bentonite seals. Constant-head injection tests on the bentonite seals were initiated, but stable injection and collection rates were not achieved in the testing period and test results were not analyzed. Constant-head results were obtained from the grout seals in one of the test holes. Transient tests on the same seals yielded erroneous results due to an apparent pocket of air in the injection interval. Tracer tests were not attempted for either the betonite or grout seals. Results of the tests performed indicated that the betonite and grout installations provided sealing to water flow about equal to that provided by the intact granite.

1.2.2 Dowell Schlumberger Corporation

Dowell Schlumberger (Dowell, a subsidiary of the Dow Chemical Company) has been engaged in solving subsurface permeability problems for over 50 years. They have successfully performed work in sealing a borehole for the Atomic Energy Commission in the Huchinson salt formation near Lyons, Kansas. The purpose of the seal test was to demon-

strate sealing techniques, curing characteristics, and other qualities of the grouts (Eilers, 1974).

In 1977, Dowell sealed the Energy Research and Developement Administrations's Borehole Number 10 at the site of the Waste Isolation Pilot Plant near Calsbad, New Mexico with a cement seal. This test, was also designed to confirm the sealing techniques and quality control under field conditions for cement plugs (Roy et. al., 1985).

A chemical sealant has also been developed by the Dowell Division Laboratory of Dow Chemical Company, Tulsa, OK, for sealing groundwater monitoring wells where the groundwater is highly mineralized (Senger and Perpich, 1983). The sealant contains a polymer that swells in water and can be preformed by pouring into a mold of appropriate size and allowing it to set overnight to a consistency of soft rubber. Swelling time can be adjusted by changing the formulation of the sealant. The chemical sealant has been used in the Waterloo Multilevel Piezometer measuring system and has been considered as a borehole seal for nuclear waste isolation (Cherry and Johnson, 1982).

1.2.3 Sandia National Laboratories

Sandia National Laboratories has performed seal tests at the Waste Isolation Pilot Plant, (WIPP), facility as part of their Plugging and Sealing Program, (PSP). The U.S. Department of Energy (DOE) is developing the WIPP facility in southeast New Mexico for the purpose of provid-

ing a research and development (R&D) facility to demonstrate the safe disposal of radioactive waste resulting from defense programs of the United States. The WIPP disposal horizon is located 656 m below ground in a bedded-salt deposit. The PSP is an integrated program of modeling, laboratory materials testing, and in situ tests to develop acceptable sealing technology for the eventual decommission of the WIPP facility.

Sealing design concepts have been presented for WIPP penetrations by Christensen and Peterson, 1982, Christensen, Gulick, and Lambert, 1982, Stormont, 1984. These concepts include the use of cementitious materials (grouts and concretes) and "natural" materials (salt and bentonite). Primary features of the conceptual seal designs include concrete bulkhead-type seals in the the shafts and at the entries to waste disposal panels, rock and rock/bentonite mixture backfills in waste and nonwaste-containing rooms, and cementitious grouts for penetrating boreholes, (Stormont, 1986).

In 1985, Sandia began a series of sealing experiments called the Small Scale Seal Performance Tests (SSSPT). The SSSPTs are a series of in situ experiments, (designated Series A, B, and C), intended to evaluate the performance of various candidate seal materials emplaced in boreholes from 15.20 cm (6 in.) to 91.4 cm (36 in.) diameter in salt. The performance of the seals was evaluated using thermal/mechanical and fluid flow data generated by the tests under expected repository conditions. For Series A and B, inclined holes intercepted the lower or far end of each of the sealed boreholes enabling access to the remote ends

of the seals for instrumentation and flow testing. Transient and steady-state flow tests using gas and saturated brine solutions were performed on the three test series. Flow tests were analyzed in terms of both one-dimesional and axisymmetric three-dimensional steady-state analytical models and one-dimensional and axisymetric three-dimensional transient numerical models. The analyses for determining the flow properties of the seal assumed the rock formation impermeable. The analyses for the flow properties of the surrounding rock formation assumed the seal is impermeable, (Stormont (ed.), 1986).

1.2.4 Stripa Project

The International Stripa Project in cooperation with the Organization for Economic Cooperation and Development (OECD) has performed tests on both bentonite and expansive concrete seals. The tests have been performed in a granite rock mass of an underground experimental facility located in an abandoned iron-ore mine near Stripa, Sweden. The project has included testing on pure sodium benonite seals which have been successfully tested in 5.6 cm diameter holes, 100 m in length and in 7.6 cm diameter holes, 4 m in length, (Pusch and Borgesson, 1989). Shaft seals composed of expansive concrete have been tested in vertical shafts ranging from 1 to 1.3 m in diameter. The concrete seals had an average length of 0.5 m. The flow testing of these seals indicated that the primary flow path was along the seal/rock interface.

1.3 Other Uses of Borehole Seals

In abandoned wells, seals are used to isolate fluid-bearing units, preventing unwanted mixing of fluids. A similar use of borehole seals is the abandonment of wastewater-injection wells (Warner and Lehr, 1977, p. 320). In this case the seal is installed to direct an injected contaminant into the geologic interval selected to receive it. The oil and gas industries use borehole seals to isolate portions of a producing well or as part of abandonment for a dry or depleted hole. Borehole seals also are used to preserve artesian pressure in wells penetrating confined aquifers or multiple aquifers. In the installation of field piezometers, borehole seals are used both above and below the piezometer to isolate the tip area (Bartholomew and Haverland, 1987, p 28., Dunnicliff, 1988, pp 155-161).

1.4 Emplacement Methods of Seals

The primary method for installing bentonite seals is through the deposition of compressed dry bentonite tablets or pellets. Compressed dry bentonite pellets have been shown to form an adequate seal (Filho, 1976) provided that they can be inserted in the borehole at the required location. The swelling properties of bentonite pellets depend both on the properties of the constituents of the pellets and on the chemistry of the water in which they are immersed (Dunnicliff, 1988, p 158).

The oil and gas industry commonly use a bailer to install grout seals in gas and oil wells. Smith, (1976, pp. 99-101) discusses the variations of the bailer method. The Environmental Protection Agency recommends for placing of grout seals in water wells the use of either a tremie, grout pipe, or dump-bailer (EPA, 1975, p. 140). A dump-bailer method was utilized for the installation of a cement seal both in the laboratory trials, (Chap. 4) and in the field.

CHAPTER TWO

TEST DESCRIPTIONS

2.1 Introduction

This chapter describes three in-situ tests used to determine hydraulic properties of borehole seals and of intact rock mass surrounding a borehole. These tests are the steady constant-head tests, transient constant-head test and head buildup test (recovery variation). All the described tests are performed on the neat cement seal. Only the steady constant-head test is performed on a crushed tuff/bentonite seal.

2.2 Steady Constant-Head Injection Tests and Falling Head Tests For Determination of Rock Mass Permeability

2.2.1 Rock Mass Permeability

The steady constant-head injection test is a field procedure which is very similar to the steady constant-head seal test. The injection test configuration consists of an isolated interval in a borehole fixed between two pneumatic packers or between a packer and the bottom of the hole. Water is injected into the interval under constant pressure. As the flow rate, Q_{ij} approaches a constant value, it is assumed that

steady flow has been achieved, and that the rock mass is saturated.

The most commonly used expressions for hydraulic conductivity from a steady constant-head injection test are an expression presented by Hvorslev (1951) and one based on the Thiem equation for steady, radial flow to a well (Todd, 1980, p 117; Bear, 1979, p 306).

The derivation of Hvorslev's expression assumes that all flow emerges uniformly from a line source at the vertical axis of the borehole. The equipotential surfaces that result are confocal prolate ellipsoids whose foci are the endpoints of the line source (Figure 2.1a). An expression for the hydraulic conductivity of the surrounding rock mass is obtained by establishing the injection head beginning from the ground surface to a circle with radius equal to the radius of the borehole and in a plane normal to the line source located at the injection interval midpoint. The derivation of the expression is given by Hsieh (1983) and also by Marinelli (1984, pp. 33-36) as:

$$K_r = \frac{Q}{2\pi LH} \ln\left[\frac{L}{D} + \sqrt{1 + \left(\frac{L}{D}\right)^2}\right] \qquad (2.1)$$

where: Q = steady state injection rate [L^3/T]
L = length of injection interval [L]
D = diameter of borehole [L]
H = injection head [L]

The assumptions based upon the Thiem equation are that flow is radial and confined between the upper and lower impermeable boundaries

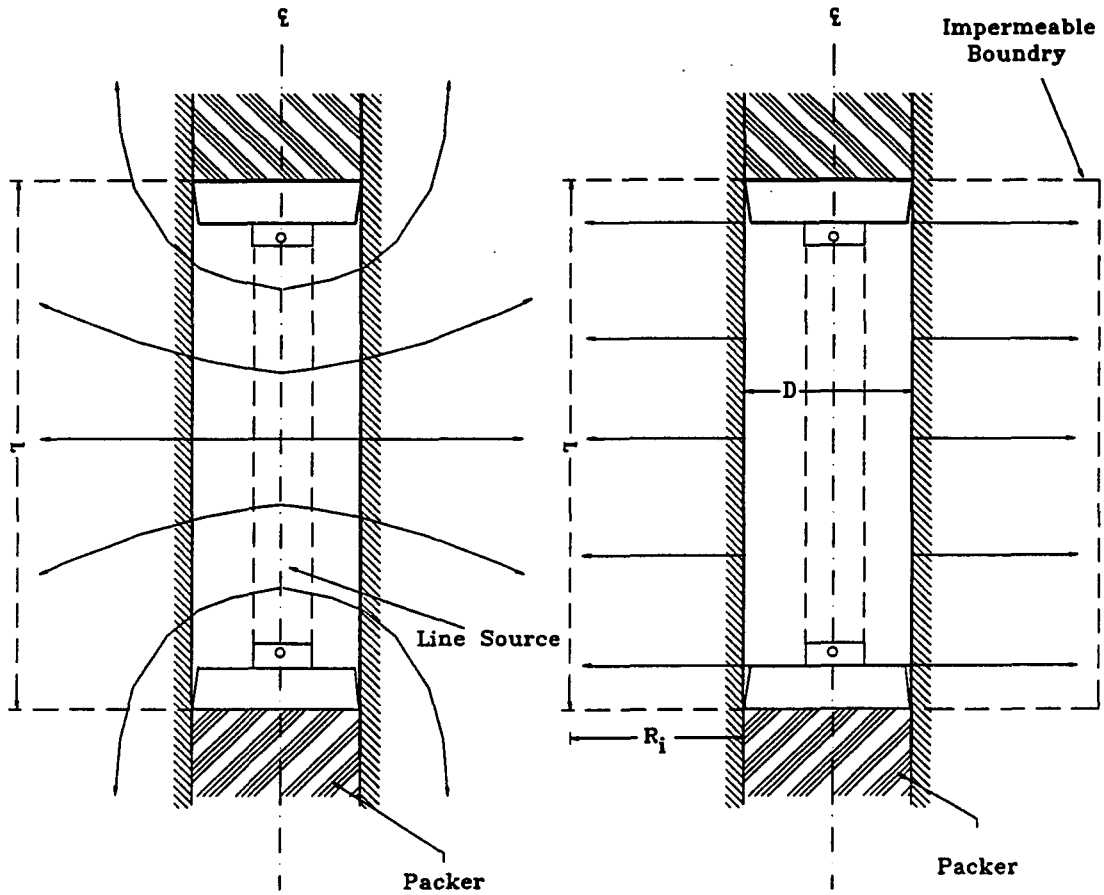

(a) prolate – ellipsoidal flow (b) radial flow

Figure 2.1 Assumed flow patterns in analysis of straddle packer tests.

(upper and lower packers), Figure 2.1b; the rock mass around the isolated injection interval is homogeneous and radially isotropic; at a distance equal to the radius of influence, R_i, a circular boundary of constant head equal to ambient exists; and the injection flow rate and positive head are constant. The solution for hydraulic conductivity described by Hsieh, 1983, and Zeigler, 1976 is:

$$K_r = \frac{Q}{2\pi LH}\ln\left(\frac{R_i}{d}\right) \qquad (2.2)$$

where:

R_i = radius of influence [L]
Other terms are previously defined.

Generally, unless an observation well or piezometer is installed, a radius of influence, R_i, cannot be determined. The significance of the radius of influence, R_i, in calculating hydraulic conductivity values is shown in Figure 2.2. As R_i is increased from two and a half times the borehole radius to nearly 30 times the borehole radius, the computed permeability increases by less than one order of magnitude. To remain consistent in calculating the hydraulic conductivity from various tests, R_i is taken equal to the injection interval length, L. In addition, if L >> D and R_i is equal to L, then Eq. 2.2 is equal to the Hvorslev expression (Eq. 2.1).

The falling head test is performed when the steady constant-head injection test shows a high rate of flow in a given interval. A falling

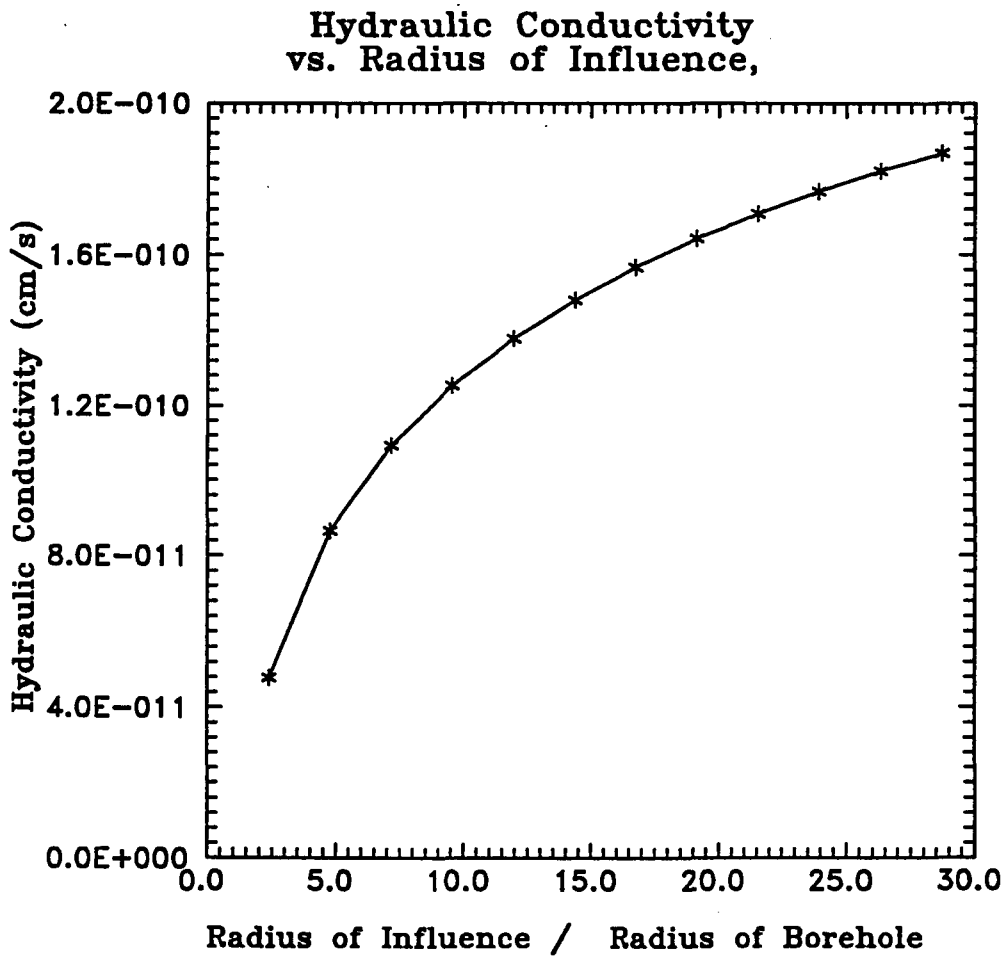

Figure 2.2 Significance of radius of influence, R_i, in calculating hydraulic conductivity, K_r. Overall change is less than one order of magnitude.

head permeameter is spliced into the injection line.

For the falling head permeameter test, the hydraulic conductivity is calculated from an equation derived from Bear (1979, pp. 305-306) and Freeze and Cherry (1979, p 336):

$$K = \frac{a \ln(R_i/R_H) \ln(h_0/h_1)}{2\pi L(t_1 - t_0)} \qquad (2.3)$$

where: a = cross-sectional area of the falling permeameter [L^2]
R_H = hole radius [L]
h_0 = initial height of water in the permeameter measured from the middle of the test interval at time t_0 [L]
h_1 = height of water in the permeameter measured from the middle of the test interval at time t_1 [L].
t_1, t_0 = time in seconds at final height h_1 and at initial height h_0.
Other terms are previously defined.

The above equation assumes that fluid flow is laminar, that all connective voids are filled with water, and that Darcy's law is valid.

2.2.2 Measurement of Bottom Borehole Seal Permeability

This section describes a method to determine inflow rates and hydraulic conductivities of the rock around the borehole and of a bottom cement seal through the use of a single packer. The test configuration is given in Figure 2.3. The analytical solutions assume that the materials are homogeneous and fully saturated, that Darcy's law is valid, and that the flow paths through the rock and bottom seal are radial and

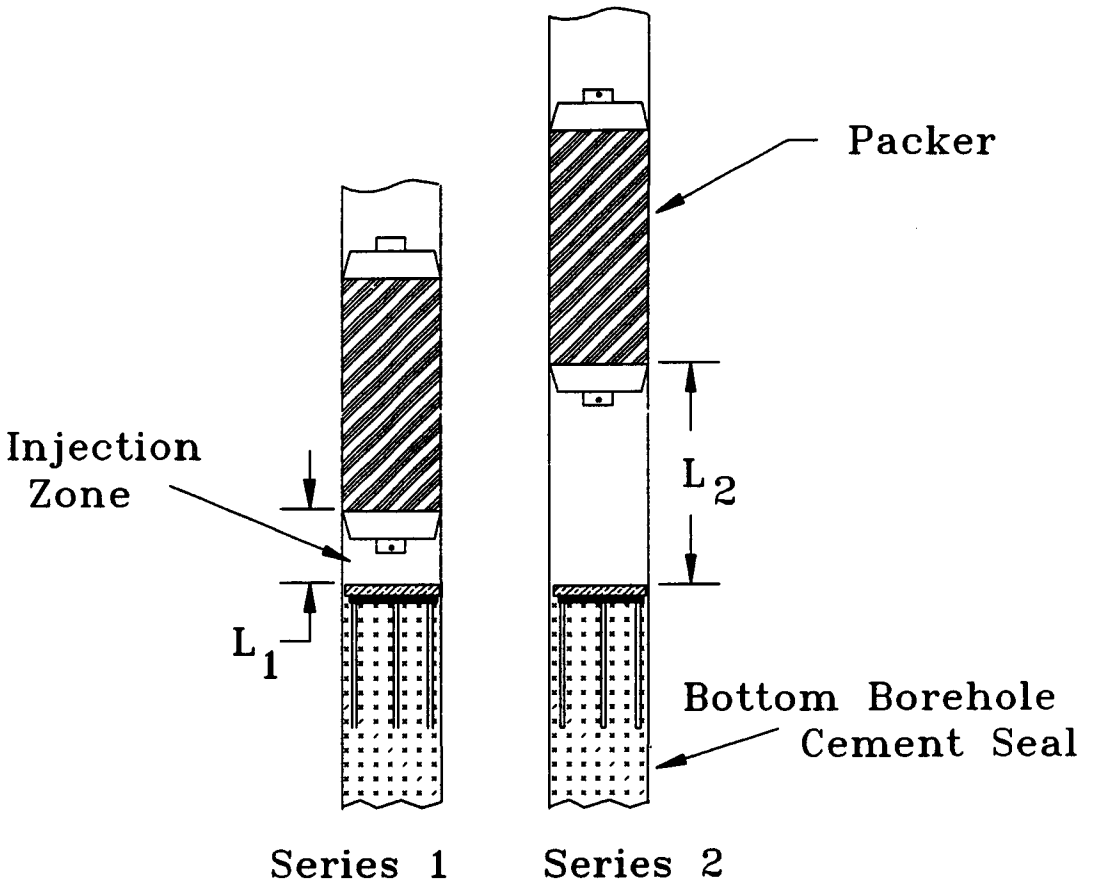

Figure 2.3 Single packer flow test for determination of rock and bottom borehole seal permeablility.

longitudinal, respectively. Data used in the calculations are the inflow rates measured after a steady-state flow (constant flow rate) has been reached for each test series (i.e. each injection zone length).

If the injection pressures are the same for all the tests, the flow rate through the rock for test series #1 can be determined from:

$$Q_{R_1} = \frac{Q_{T_2} - Q_{T_1}}{\frac{L_2}{L_1} - 1} \tag{2.4}$$

where: Q_{R_1} = flow rate through the rock for test series #1

Q_{T_1} Q_{T_2} = flow rates measured from the injection pump of test series #1 and #2, respectively.

L_1, L_2 = length of injection zones of test series #1 and #2, respectively.

The flow rate through the bottom seal of the test series #1 is obtained from:

$$Q_{BS_1} = Q_{T_1} - Q_{R_1} \tag{2.5}$$

where Q_{BS_1} = rate of longitudinal flow through the bottom cement seal.

If the injection pressures for the first and second test series are not the same, then the flow rate into the rock mass can be determined from:

$$Q_{R_1} = L_1\left(\frac{Q_{T_2}P_{i_1} - Q_{T_1}P_{i_2}}{L_2P_{i_1} - L_1P_{i_2}}\right) \tag{2.6}$$

where: P_{i_1}, P_{i_2} = injection pressures of test series #1 and #2, respectively.

The hydraulic conductivity of the intact rock mass can be calculated from Eqns. 2.1 and 2.2, or, under high flow rates and single fracture conditions, from Eqn. 2.3.

2.3 Fluid Flow Through a Porous-Medium Borehole Seal

2.3.1 One Dimensional Flow Through A Borehole Seal

The one-dimensional model assumes flow is steady and axial through a porous-medium seal. The surrounding rock mass is assumed an impermeable barrier, and $Q_i = Q_o$ (Figure 2.4). Assuming Darcy's law is valid, and that all connecting voids are water filled, the basic governing differential equation is:

$$\frac{d^2h}{dx^2} = 0 \tag{2.7}$$

The boundry conditions for a borehole seal are:

$$h = 0, \quad x = 0 \tag{2.8}$$

$$h = H_i, \quad x = L_s \tag{2.9}$$

The basic expression for outflow from the plug is:

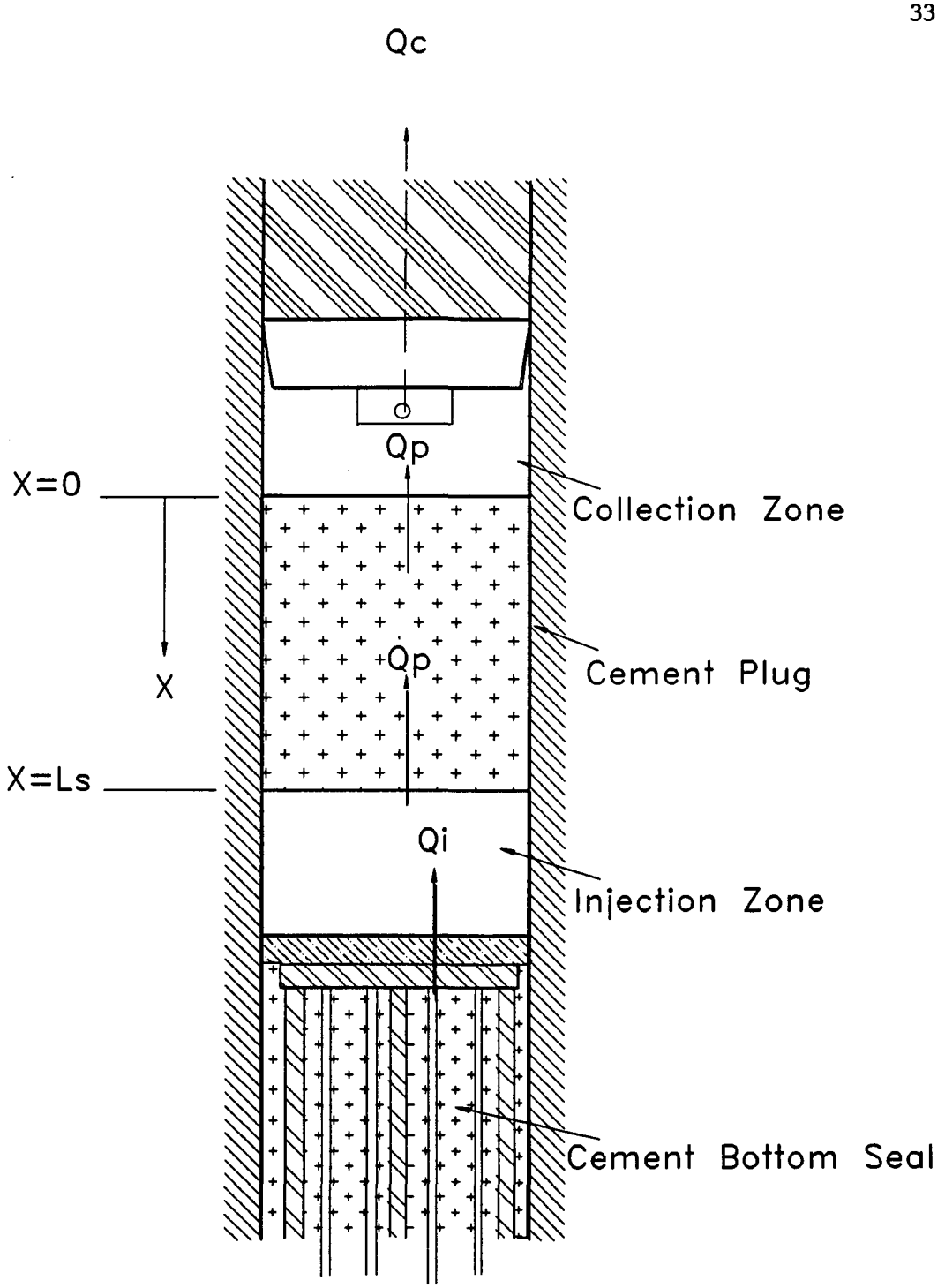

Figure 2.4 One-dimensional flow through a borehole seal.

$$Q_p = K_s A \frac{dh}{dx} \tag{2.10}$$

where:

Q_p = Flow rate through the cement plug & plug interface [L^3/T]
K_s = Hydraulic conducitivity of the seal [L/T]
A = Cross-sectional area of the seal [L^2]
h = Applied hydraulic head [L]
x = Distance from the injection face to the collection face [L]
L_s = Length of the seal [L]

Integrating the governing differential equation (Eq. 2.7) twice and applying the boundary conditions (Eqs. 2.8, 2.9) yields an expression for the hydraulic head as a linear function of x. Differentiating this expression with respect to x and subsituting into Eq. 2.10 yields:

$$Q_p = K_s A \frac{H}{L_s} \tag{2.11}$$

rearranging terms yields:

$$K_s = \frac{Q_p L_s}{AH} \tag{2.12}$$

Eq. 2.12 can be used to yield an estimate of the hydraulic conductivity of the seal. Because the cement plug is considered to be 1 to 2 orders of magnitude higher in permeability than the surrounding rock, (Fuenkajorn and Daemen, 1990, Greer and Daemen, 1991), then $Q_p \gg Q_{fc}$, where Q_{fc} is flow from the formation into the collection reservoir. Q_c

can then be substituted for Q_p and considered an upper limit of Q_p. This assumes flow is very nearly one-dimensional through the seal and that Q_i and Q_c are approximately equal and yield about the same value of K_s. In general however, the injection flow Q_i includes significant components into the rock mass as well as axial components into the borehole plug and bottom seal (Q_{if}, Q_{bs}), as described in Figure 2.5. Similarly, Q_c includes components from both the rock mass and the seal (Q_p, Q_{fc}). The flow components are described in Table 2.1. Assuming that the compressibility of water is negligible, that the injection and collection zones are completely water-filled, and that the hydraulic head in the rock mass is at ambient at some axial and radial distances from the seal, the following equation is true by simple continuity:

$$Q_p \leq Q_c \leq Q_i \tag{2.13}$$

Thus using Eq. 2.12 gives upper limit values for K_s by using either Q_i or Q_c. Q_c gives a smaller and more realistic upper limit than one obtained with Q_i, assuming that Q_c contains no inflow from the rock mass.

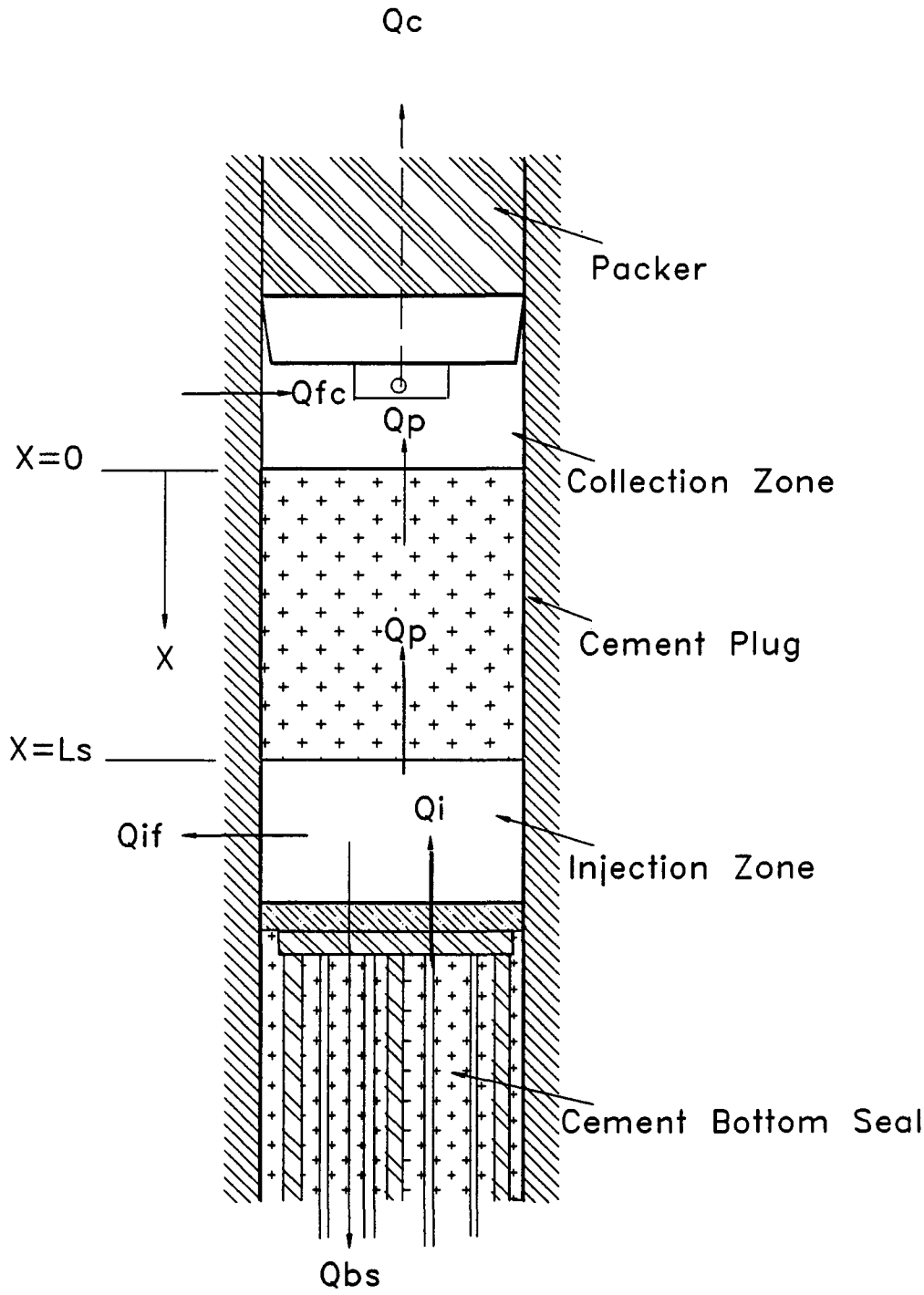

Figure 2.5 Flow components associated with the borehole seal test performed in this study.

Table 2.1 Flow Components of Borehole Seal Test

Flow Component	Definition
Q_i	Measured Injection Flow Rate
Q_{if}	Flow Rate from Injection Zone Into Formation
Q_p	Flow Rate Through Cement Plug & Plug Interface
Q_{bs}	Flow Rate Through Cement Bottom Seal
Q_{fc}	Flow Rate From Formation Into Collection Zone
H_i	Injection Zone Head
H_c	Collection Zone Head
H_{if}	Formation Head Near Injection Zone
H_{fc}	Formation Head Near Collection Zone
Q_c	Measured Collection Zone Outflow Rate

2.3.2 Head-buildup Test

The head-buildup test is a transient test which yields an effective longitudinal permeability and specific storage for a borehole plug. The head buildup test described here is of the recovery variation. The test is similar to the pressure build-up tests performed by Sandia National Laboratories in the Bell Canyon Test (Christensen and Peterson, 1981) and head-buildup tests performed by Greer and Daemen (1991). A generalized schematic of the test is shown in Figure 2.6. The head-buildup test is performed after a period of constant-head testing in which steady flow conditions are established. At the start of the test, both the injection and collection zones are water filled, and the borehole plug is saturated. It is assumed that the borehole walls are impermeable so that flow can occur only along the borehole axis (x-axis in Figure 2.6). Prior to the start of the test, the hydraulic head in the

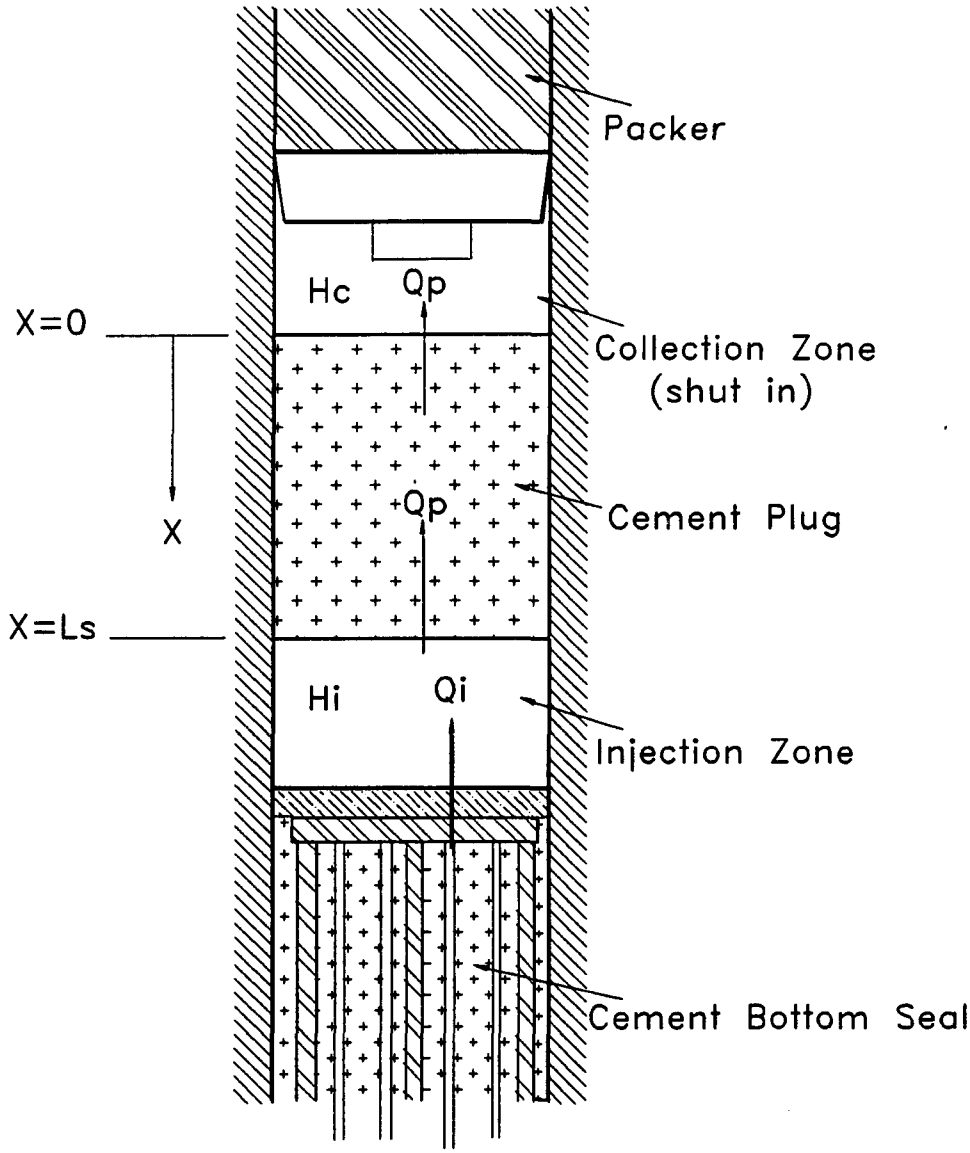

Figure 2.6 Generalized schematic of head buildup test.

collection zone is at a level defined as zero, (Hc = 0), the hydraulic head in the injection zone is at Hi (Hi > 0), and the head across the plug varies linearly from Hi to Hc. As the test proceeds, head is maintained at a constant level and flow occurs in the -x direction. As water enters the filled collection zone, the water compresses and Hc approaches Hi. The partial differential equation and boundary conditions describing the test are given as follows:

Governing partial differential equation:

$$\frac{\partial^2 h}{\partial x^2} - \frac{S_p}{K_{px}} \frac{\partial h}{\partial t} = 0 \quad for \quad 0 \le x \le L_s \quad \& \quad t > 0 \tag{2.14}$$

Initial Conditions

$$h(x,0) = f(x) = \left(\frac{x}{L_s}\right) H_i \tag{2.15}$$

$$h(L_s,t) = H_i \tag{2.16}$$

$$h(0,t) = h_c(t) \quad for \quad t \ge 0 \tag{2.17}$$

$$h_c(0) = 0 \tag{2.18}$$

Boundary Conditions:

$$\frac{S_c}{K_{xp}A}\frac{dh_c}{dt} - \frac{\partial h}{\partial x}\Big|_{x=0} = 0 \quad for \quad t>0 \tag{2.19}$$

where:

h = hydraulic head in the plug [L]

h_c = hydraulic head in the collection zone [L]

x = distance along the plug as measured from the plug on the collection zone side [L]

A = cross-sectional area of the plug measured perpendicular to the x-axis [L^2]

t = time from start of the test [T]

L_s = length of the plug in the x direction [L]

S_c = compressive storage of the collection reservoir [L^2] (measured separately, $S_c = \Delta V_c / \Delta h_c$)

K_{xp} = hydraulic conducitivity of the plug in the x direction [L/T]

H_i = constant hydraulic head in the injection zone [L]

S_s = specific storage of the plug [1/L]

An analytical solution to the initial-boundry value problem was obtained by Roko in Daemen et al., (1986, Appendix A) as follows:

$$h(x,t) =$$

$$H + 2\sum_{m=1}^{\infty} \frac{H_i \exp(-\alpha\phi_m^2)\left\{\sin\left(\frac{\phi_m(x-L_s)}{L_s}\right) - \frac{x\phi_m}{L_s}\cos\phi_m + \frac{\phi_m^2 K_{xp}}{S_s L_s^2}\lambda\sin(\phi_m)\right\}}{\sin(\phi_m)\left(\phi_m^2 + \frac{\lambda\phi_m^2 K_{xp}}{S_s L_s}\right) + \lambda\frac{\phi_m^3 K_{xp}}{S_s L_s}\cos(\phi_m)} \tag{2.20}$$

where:

$$\alpha = \frac{K_{xp}t}{S_s L_s^2} \tag{2.21}$$

$$\phi_m = roots\ of:\ \tan\phi = \frac{S_s A L_s}{S_c \phi} \tag{2.22}$$

$$\lambda = \frac{S_c}{K_{xp}A} \tag{2.23}$$

Evaluating Eq. (2.20) at x = 0 yields an expression for the head build-up in the collection zone as:

$$h_c(t) = h(0,t) = H_i + \sum_{m=1}^{\infty} \frac{-H_i \exp(-\alpha\phi_m^2)\sin\phi_m}{\sin(\phi_m)\left(\phi_m^2 + \frac{\lambda\phi_m^2 k_{xp}}{S_c L_s}\right)} + \lambda \frac{\phi_m^3}{S_c L_s}\cos(\phi_m) \qquad (2.24)$$

Substituting the value for λ and dividing the numerator and denominator of Eq. (2.24) by $\sin\phi_m$ yields:

$$h_c(t) = H + 2H \sum_{m=1}^{\infty} \frac{-\exp(-\alpha\phi_m^2)}{\phi_m^2 + \frac{S_c\phi_m^2}{AS_sL_s} + \frac{S_c\phi_m^3}{AS_sL_s\tan\phi_m}} \qquad (2.25)$$

Allowing $\xi = S_sAL_s/S_c$ and dividing both sides by H_i yields:

$$\frac{h_c(t)}{H_i} = 1 + 2\sum_{m=1}^{\infty} \frac{-\xi^2\exp(-\alpha\phi_m^2)}{\xi^2\phi_m^2 + \xi\phi_m^2 + \phi_m^4} \qquad (2.26)$$

Equation 2.26 can be used to make dimensionless plots describing the build-up of head in a collection zone. A plot of $h_c(t)/H_i$ versus $\log(\alpha\xi^2)$ is prepared with ξ as a selected parameter similar to Figure 2.7.

The compressive storage of the collection reservoir (Sc), measured seperately, is defined as the change in volume of water in the reservoir per unit change in hydraulic head in the reservoir.

2.3.3 Transient Constant-head test

The transient constant-head test is performed after a long period of

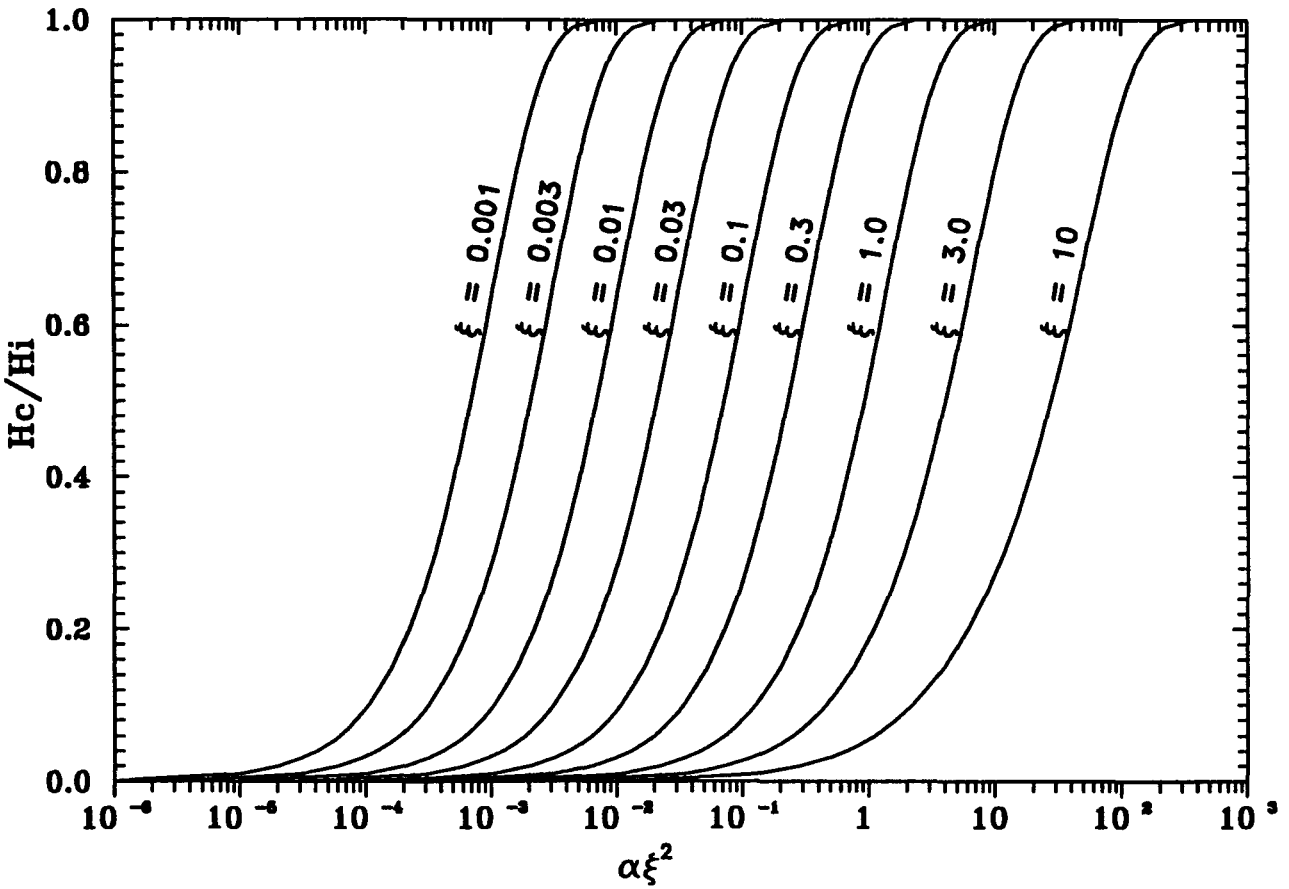

Figure 2.7 Dimensionless plots describing the buildup of head in a collection zone. Plots are derived from E_q. 2.26 with ξ as a selected parameter.

steady-state constant head testing in which steady flow conditions are established. Results of the transient flow test yield the hydraulic diffusivity (K_s / S_{ss}) of the seal. With K_s determined from steady-state tests, S_{ss}, specific storage of the seal, can be obtained from the hydraulic diffusivity. This test is similar to tests performed by Greer and Daemen (1991). A generalized schematic of the test is shown in Figure 2.8.

In the transient constant-head test, the injection head, H_i is assumed to vary linearly from positive H_{i1} to H_c = 0 on the collection side of the plug. At the start of the test, H_{i1} is changed to H_{i2}, where $H_{i2} \neq 0$ and is maintained throughout the test. Both the transient injection flow Q_i and the transient collection flow Q_c are monitored until steady-state conditions are achieved.

Greer and Daemen (1991) describe the one-dimensional axial flow model with the following initial-boundary value problem:

Governing equation:

$$\frac{\partial^2 h}{\partial x} - \frac{S_{ss}}{K_s}\frac{\partial h}{\partial t} = 0 \quad for \quad 0 < x < L_s \tag{2.27}$$

Boundary conditions:

$$h(0,t) = 0 \quad for \quad t \geq 0 \tag{2.28}$$

$$h(L_s,t) = H_{i2} \quad for \quad t > 0 \tag{2.29}$$

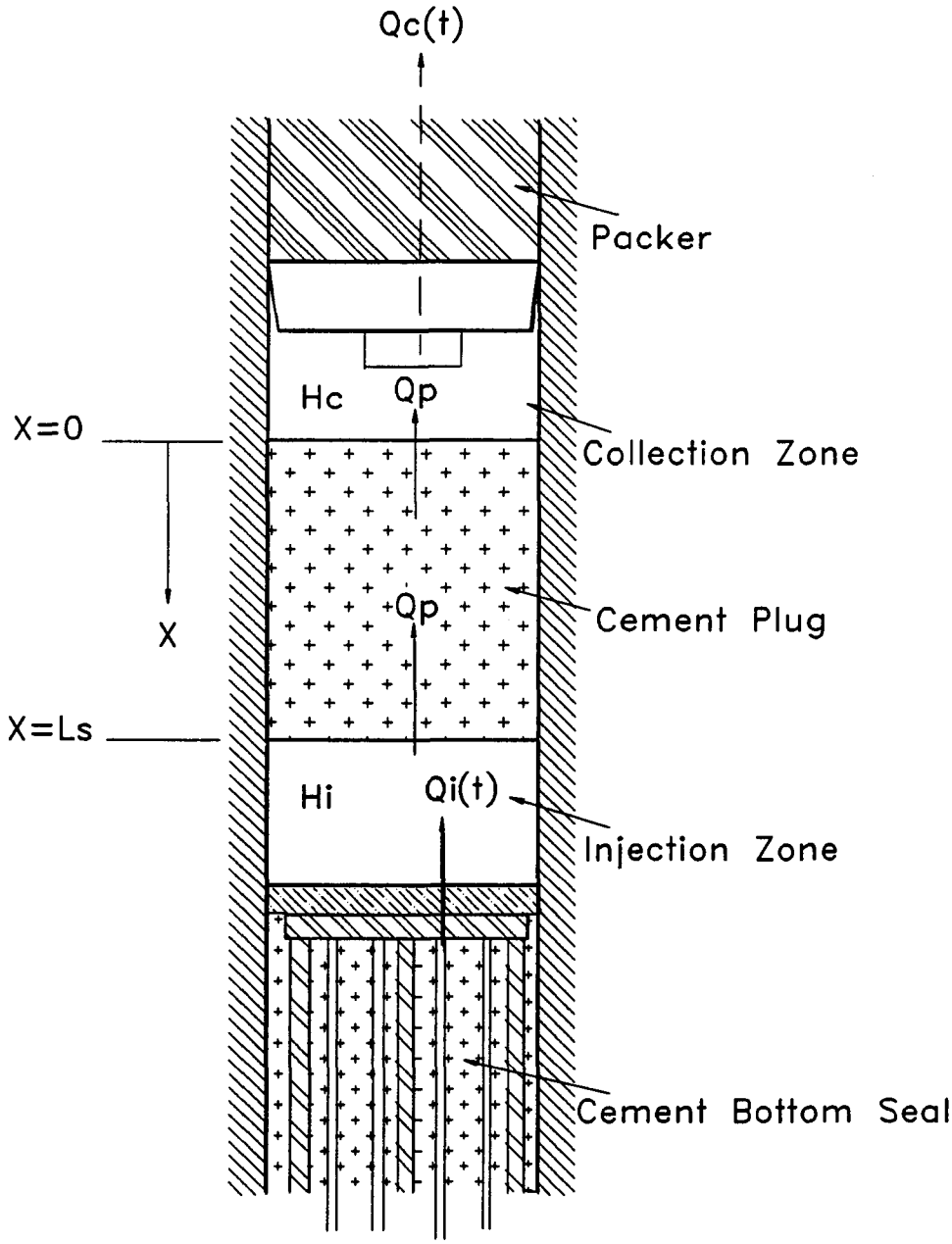

Figure 2.8 Generalized schematic of the transient constant head test. $Q_c(t)$ and $Q_i(t)$ are measured as a function of time.

Initial condition:

$$h(x,0) = \frac{x}{L_s} H_{i1} \tag{2.30}$$

Discharge conditions:

$$Q_i = K_s A \frac{\partial h}{\partial x}\Big|_{x=L_s} \tag{2.31}$$

$$Q_c = K_s A \frac{\partial h}{\partial x}\Big|_{x=0} \tag{2.32}$$

Carslaw and Jaeger (1959, pp 99-100) give the general analytical solution to the transient constant head test as:

$$h(x,t) = \frac{H_{i2}x}{L_s} + \frac{2(H_{i2}-H_{i1})}{\pi} \sum_{m=1}^{\infty} \left\{ \sin\left(\frac{m\pi x}{L_s}\right) \frac{\cos(m\pi)}{m} \exp(-m^2\pi^2 t_d^*) \right\} \tag{2.33}$$

All of the above terms are defined in the description of the head-buildup test with the exception of t_d^*. The quantity t_d^* is a dimensionless expression for time in terms of the hydraulic properties and the length of the seal, L_s. This quantity is defined as:

$$t_d^* = \frac{K_{ss} t}{S_s L_s^2} \tag{2.34}$$

Greer and Daemen (1991) derive Q_i and Q_c from the general analytical solution as:

$$Q_i = \frac{kA_s H_{i2}}{L_s} + \frac{2kA_s(H_{i2}-H_{i1})}{L_s}\sum_{m=1}^{\infty}\exp(-m^2\pi^2 t_d^*) \tag{2.35}$$

$$Q_c = \frac{kA_s H_{i2}}{L_s} + \frac{2kA_s(H_{i2}-H_{i1})}{L_s}\sum_{m=1}^{\infty}\cos(m\pi)\exp(-m^2\pi^2 t_d^*) \tag{2.36}$$

Letting Q_o be the steady-state flow rate established at the end of the test, Q_o is derived from Eq. 2.11 as:

$$Q_o = \frac{K_s A H_{i2}}{L_s} \tag{2.37}$$

Dividing Eq. 2.34 and 2.35 by 2.36 and rearranging terms yields:

$$\frac{(Q_i - Q_o)H_{i2}}{(Q_o(H_{i2}-H_{i1}))} = 2\sum_{m=1}^{\infty}\exp(-m^2\pi^2 t_d^*) \tag{2.38}$$

$$\frac{(Q_o - Q_c)H_{i2}}{(Q_o(H_{i2}-H_{i1}))} = -2\sum_{m=1}^{\infty}\cos(m\pi)\exp(-m^2\pi^2 t_d^*) \tag{2.39}$$

Using Eq. 2.37 and 2.38, semilog plots of $(Q_i-Q_o)H_{i2}/(Q_o(H_{i2}-H_{i1}))$ or $(Q_o-Q_c)H_{i2}/Q_o(H_{i2}-H_{i1})$ versus t_d^* are made (Figure 2.9). These plots represent type curves for the transient constant head test. Semilog plots are drawn of the same parameters versus time t, using the data from the test are made. This plot represents the data curve to be superimposed over the type curves.

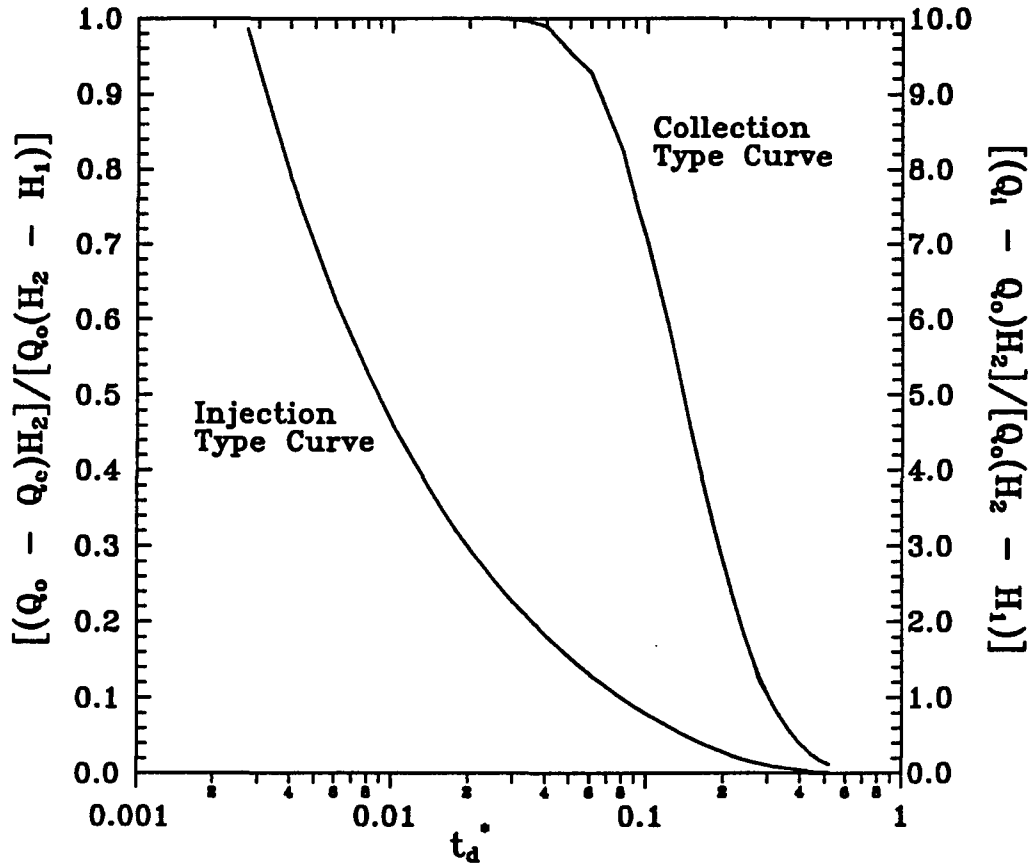

Figure 2.9 Collection and injection type curves for transient constant-head test.

CHAPTER THREE

SITE SELECTION AND CHARACTERIZATION

3.1 Introduction

This chapter presents criteria used for site selection, and the methods of characterization used to investigate each site. Each site must provide rock with appropriate lithology. Boreholes must be deep enough for testing and must include intervals of relatively competent rock. The regional setting must provide year-round access and must permit research installations. Work was begun on the field site in April 1988. The site is approximately 110 miles north of Tucson. Characterization methods used include corelogging, down borehole color videologging, joint orientation mapping, ground penetrating radar and hydraulic characterization through packer tests.

3.2 Regional Geological Setting and General Setting

A dacitic ash flow (Apache Leap tuff) sheet near Superior, Arizona was selected for the field experiments. The Apache Leap tuff is exposed approximately from 30 ° 15 min. N to 30 ° 45 min. N, and from 110° 45

min. W to 111° 30 min. W. The exposure is around the interconnections of Maricopa, Pinal and Gila counties. The easternmost exposure of the tuff is found at Miami Arizona, the westernmost exposure is at Apache Junction (on Highway 60). The tuff unit covers over 100 square miles and may have once stretched over 1500 square miles (Peterson, 1961).

The tuff around Superior has been dated by isotopic age dating techniques, to be Miocene in age (Creasey and Kistler, 1964). Peterson (1961) divided the ash flow into five units. In descending order (from top to bottom) they are: white zone, grey zone, brown zone, vitrophyre and basal tuff. The tuff in the brown zone has the highest degree of welding and has been selected for field testing.

The brown zone ranges in thickness from 6 to 135 meters with a maximum thickness in Queen Creek Canyon (Peterson, 1961). The unit is comprised of a densely welded, devitrified, aphanitic groundmass with lithic fragments consisting of 5 to 20 percent of its make-up (Evans, 1983). Phenocrysts in the unit are set in a dense aphanitic, brownish-orange, cryptocrystalline matrix composed mostly of K-feldspar.

The ground water level at the Superior site is at least 500 meters below the ground surface due to dewatering from the Magma Mine Corporation for its nearby underground copper mine (Magma Mine). However, drilling performed by DOE in the same vicinity has encountered perched water tables as shallow as 100 meters below ground surface. All three borehole test sites are in the unsaturated zone, well above the local

water table.

Superior is in part of a semi-arid region of Arizona with average rainfall annual of less than 50 cm. Average elevation of the field site is 1040 m above sea level. The upper reaches of the tuff reach 1500 m. Temperatures at the site range from -5 to 40 °C, with an average temperature of 23 °C.

A geological investigation was made for selection of an appropriate site for field testing. The site selection is based upon the following criteria:

1) Rock as similar as possible to Yucca mountain, especially Topopah Spring tuff

2) Rock quality: The rock at the site should have a low frequency of joints and fractures and a low degree of weathering.

3) Accessibility: The site should be reachable by 3/4 ton truck. Water must be within reasonable distance. Access must be year round.

4) Security: The site should be, more or less, isolated from the public as much as possible.

5) Rock Type: The tuff tested must be highly welded (i.e. must be brown unit of the Apache Leap formation).

East of Superior, the Apache Leap tuff is exposed as a trend cover from the Queen Creek road tunnel to 3.5 miles southeast of Superior (along Highway 177). The brown zone tuff is found along the road cut (old and new Highway 60). The selected field site is in this area in

the Queen Creek canyon. Figure 3.1 gives the locations of field sites A, B and C along the old Highway 60. Each location represents a test hole (vertical hole) and an intersecting inclined hole. The field site is approximately 0.6 miles from a water source. Location A is on the east side of the old highway tunnel, location B on the west side and location C inside the tunnel. Selection of the locations for the test holes is based upon the quality of the tuff exposed on the surface. The test holes are located where the rock has a low fracture frequency.

3.3 Drilling of Inclined Access Holes

An inclined hole with a nominal diameter of 50 mm has been drilled at each of the three sites. The drilling was commenced on September 29, 1988, and completed on January 11, 1989. An Acker Ambassador electric coring drill was used to drill the inclined holes. A theodolite was used to align the drill orientation prior to and during drilling. Prior to drilling the 50 mm diameter hole, a 150 mm diameter impregnated diamond bit was used to drill to a depth of approximately 0.7 m. After the core was removed, a 150 mm O.D. and 0.9 m long casing (PVC tube) was placed into the hole. Bolt anchor cement (Sulfaset F-181) was then poured into the hole and into the spacing between the hole and casing to stabilize the casing. The top of the casing is 0.2 m higher than the ground surface. A 50 mm diameter impregnated diamond coring bit was

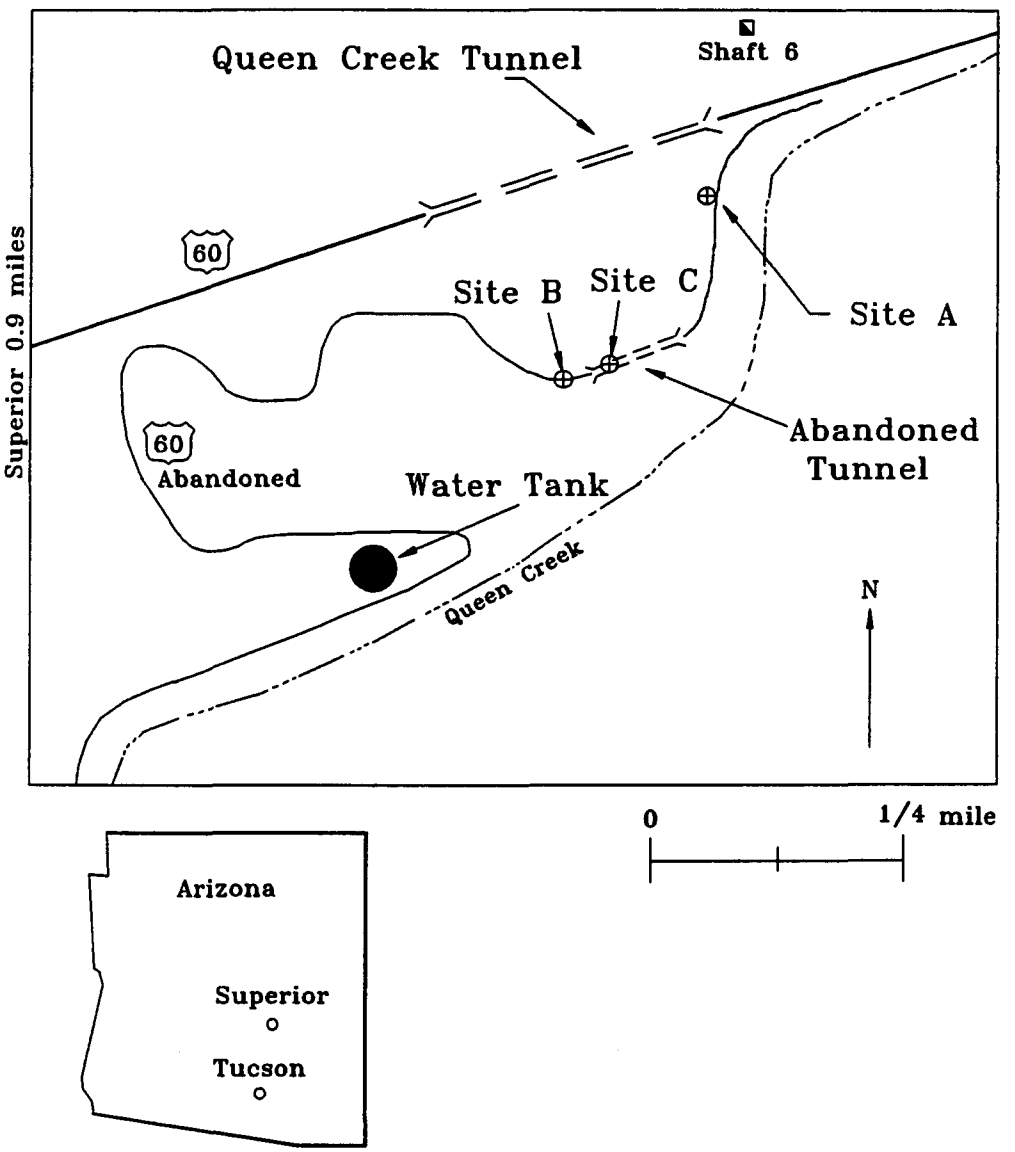

Figure 3.1 Location of field sites near Superior, Arizona.

used to drill through the cement and rock. All the drill bits used were Longyear thinwall series II - series III models. Fresh water was used as the drilling fluid. The core was recovered every 0.6 - 0.9 m of bit penetration. The drill bit was replaced when the bit teeth were worn out or sheared off. In portions of highly fractured zones or when numerous bit teeth were lost in the hole, a 45 mm diameter impregnated diamond blind bit was used to drill until the hole integrity improved.

3.4 Drilling of 150 mm Diameter Vertical Holes

Six inch (150 mm) diameter vertical holes have been drilled at each location (A, B and C). Each hole is located so as to intersect a previously drilled inclined hole at a depth of approximately 5 to 6 meters. Drilling commenced on April 11, 1989, and was completed on April 22. The work was performed by the Boyles Bros. Drilling Co. using a Joy 22HDH hydrostatic diamond core drill.

The location of the vertical hole to be drilled is determined by the information obtained from inclined holes (core log and flow test results) and by the rock quality on the cliff and ground surfaces. The position and orientation of the drill rig mounted on a 6-ton truck are specified by using a theodolite. After the drill rig is been aligned, the truck is stabilized using hydraulic jacks.

A 178 mm diameter thin wall diamond impregnated bit mounted on a 50

mm diameter drill rod was used to drill through concrete poured earlier to provide a smooth drilling surface and through the rock to a depth of approximately 1.3 m. Fresh water was used as the drilling fluid. A 175 mm OD, 162 mm ID steel casing about 2 m long is then placed in the hole. The casing is stabilized by pouring cement into the gap between the hole and casing. The cement is allowed to cure for ten hours before resuming drilling.

A 150 mm OD, 100 mm ID diamond impregnated bit mounted on a 2.74 m long core barrel is used to drill the vertical hole below the cased hole. Fresh water is used as the drilling fluid. The rate of bit penetration varied from 15 to 100 cm/hr. The core is recovered every 1-2 m of bit penetration. The rotational speed of the drill bit ranged from 60-100 rpm. The nominal core diameter recovered is 100 mm (4 in). The core log is given in Appendix A2.

The core obtained from the vertical hole A shows vertical natural fractures from the ground surface to a depth of 7.6m (near the intersection point of the inclined access and vertical holes). The dip direction of the fractures is nearly parallel to the trend of the inclined hole (A). Natural fractures are absent below the intersection point. The core recovered from site B is badly broken up between 2.44 and 6.10 m. This is probably due to the drilling process and the presence of natural fractures. The vertical hole C (inside the tunnel) gave good intact core throughout the hole length. Only a few natural fractures

are observed. Most are nearly horizontal in orientation. Figure 3.2 describes the dimensions of the inclined and vertical holes of each site.

3.5 Joint Orientation Measurement

Joint orientations are measured along the roadcut primarily near sites A and B. The primary purpose is to obtain information as to the structural geology of the field site and to predict the orientation and extent of the fractures intersected by the inclined and vertical holes. The results have been used to select the location of the vertical holes prior to drilling, and the location of the borehole plug (test zone).

3.5.1 Method of Measurement

Five survey lines are laid out parallel to the rock wall along the roadway near both ends of the tunnel near locations A and B (Figure 3.3). The lengths of the survey lines vary from 15 to 76 m. Orientation of the joint planes is measured using a Brunton compass, which provides strike of the planes as well as dip angle and dip direction. The direction (trend) of the survey lines and length are measured. The joint spacing of the same joint set is determined by recording the locations of the intersection between joints and the survey line. Details

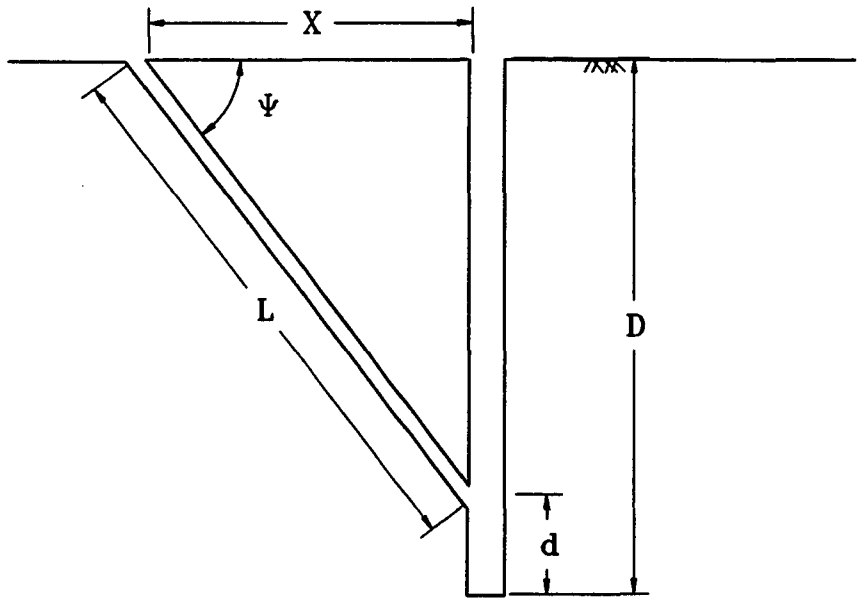

D = total depth of vertical hole
d = length of vertical hole below intersection point
L = length of inclined hole
X = horizontal distance between vertical and inclined holes
Ψ = dip angle of inclined hole
Φ = dip direction of inclined hole

Site	D (m)	d (m)	L (m)	X (m)	Ψ	Φ
A	7.47	1.68	8.84	4.72	57°	S 10° W
B	6.71	1.83	7.48	4.57	52°	N 88° W
C	6.22	0.74	7.01	4.11	52°	N 80° E

Figure 3.2 Dimensions of holes at sites A, B, and C.

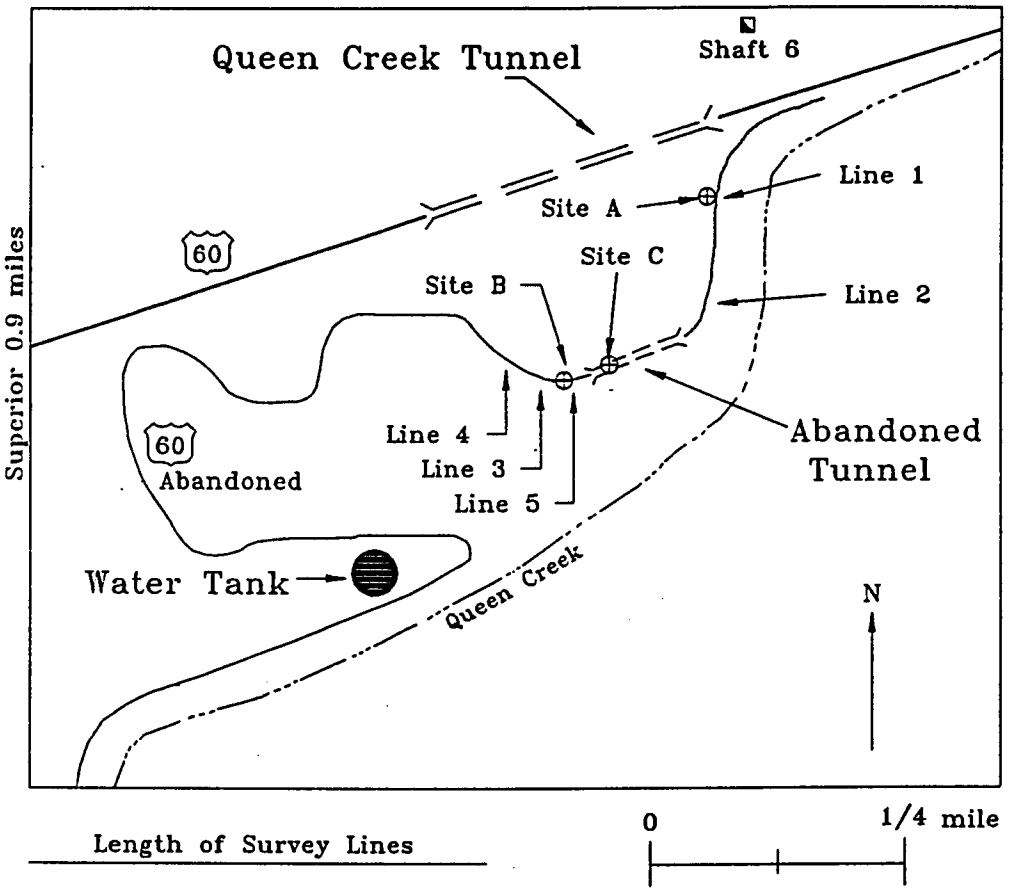

Length of Survey Lines

Line 1 = 76.3 m
Line 2 = 30.5 m
Line 3 = 30.5 m
Line 4 = 15 m
Line 5 = 17 m

Figure 3.3 Location of survey lines L1 - L5 for joint orientation measurements near sites A and B.

and variations of this technique are given by Call et. al., (1976). The field data gives only the apparent spacing of the joints. True spacing, S, is given by Goodman (1980, p. 149),

$$S = S_{app} x (\cos \alpha_H) \qquad (3.1)$$

where:

S =true spacing

S_{app} =apparent spacing

α_H =the angle between the normal to the joint and the survey line

3.5.2 Results of Joint Orientation

From the joint orientation measurements the strike and dip of the joint planes are entered into a computer program (SPLOT - Darton Software, 1987) to plot the poles on a stereographic equal area projection. Different survey lines are represented by different symbols. Figure 3.4 gives a contour plot of the poles. Four joint sets are recognized. The joint measurements are tabulated in Appendix A. The results of the analysis are given in Table 3.1.

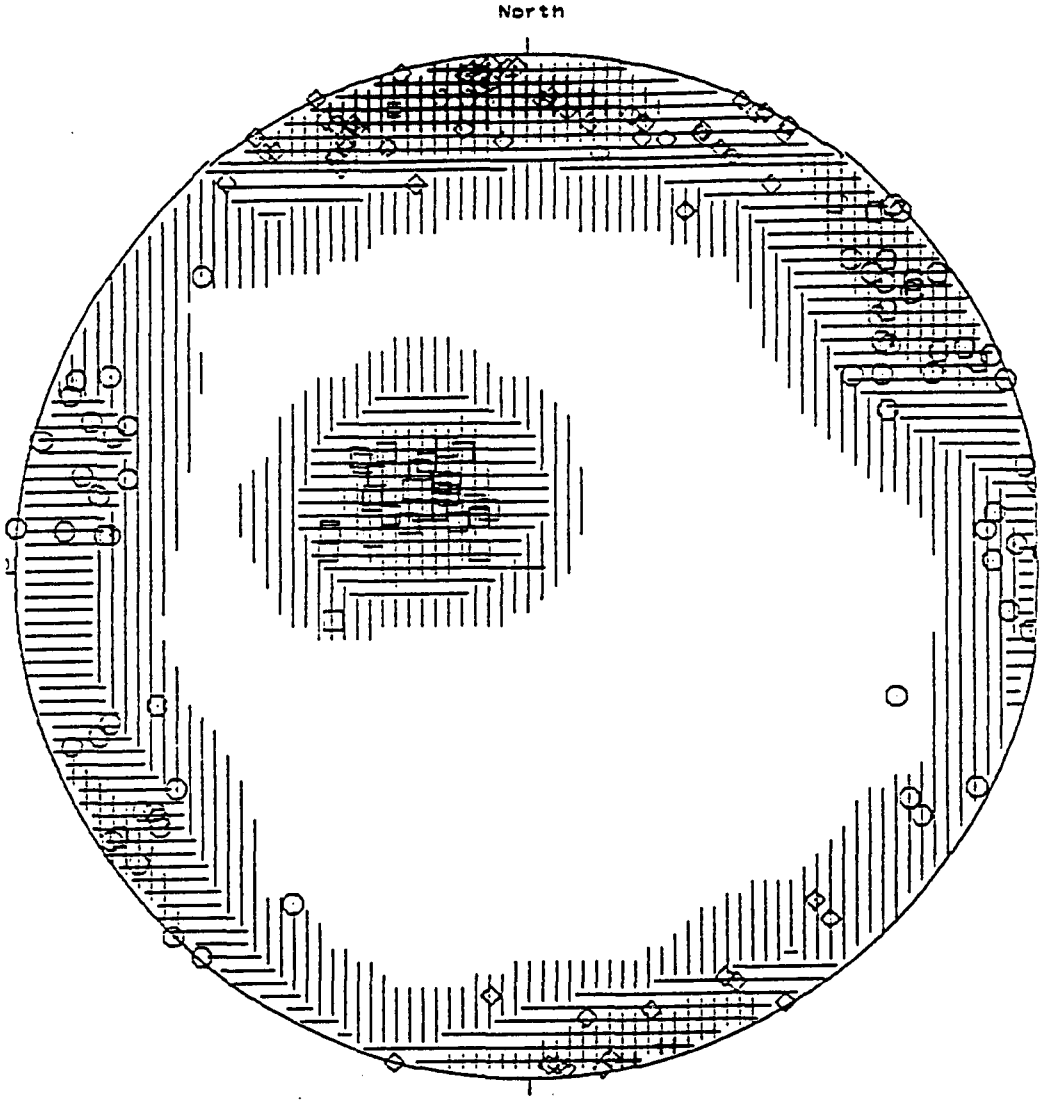

Figure 3.4 Contour plot of the poles of the joint planes. Four joint sets are recognized.

Table 3.1 Orientation and spacing of the four recognized joint sets in quadrant format

Joint Set # 1	Strike N30E	Dip 21SE	Avg Spacing:	0.37 m
Joint Set # 2	Strike N88E	Dip 74SE	Avg Spacing:	0.64 m
Joint Set # 3	Strike N12E	Dip 59SE	Avg Spacing:	0.49 m
Joint Set # 4	Strike N25W	Dip 63SW	Avg Spacing:	0.67 m

3.6 Video Logging of Vertical Holes

Borehole video logging has been performed to investigate the characteristics of the rock on the wall of vertical holes and to select a location at which to place a borehole plug. The work was performed on May 19, 1989, by "Well Scan Inc." of Phoenix, Az. A 76 mm OD color video camera (Wellcam, WC-9941) with headlight is lowered into the hole using a steel cable. The borehole image is monitored using a control unit (WC-9541) and is simultaneously recorded by a videocassette recorder. A nylon line is attached to a fixed point along the borehole wall to provide a reference orientation inside the hole. The depth of the camera is measured from the encoder at the cable reel.

The investigation is made from the top end of the casing to the bottom of the borehole. The observations agree well with the core log. The vertical hole C seems to be the best (i.e. less fractured) for seal testing purposes. Holes A and B show highly fractured rock. Most fractures are nearly vertical. The video log indicate that hole B is

not suitable for packer tests due to the poor integrity of the hole and large fracture apertures (3-30 mm). Performance of packer tests under such conditions could easily damage the pneumatic packers.

3.7 Fracture Detection Using Ground Penetrating Radar

The purpose of this investigation is to evaluate the subsurface rock quality. The investigation has been made at the original location of the inclined hole C where highly fractured rock was found at a depth of 2 to 3 meters during coring. The results supported the decision to relocate the inclined hole C.

3.7.1 Methods of Investigation

Ground penetrating radar (GPR) detects changes in subsurface electrical properties, which are often related to differences in water content. A subsurface interface radar (SIR System-3) manufactured by Geophysical Survey Systems, Inc., has been used. The SIR System-3 includes a profiling recorder (GSSI Model PR-8315) providing a facsimile printout of the radar returns, and a transducer transmitting and receiving the radar signal. The transducer (antenna) has a frequency of 100 MHz.

The transducer is pulled over the ground surface where the subsurface rock quality needs to be examined. Fiberglass measurement tapes indicating the path of the profile are used to prevent interference with the radar signal. Reference points can be marked on the recorder while the antenna is being towed. The resolution of the results depends upon the towing speed, frequency of the introduced signal, and the electrical conductivity of the rock. Maximum penetration depth of the GPR system used is approximately 2 meters. In moist ground cover or when water is present, the overall penetration depth is reduced due to scattering of the beams.

3.7.2 Results of the GPR

Figure 3.5 gives the facsimile printout of the radar returns obtained at the original location of inclined hole C. The printout is overlaid with the cross-section of the inclined hole C. The depth of the investigation is 2.5 m. Dark smooth bands appear at the left and right sides of the printout and indicate the intact rock. The fluctuating bands (called "no signal return area") at the middle of the printout indicate fractured rock. The length and width of the investigated area are 6 and 4.5 m, respectively. The results tend to agree with the core log. The original location of site C was abandoned based upon preliminary drilling of the inclined access hole and upon the GPR results.

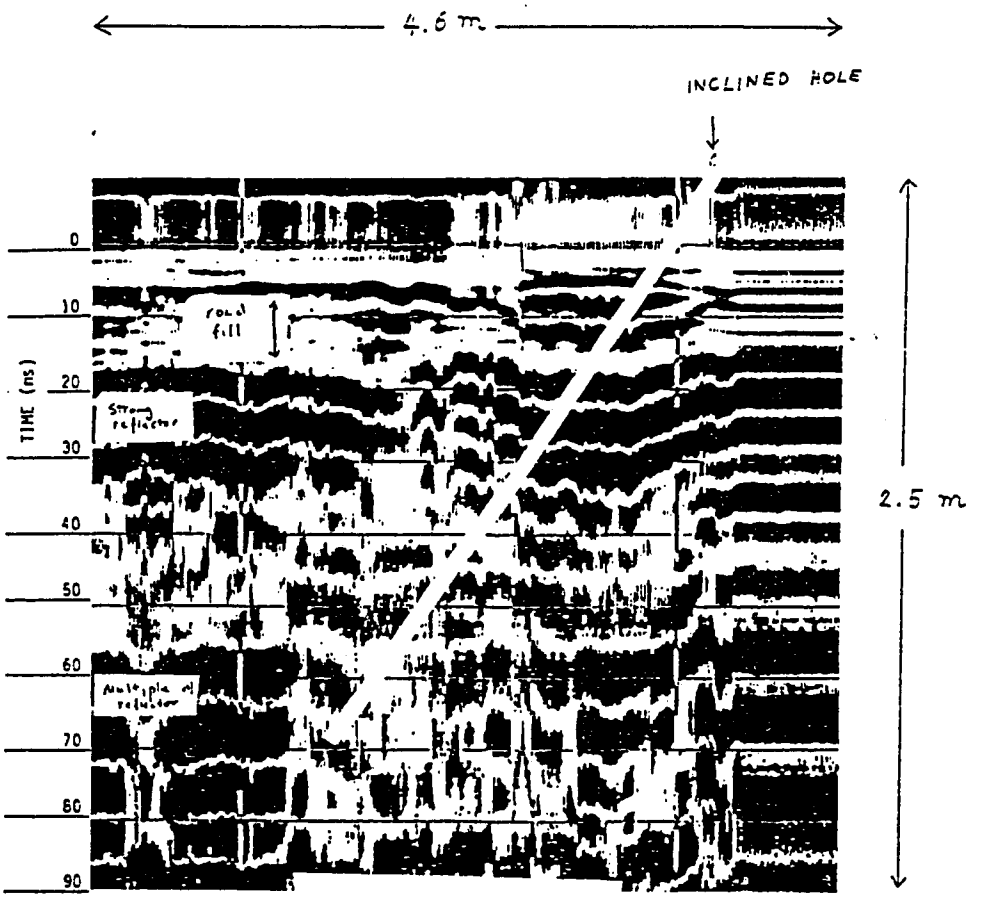

Figure 3.5 Facsimile printout of the radar returns obtained at the original location of inclined hole C. The printout is overlaid with the cross-section of the inclined hole C.

3.8 Hydraulic Characterization of Inclined Holes

Constant pressure (steady-state flow) and falling head packer tests using a straddle packer system is conducted on the inclined holes of all three sites to aid in locating the vertical boreholes and plugs and to obtain an estimate of the hydraulic conductivity of the rock. Analysis of the tests is in terms of hydraulic conductivity calculated using Darcy's law, based on the assumption of a homogeneous, isotropic porous medium.

3.8.1 Test Method

Both the constant pressure injection tests and the falling head tests use straddle packers to isolate a borehole test interval. The test interval is fixed at 37 cm between the upper and lower packer assembly and is lowered to the depth at which the interval to be tested will be isolated when the packers are inflated.

If the test interval consists of relatively intact rock, the injection pressure will stabilize, allowing use of the steady-state injection system. If fractures are present in the test interval, allowing water to quickly flow out of the test interval, the falling head system is implemented to measure the hydraulic conductivity.

3.8.2 Test Results

Figure 3.6 gives the hydraulic conductivity as a function of position at locations A, B and C, respectively. Two distinct hydraulic conductivities are observed: $k = 10^{-5}$ to 10^{-4} cm/s probably represents a lower bound estimate of the fracture zone permeability, and $k < 1.9 \times 10^{-8}$ cm/s represents the intact rock permeability.

Falling head tests indicate that nearly all of the fracture zones in the inclined boreholes have a calculated hydraulic conductivity (k) on the order of 10^{-5} cm/s. With the lower packer deflated and the injection water allowed to flow past the lower packer, the hydraulic conductivity of the test system ranges from 8.0×10^{-4} to 1.0×10^{-5} cm/s. This indicates that in some highly fractured zones of the borehole, the injected water flows out of the test interval nearly as fast as the injection system can provide. In less fractured zones, the magnitude of flow out of the test interval decreases and can be calculated if it is less than the outflow of the injection system.

For steady-state tests, the accuracy of the injection system and test duration limit the minimum measurable hydraulic conductivity, which is 1.9×10^{-8} cm/s. Therefore, when intact zones are encountered in the borehole, and the flow into the injection zone is less than can be measured, the hydraulic conductivity of that test interval is considered less than 1.9×10^{-8} cm/s (ie. less than what the hydraulic test system

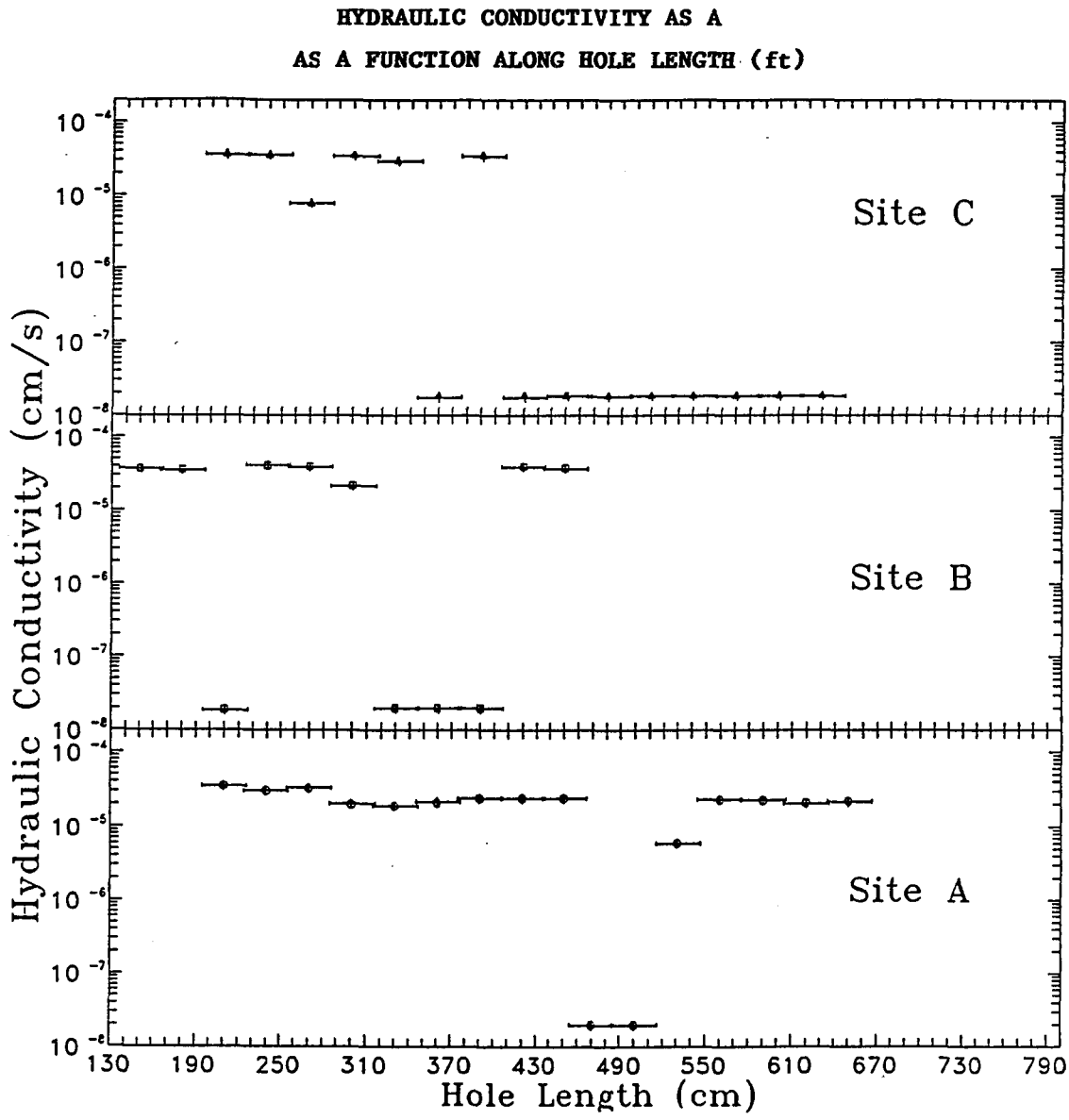

Figure 3.6 **Hydraulic conductivity as a function of hole depth of locations A, B and C respectively. The centered symbol represents the center of the test interval.**

can measure).

For inclined hole A, the intact rock is found at a depth from 470 to 520 cm. The hydraulic conductivity of this zone is less than 1.9 x 10^{-8} cm/s. The intact zones are found in inclined hole B at depths from 200 to 220 cm and from 320 to 400 cm. For inclined hole C, the intact rock (i.e. $k < 1.9 \times 10^{-8}$ cm/s) is found at a depth from 420 to 620 cm. Correlation of the permeability results with the core obtained from the inclined holes is uncertain due to extensive breakage of the core caused by drilling.

3.8.3 Long Term Straddle Packer Test of Inclined Hole C

A long term steady state flow test was performed in the inclined hole near the intersection between the vertical and inclined holes at site C. Position of the test is 4.8 - 5.2 m along the inclined hole. The test has been performed for approximately 6 days under an injection pressure of 0.5 MPa. Results (Figure 3.7) show that at the time of termination of the test, the flow rate into the injection zone is still decreasing (i.e. saturation has not been reached). The calculated hydraulic conductivity of the rock (k_r), assuming a radial flow path and a radius of influence, R_i = 0.42 m, is 8.85 x 10^{-11} cm/s. Assuming prolate ellipsoidal flow or radial flow, the hydraulic conductivity overestimates the actual permeability of the rock since the flow rate

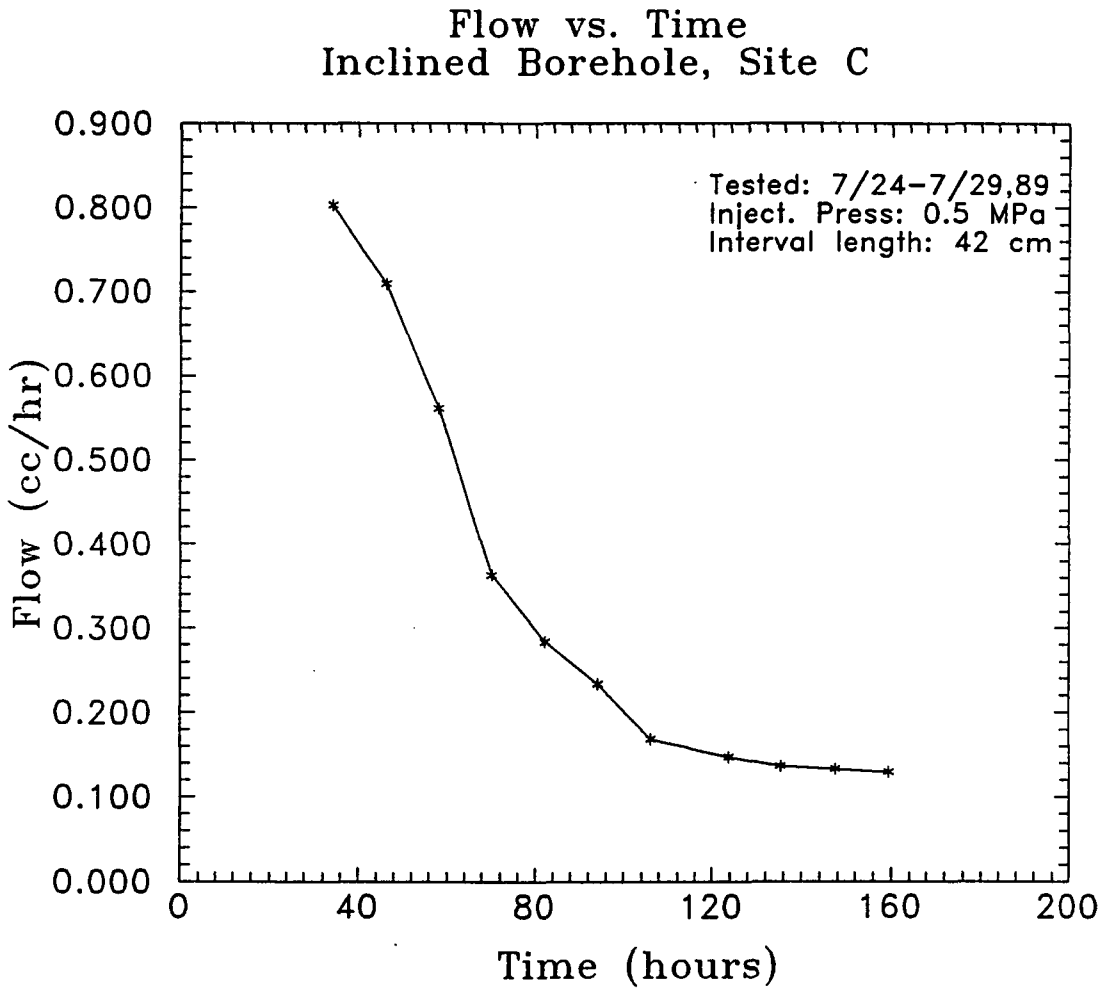

Figure 3.7 Long term straddle packer flow test, inclined hole C. Injection pressure is 0.5 MPa. Length of the test interval is 42 cm. Test conducted 7/24 - 7/29, 1989.

used in the calculation has not reached a steady state.

3.9 Hydraulic Characterization of The Vertical Boreholes

A prime goal of vertical borehole flow testing is to aid in selecting a location for the borehole plug to be installed and tested, and to obtain an estimate of the hydraulic conductivity of the rock. Steady-state analysis requires that injection into the packed-off interval continue until the flow rate has stabilized. A constant flow rate indicates that the rock around the borehole is fully-saturated.

3.9.1 Steady State Flow Test with Straddle Packer System

Two 127 mm diameter and 2.1 m long pneumatic packers were initially used for this test. Because of the length of the packer the maximum depth is limited of the vertical hole that can be tested without exposing the packer gland to the opening of the inclined hole. Replacing the bottom 127 mm packer by a modified 76 mm diameter packer allows testing of the vertical borehole to greater depths, and allows inflation of the modified packer at or near the intersecting inclined hole without damage to the packer. However, because of the shorter packer gland length and overall configuration, the risk is higher of poor sealing by the packer.

3.9.2 Results of Packer Flow Testing at Site C.

Figure 3.8 gives the results of the falling head tests in vertical hole C. The hole is tested from 2.39 m to 3.57 m in depth. The injection zone length is 0.48 m. The triangles represent the center of the injection zones. Distance between the centers of the adjacent injections zone is 0.1 m. The hydraulic conductivity of each zone is averaged from a minimum of 45 readings. The hydraulic conductivities along the depth intervals of 2.39 to 3.57 m range from 2×10^{-6} to 10^{-5} cm/s. The maximum permeability that can be measured with the test system is 1.5×10^{-4} cm/s.

Figure 3.9 shows the results of the steady state constant head tests of the vertical hole C from 3.42 to 5.31 m hole depth. The injection pressure for all tests is approximately 0.4 MPa. Flow rates decrease with time. The maximum test duration is 19 hours, the minimum is 4 hours. The flow tests are terminated prematurely (i.e. before a constant flow rate is obtained) due to the low permeability of the rock. The low flow rates indicate that the rock mass in these intervals is intact from 3.42 to 5.31 m. Each interval (Figure 3.9) is represented by a number which denotes the depth of the center of the interval in feet. A 19-hour test was carried out at interval 16 (Figure 3.10). A power curve fitted to the data describes the decay curve of the flow

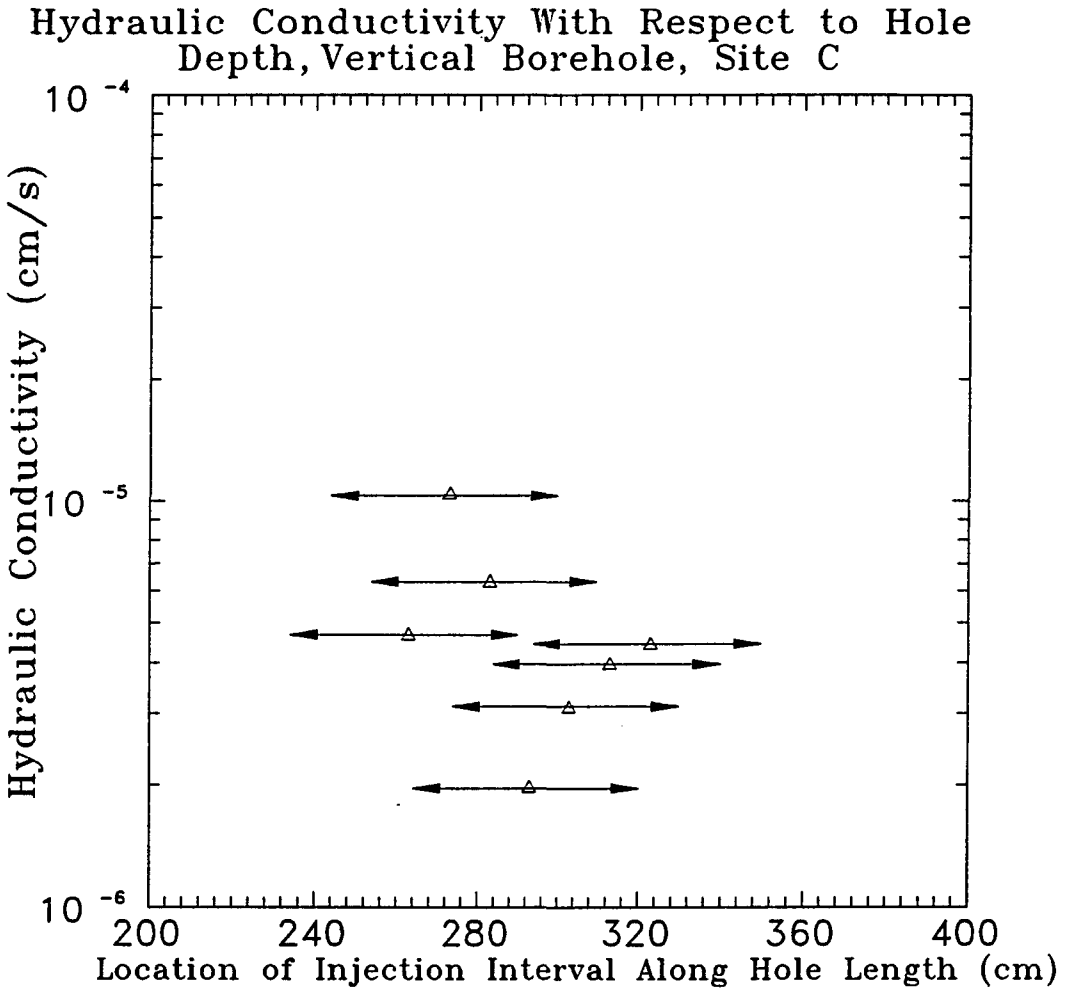

Figure 3.8 Results of the falling head tests conducted in vertical hole C. The hole is tested from 239 cm to 357 cm in depth. The injection zone length is 48 cm. The triangles represent the center of the injection zones.

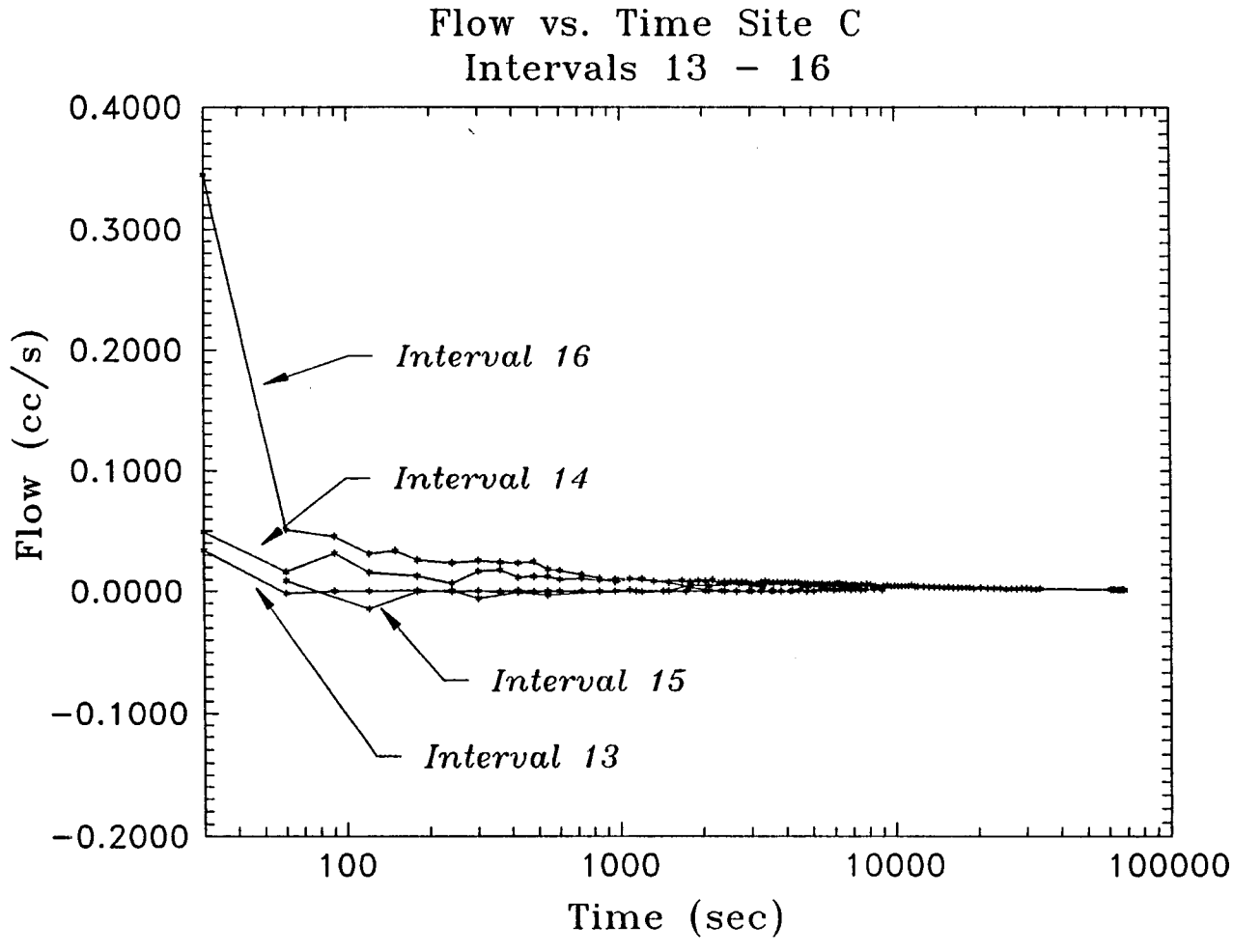

Figure 3.9 Results of the steady - state constant head test of the vertical hole C from 342 - 531 cm hole depth. The injection pressure for all tests is approximately 0.4 MPa. Each interval is the depth of the center of the injection interval in feet measured from ground surface.

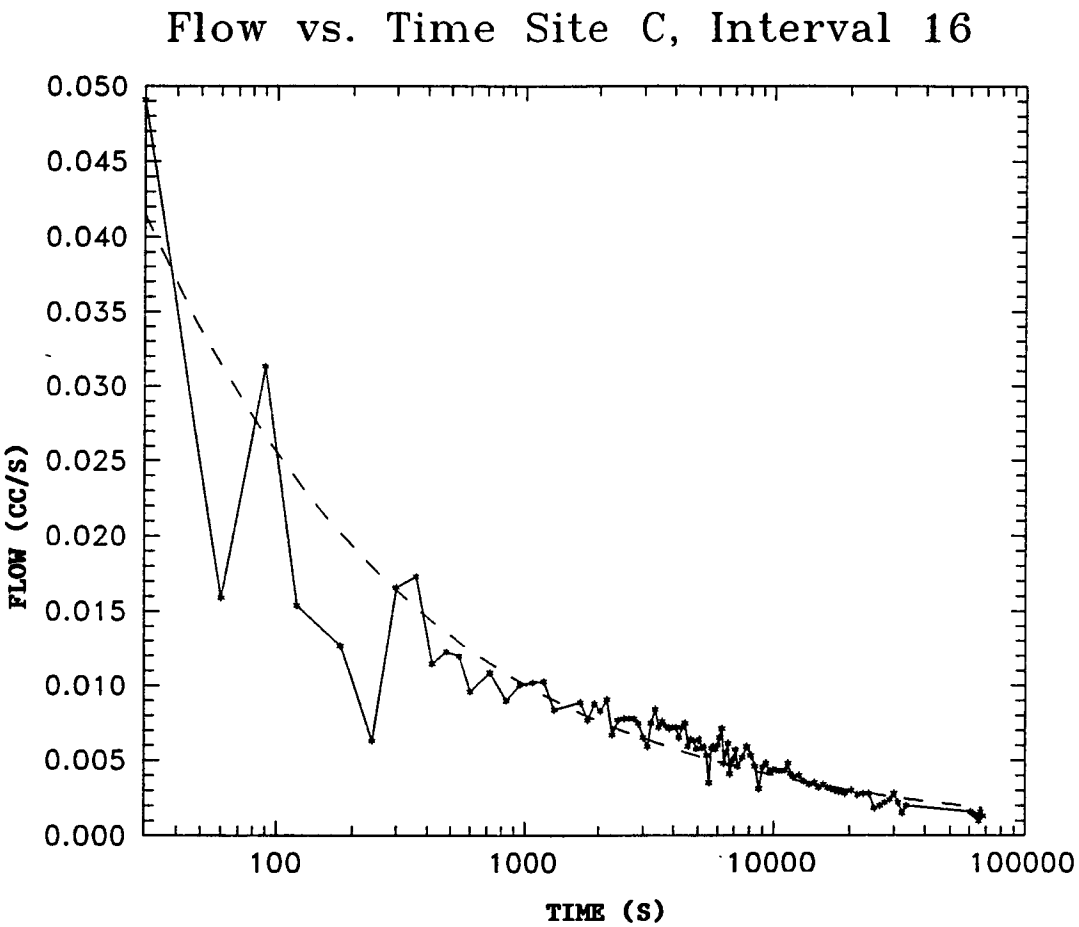

Figure 3.10 Extended steady-state constant head test performed for 19 hours at interval 16.

rate as a function of time (as the rock around the hole becomes saturated). If the rock were to become fully saturated, the flow rate should equilibrate to a constant value. Figure 3.10 indicates that a constant flow rate has not been achieved at the end of the test. The hydraulic conductivity of interval 16, averaged over the flow values of the last 3 hours, is 1.5 x 10^{-9} cm/s. This assumes that the flow is radial from the center axis of the borehole and the radius of influence, (R_i) is 0.87 m (equal to injection interval length). If prolate ellipsoidal flow is assumed, then the hydraulic conductivity solution is 1.56 x 10^{-9} cm/s. The hydraulic conductivities calculated from both solutions (i.e. radial flow method and ellipsoidal method) overestimate the permeability since the flow rates used in the calculations are obtained before the rock is fully saturated.

The intact interval of 3.42 to 5.31 m in vertical hole C has been designated as the test interval most suitable for installation and testing of a cementitous seal. The interval is sufficiently long for emplacement of a plug in intact rock and yields zones both above and below the plug which are intact and can be confined for flow testing.

3.9.3 Results of Packer Flow Testing at Site A

Figure 3.11 gives the results of the falling head permeameter tests: hydraulic conductivity as a function of position along the bore-

hole. Borehole videologging and the core log suggest that finding an intact interval of rock would be unlikely. Tests have been performed with two 127 mm diameter and 2.08 m length packers. The borehole is 8.7 meters in depth and the casing extends 1.7 meters below the ground surface. This limits the length of the borehole that can be tested. The squares represent the center of the injection zones. The distance between the centers of the adjacent injection zones is 0.3 m. The injection interval length between the packers is 0.56 m. The hydraulic conductivity of each zone is averaged from a minimum of 35 readings. The hydraulic conductivities along the tested borehole length range from 1.5×10^{-7} cm/s to 1.8×10^{-5} cm/s. The measured hydraulic conductivity of the system is 5.5×10^{-5} cm/s. None of the tested zones in this borehole are intact.

CHAPTER FOUR

LABORATORY SIMULATION OF FIELD EMPLACEMENT

4.1 Introduction

Full-scale laboratory tests have been carried out on both a expansive cement formula developed by Dowell Schlumberger Corp., and a crushed tuff/bentonite mixture developed by Ouyang and Daemen (1991). Two particular goals of performing the full scale laboratory tests are to develop procedures for installation in the field under various in-situ conditions and study the effects of these conditions on the seals. In addition, reproduction of the installation procedures allows development of tools and devices to refine installation and testing of the seals in the field. Similar tests have been performed by Daemen et. al., (1983) on cement seals in galvanized pipe and plastic tubing both in a vertical orientation and 10° above horizontal, respectively.

4.2 Laboratory Model of Cementitous Plugs

A full-scale laboratory model was constructed to aid in determining the optimum cement plug installation techniques and retrieval devices for the field test. The model simulates the vertical

and inclined holes near their intersection. A 165 mm diameter clear plastic tube simulates the vertical borehole. A 57 mm diameter clear plastic tube is used for the inclined hole. The clear tubes permit visual observation of the events taking place during plug emplacement, e.g. turbulence, mixing with standing water, channel development, as well as of some cement plug characteristics (uniformity, piping, etc.).

A specific objective is to determine an appropriate size distribution of clean sand to be used in the injection zone beneath the cement plug. The sand layer, 60 to 80 mm thick, will be placed on top of the injection stand (Chap. 5.3) to prevent the cement slurry from penetrating into the injection tubes mounted in the injection stand and to obtain a flat and smooth bottom surface of the cement plug. The grain sizes of the sand must be sufficiently large to obtain a high permeability injection zone and to prevent the sand grains from falling into the injection tubes. However, the grain sizes should be sufficiently small to prevent the cement slurry from penetrating into the injection tubes. The sand layer is saturated prior to the cement pouring.

4.2.1 Results of Pouring With Water Present

Three cement pouring simulations were made. For the first trial (Figure 4.1), cement was poured on a layer of sand with diameters >0.249 mm and < 0.419 mm, (#40 mesh), under 30.5 cm of water. A few minutes after pouring, the cement has penetrated 10 to 12 mm into the sand

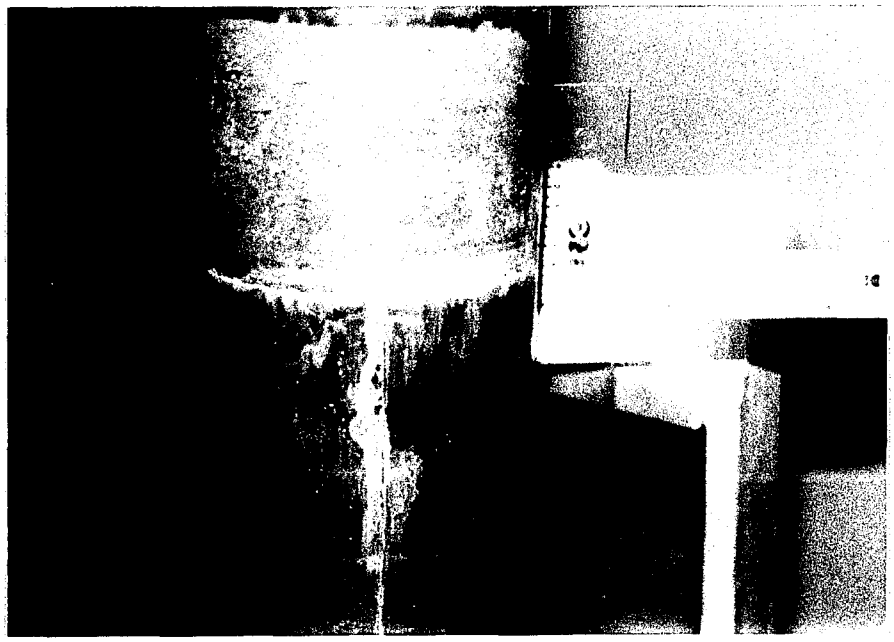

Figure 4.1 First trial of laboratory simulation of field cement pouring; sand grain sizes between 0.249 and 0.419 mm under 30.5 cm of water.

layer. A significant amount of upflow water (piping, which can degrade the sealing capability of the cement plug), was seen along the interface between the tube and cement as dark streaks. The second trial, (Figure 4.2), was poured over clean sand with diameters > 0.106 mm and < 0.249 mm, (#60 mesh), and under 30.5 cm of water. The cement mixture penetrated only 2-3 mm into the underlying sand layer. Significant piping was seen soon after pouring the cement as dark vertical streaks along the tube and cement interface. The severity of the piping decreased slightly approximately 12 hours after the cement plug was poured. The third trial was poured over sand with the same diameter as used in trial 2 but with only 2.5 cm of standing water. Significant piping was again recognized soon after pouring the cement. The severity of the piping decreased considerably within approximately 12 hours after pouring. The cement intruded only 2-3 mm into the sand (Figure 4.3).

4.2.2 Results of Pouring Without Water Present

The fourth trial was poured over saturated sand with the same grain size used for trail 2 and 3 but saturated only to within approximately 2 cm below the top of the sand layer, (Figure 4.4). The bailer used in the pouring of this trial was modified with a 2 mm screen mesh fitted to the outlet to reduce the disturbance of the sand layer as the cement pour out. The least amount of piping developed in this trial. After a

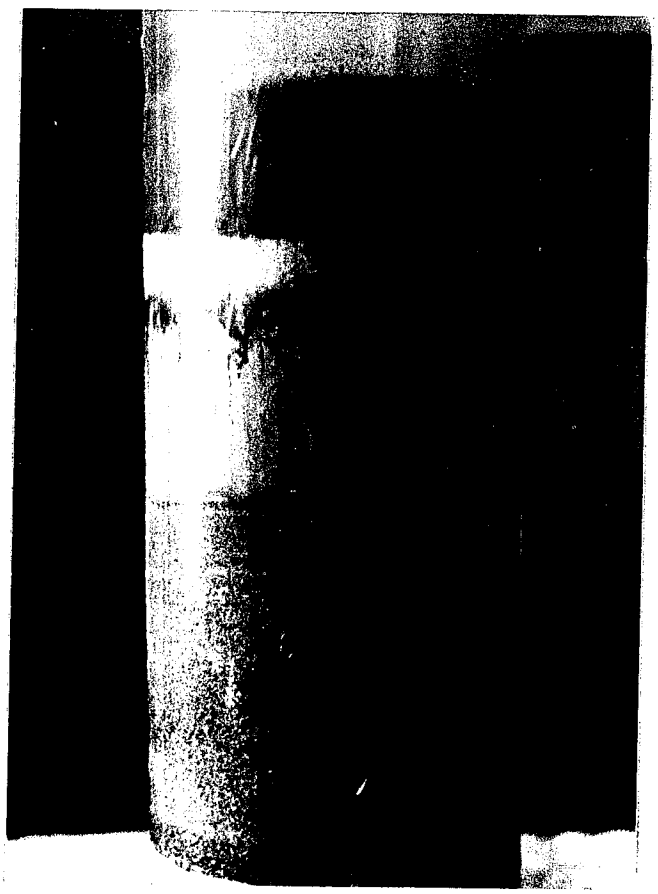

Figure 4.2 Second plug pouring trial. Extensive piping can be seen just below the dark band which is the top of the plug. Sand grain sizes between 0.106 and 0.249 mm.

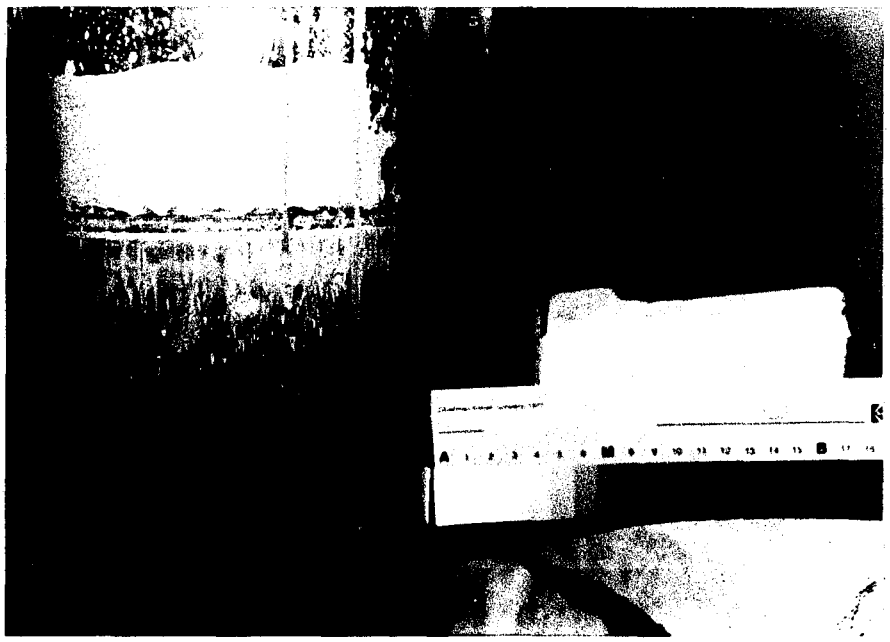

Figure 4.3 Third trial of cement pouring; sand grain sizes between 0.106 and 0.249 mm under 2.5 cm water.

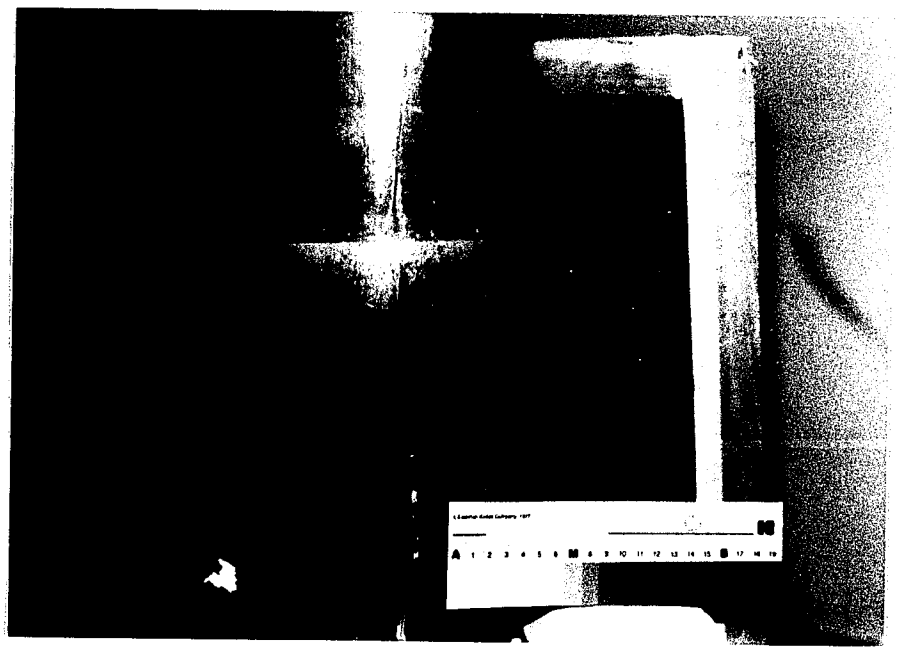

Figure 4.4 Fourth trial of cement pouring; sand grain sizes between 0.106 mm and 0.249 mm. Water level 2 cm below the top of the sand layer

period of 12 hours, piping effects along the interface were not visible. Air, however, was trapped between the sand grains beneath the cement plug.

4.2.3 Conclusions and Recommendations

The results of the four trials indicate that a sand layer of 4 to 6 cm thick with a grain diameter > 0.249 mm, (#40 mesh), should be placed on top of the injection stand in the field and followed with a 2 to 4 cm high layer of sand > 0.106 mm and < 0.249 mm, (#60 mesh), in diameter. This combination will adequately prevent the cement slurry from penetrating into the injection tubes, and prevent clogging of the tubes by the sand. The modification to the bailer significantly reduced the disturbance of the sand layer as the cement slurry was poured. This resulted in a smoother and flatter interface between the cement slurry and sand after the pour. The optimum level of water was found to be 1 - 2 cm below the sand layer. Although a certain amount of air may be trapped below the plug in the upper sand layer, piping caused by water being displaced by the cement as it is poured is greatly reduced or eliminated entirely. Too much air trapped in the injection zone beneath the plug, however, can significantly interfere with the flow analysis for the plug test. In the field, the presence of the trapped air can be minimized by a recurculating or flush line installed parallel to the injection line which can be used to expel most of the trapped air out of

the injection zone. Similar piping effects after pouring cement plugs underwater were observed by Daemen et. al., (p. 71, 1983). Piping channels in eight seperate trials poured underwater were recognized as dark streaks along the tube and plug interface. After curing, a cross-section of each plug revealed that many of the streaks were open channels.

4.3 Laboratory Model of Crushed Tuff and Bentonite Seals Simulating In-Situ Conditions

The full-scale laboratory model used for testing emplacement of Self Stress II expansive cement plugs was modified for emplacement and flow testing of crushed tuff and bentonite seals. The primary purpose is to develop a successful procedure for installation of the crushed tuff/bentonite seal. The installed material must be as homogeneous as achievable and have an adequate bulk density obtained through dynamic compaction of the material.

The crushed tuff bentonite seal installed in the full-scale model is comprised of a Type A crushed tuff gradation developed by Ouyang and Daemen (1991). The crushed tuff/bentonite plug is comprised of 35 % by weight C/S Granular Bentonite, with the remaining material Type A crushed tuff. Ouyang and Daemen (1991) have shown promising results of this mixture on laboratory constructed specimens. Hydraulic conductivities of 10^{-10} - 10^{-8} cm/s have been determined from falling head permeameter tests performed by Ouyang and Daemen (1991).

Two full scale (180 mm diam.) plugs were tested in the model described above to develop a methodology of installation and construction for a crushed tuff/bentonite mixture plug in the field. A third plug was tested in a second model of similar size, yet with a stiffer wall construction and with pore pressure measuring points located at various heights along the cylinder wall. The physical characteristics and results of the flow tests are given in Table 4.1. The measured permeability assumes a one dimensional flow which is steady and axial through a saturated pourous-medium seal. Chapter 2, Sec. 2.2.1 describes the one dimensional flow model. The measured permeability values are given for comparison purposes. Preferential flow was recognized due to piping effects in the first two trials, yet the permeability is determined based upon flow through the entire cross-sectional area. The third trial was not fully saturated throughout its axial length and also does not fully meet the one dimensional model criteria.

Table 4.1 Physical and Hydraulic Characteristics of Laboratory Trials

Trial #	Bulk Density (g/cm^3)	L:D Ratio	# of layers used in construction	Average Flow Values (cc/hr)	Measured Permeability(cm/s)
1	1.22	1.2:1	2	20.9	4.2×10^{-6}
2	1.36	1.2:1	4	15.4	2.1×10^{-6}
3	1.57	1.2:1	4	0.25	1.1×10^{-8}

4.3.1 Trial 1

The first plug installed has an estimated bulk density of 1.22 g/cm^3 and a length to diameter ratio, (L:D), of 1.2:1. The plug has been installed in two layers with a bailer. Separation of the mixed particles made the distribution of the tuff and bentonite very poor and made the resulting plug relatively heterogeneous. This separation is mainly due to the bailer used which is designed for emplacement of liquids, specifically neat cement. As the stopper of the bailer was lifted through the plug material, filtering of the largest materials occurred, allowing them to drop out last. A new bailer, larger in diameter and with a spring loaded opening which opens quickly to allow dropping the material with minimal separation was built. This bailer is designed for emplacement of dry granular materials rather than liquids.

Flow testing of the plug with a falling head injection from beneath indicated that due to the lack of homogeneity, channeling occurred along one side of the plug and pipe interface as seen in Figure 4.5a. Figure 4.5b shows the opposite side of the plug with layering of medium to fine particle grains and uneven wetting. Figure 4.6b shows the results of falling head flow tests with an average applied head of 6 meters, similar to what would be encountered if the plug were installed in the vertical borehole of site A. Flow tests carried out 2 days, 14 days, and 21 days after installation show little indication of bentonite healing. This is mainly due to the severity of the channeling along the

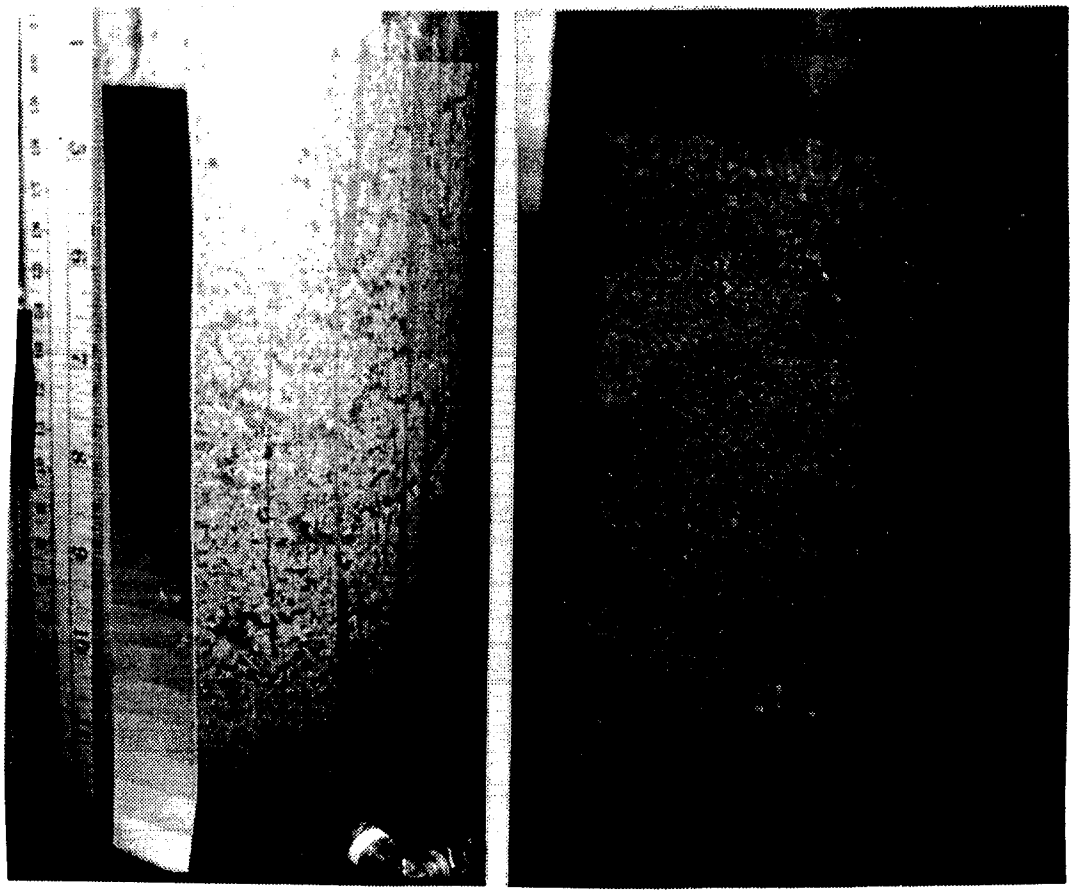

Figure 4.5 a,b Trial 1 of the laboratory crushed tuff/ bentonite plugs.
a) Severe channeling along the plug and pipe interface due to inhomogenieties of the plug
b) Fine particles on the opposite (180°) side with uneven wetting due to the higher content of bentonite

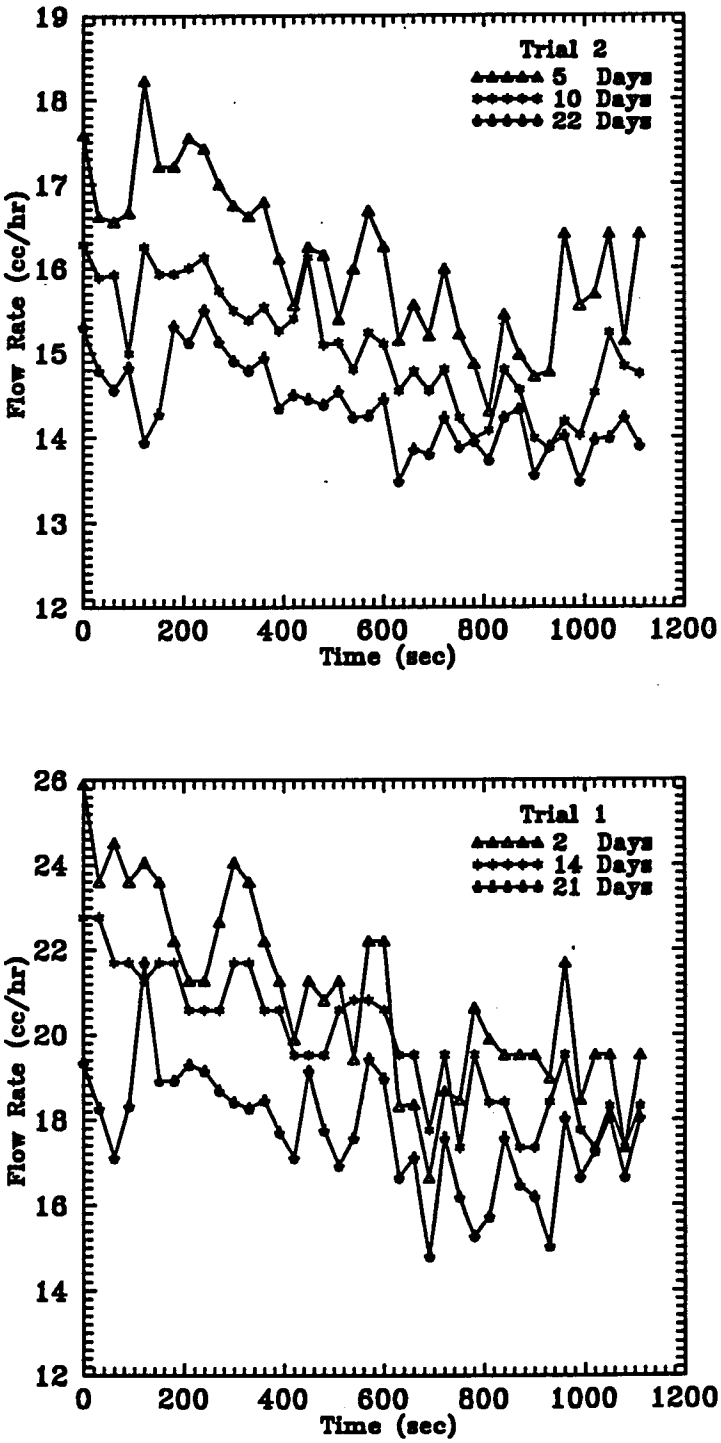

Figure 4.6 Falling head flow tests performed on two laboratory trial crushed tuff/bentonite mixture plugs.

interface, poor confinement and an overall low bulk density of the plug due to poor compaction procedures. Compaction is limited by the relatively thin wall thickness of the test pipe.

4.3.2 Trial 2

A second laboratory plug was constructed of four layers with a redesigned bailer. Confinement for the second trial is 2.5 times greater than for the first test and more evenly distributed, with a 4 cm thick sand layer on top of the plug. Length to diameter ratio, (L:D), is the same as the first trial of 1.2:1. The estimated bulk density of this plug is 1.36 g/cm^3. The redesigned bailer is a significant improvement over the first one, however the installed second plug still suffered from heterogeneities, although less severe ones than the first test, (Figure 4.7). Because of the inhomogeneity, piping occurred in the plug internally. Flow tests performed 5, 10, and 22 days after installation with the same average head as trial 1, indicated that the plug was not homogeneous due to the relatively high permeability measured, (Table 4.1, Figure 4.6a). Little indication of bentonite healing is suggested by the falling head flow tests which approximately yielded the same average flow results.

It is felt that the second trial failed primarily due to inhomogeneities of the installed plug, inadequate confinement and, most importantly, inadequate and uneven compaction. Although these were

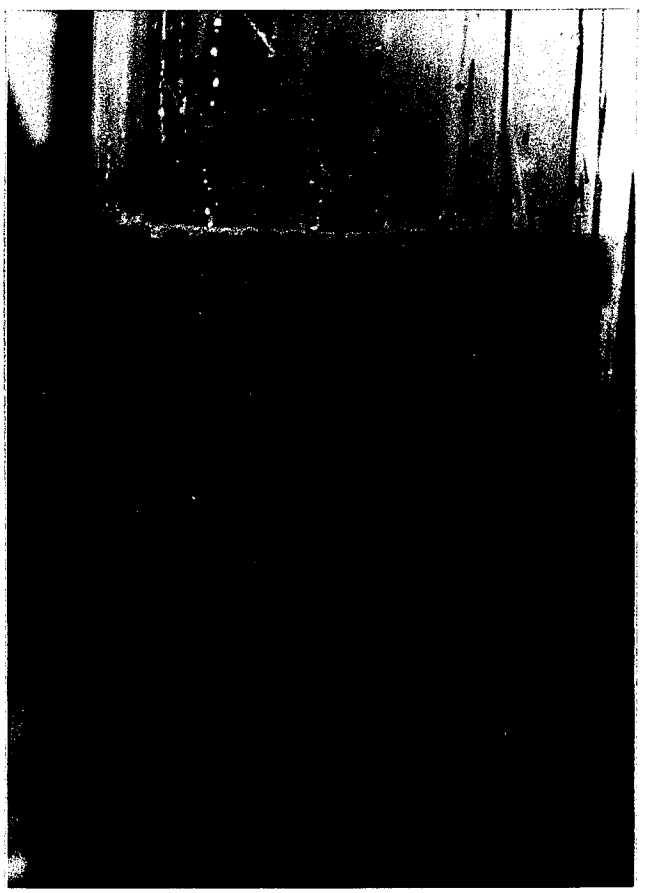

Figure 4.7 Second trial of the crushed tuff/bentonite plug. Piping occured internally due to the poor compaction and inhomogeneity of the plug

improved significantly compared to the first trial, in order for the crushed tuff/bentonite material to perform properly, compaction and confinement must be further increased. A static compaction method has been considered, yet duplication in the field would be expensive and difficult due to the installation depth.

4.3.3 Trial 3

A third laboratory plug was performed in a plexiglas cylinder of similar diameter as the first two trials, yet with twice the wall thickness. The greater wall thickness allows a higher degree of compaction of the plug material while reducing the risk of cracking the cylinder during the compaction process. In addition, it provides greater stiffness which is more comparable to the insitu conditions.

The third trial was constructed of four layers, compacted individually. The resulting bulk density is 1.57 g/cm^3. The bailer was further modified after the second trial by reducing its overall length by one half. This in turn allowed less seperation of the mixture as it was loaded into the bailer.

Flow testing was carried out under a falling head test with an average applied head of 6 meters. Figure 4.8 shows the results over a 2500 hour test period. The average flow rate at the end of the test was 0.25 cc/h. At the end of the test, the plug was still not fully saturated as can be seen in Figure 4.9. Two pressure transducers are

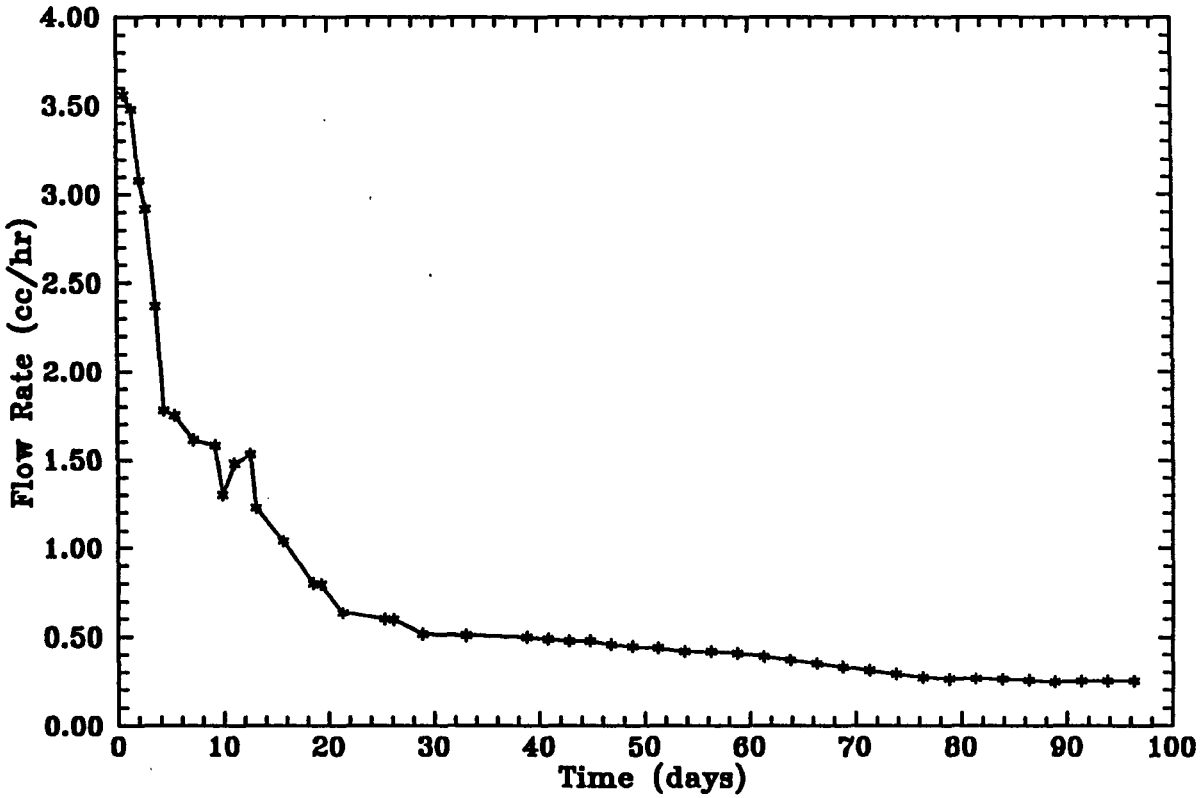

Figure 4.8 Results of falling head tests on the third trial.

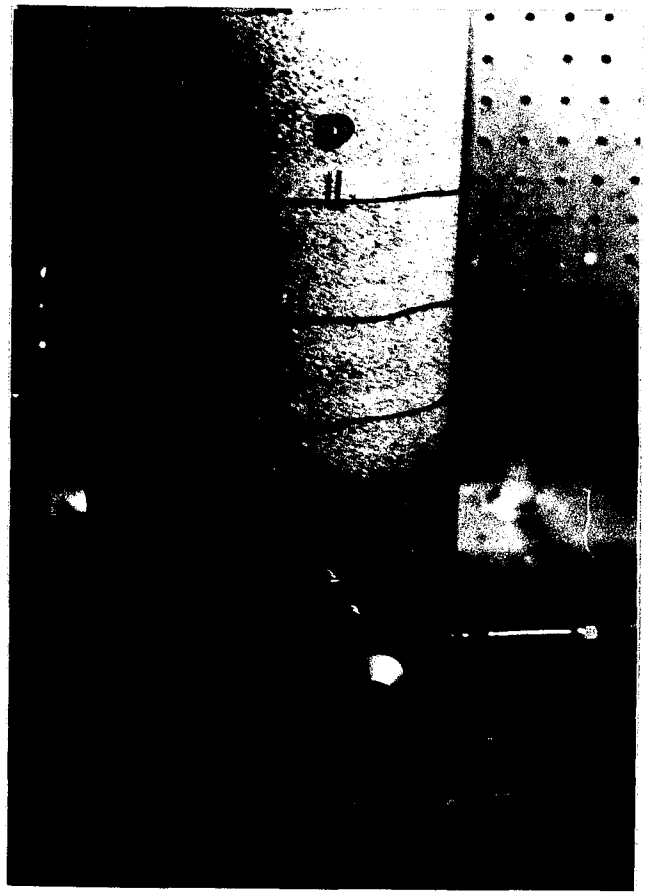

Figure 4.9 Third trial of installation of a laboratory crushed tuff/bentonite plug. Plug is not fully saturated.

mounted 1/3 and 2/3 from the center of the injection zone beneath the plug to measure the distribution of pore pressure within the mixture. The pressure transducer near the top did not register a pore pressure due to the fact that the plug never fully saturated up to that level. The lower pressure transducer however, near the end of the test, did read a positive pore pressure.

4.3.4 Conclusions and Recommendations

The three trials indicated that for the crushed tuff/bentonite plug to seal properly in the field, a great deal of attention must be addressed to installation procedures. Homogeneity of the material, compaction, which is directly related to the bulk density, and particle size of the crushed tuff aggregate play significant roles in the sealing capability of this material.

The first trial was impaired primarily because of a bailer, which caused severe seperation of the larger crushed tuff particles from the bentonite and in turn the material had severe nonhomogenous characteristics. These chracteristics include uneven bentonite content throughout the plug, where in some areas it was nearly absent. Another significant factor affecting the performance of the first trial was that the compaction process during installation, which was inadequate with only

two layers comprising the plug. In addition, the confinement above the plug was insufficient to reduce volumetric swelling.

The second trial was compromised by the same factors described above, hovever to a lesser degree. The two most significant factors include inadequate compaction, even though it was increased from the first trial, and, to a lesser degree nonhomogeneous characteristics of the installed plug, contributed by the redesigned bailer. Because of the length of the bailer, as the material was loaded into the tube of the bailer, it dropped 24 - 32 inches (60 - 80 cm). As the material fell to the base of the bailer, a certain degree of separation between the larger and smaller particles occured. This was seen when the material was deposited in the borehole, where the largest particles dropped out first and the fines were deposited last. This in turn resulted in a inhomogeous plug which aggravated the piping effect during flow tests.

The third trial plug was installed in a plexiglas cylinder with a thicker wall. This larger stiffness of the cylinder allowed greater compaction of the plug and resulted in a higher bulk density. The bailer was further modified by reducing it overall length to limit seperation of the plug mixture during filling of the bailer and deposition of the material in the borehole. This significantly improved the overall homogeneity of the third trial plug. The bailer can be further improved by making the trap door split in the center to allow

the material to fall into the center of the borehole rather than to one side. This adjustment should further enhance the homogeneity of the plug.

CHAPTER 5

INSITU TESTING OF CEMENT BOREHOLE PLUGS

5.1 Introduction

This chapter presents the application of the hydraulic tests described in Chapter 2 to in-situ testing of a cement borehole plug. After a suitable test zone was selected at site C, (Chap. 3), the portion of the borehole below the test interval had to be sealed and equipment had to be permanently installed for flow tests. After the installation of the bottom seal and equipment, single packer tests were performed to determine the permeability of the bottom seal before installation of a test plug.

Once the testing of the bottom borehole seal had been completed, a neat cement borehole plug was installed in the vertical borehole. The configuration of the test system with both a inclined and vertical borehole allowed access to both the top and bottom of the seal (i.e. collection or injection on either side of the plug), without penetration of the plug with access and injection lines.

5.2 Preparation of Vertical Borehole

Based upon packer tests and core and videologs, the inclined and vertical holes contained fractures just below the intersection point. This necessitated the sealing of the bottom portions of these holes below the intersection point before installation of a borehole plug so as to provide a low permeability region below the test zone.

Expansive cement (Self Stress II) was poured into the bottom of the vertical and inclined holes at site C to seal the holes below the intersection point. The lengths of the inclined and vertical holes below the intersection point are 914 and 737 mm, respectively. A large amount of cement slurry was needed (i.e. larger than the capacity of the available mixing container). Prior to pouring, the cement slurry was accumulated in a storage tank (5-gal. plastic can) until the desired volume was obtained. The cement slurry in the tank was stirred continuously to prevent separation of the material. The mixing and pouring durations are kept minimal.

The first layer of cement was poured in the vertical hole on June 25, 1989. The length of the cement was intended to be about 300 mm. Approximately 5,000 cc of cement slurry was prepared. The length of the cement plug was measured as 500 mm, on June 28, 1989 (3 days later). The measured length was significantly larger than the one precalculated from the volume of the slurry. This is probably due to mixing of the

cement slurry with the water standing in the hole as a result of the turbulence created by the rapid cement discharge from the bailer and by raising the bailer during pouring. A similar phenomenon was observed in the laboratory model of the cement seal, (discussed in Chap 4, Sec. 4.2).

On July 2, 1989, Self-Stress II cement was poured into the bottom of the 57-mm diameter inclined hole. A 25-mm diameter PVC pipe was used to pour the cement. The pipe was inserted into the hole until it touched the bottom. Approximately 1500 cc of cement slurry was poured through the pipe into the inclined borehole. Measurement of the cement length immediately after pouring indicated that no cement was left in the hole. The cement most likely leaked through fracture(s) at the hole bottom which must have been so large enough that the viscosity of the cement was not sufficient to stop the flow.

In order to seal the large fracture(s) at the bottom of the inclined and vertical holes, a conventional Type II Portland cement mixed with a 0.5:1 w/c ratio and with a clean sand, (60 mesh), 30% by weight, was poured into the inclined hole through the PVC pipe. The resulting cement length after pouring was approximately 300 mm. This cement-sand mixture sealed the fractures effectively, as evidenced by the standing water remaining in the hole above the intersection for a period of 24 hours. On July 3, 1989, Dowell-Schlumberger Self-Stress II expansive cement was poured on top of the sanded cement until it reached

the intersection point of the inclined and vertical boreholes. The cement was cured under water for seven days.

A stainless steel injection stand was installed in the bottom of the borehole on July 31, 1989. The injection stand, Figure 5.1, secures the end of the injection/collection water lines in the vertical hole. These lines are used to inject or collect water at the bottom of a plug to be tested. The stand was cemented in position using Self-Stress II expansive cement. In addition to securing the water lines, the stand provides a fixed surface to emplace the cement plug. The depth of the injection stand is 4.65 m below ground level, 0.60 m above the intersection point. Figure 5.2 describes the configuration of the installed injection stand.

5.3 Steady-State Flow Testing of the Rock and Bottom Borehole Seal

Steady-state flow testing of the rock and bottom borehole seal after the installation of the injection stand was performed through the use of a single packer test (Figure 5.3). The purpose of this test is to determine the sealing effectiveness and permeability of the seal below the injection stand. Chapter 2, Section 2.2.2, describes the test. In order to average out temperature effects upon the test system, residual stick slip effects from the injection pump, extremely low flow levels and electronic noise from the measuring devices, flow values are

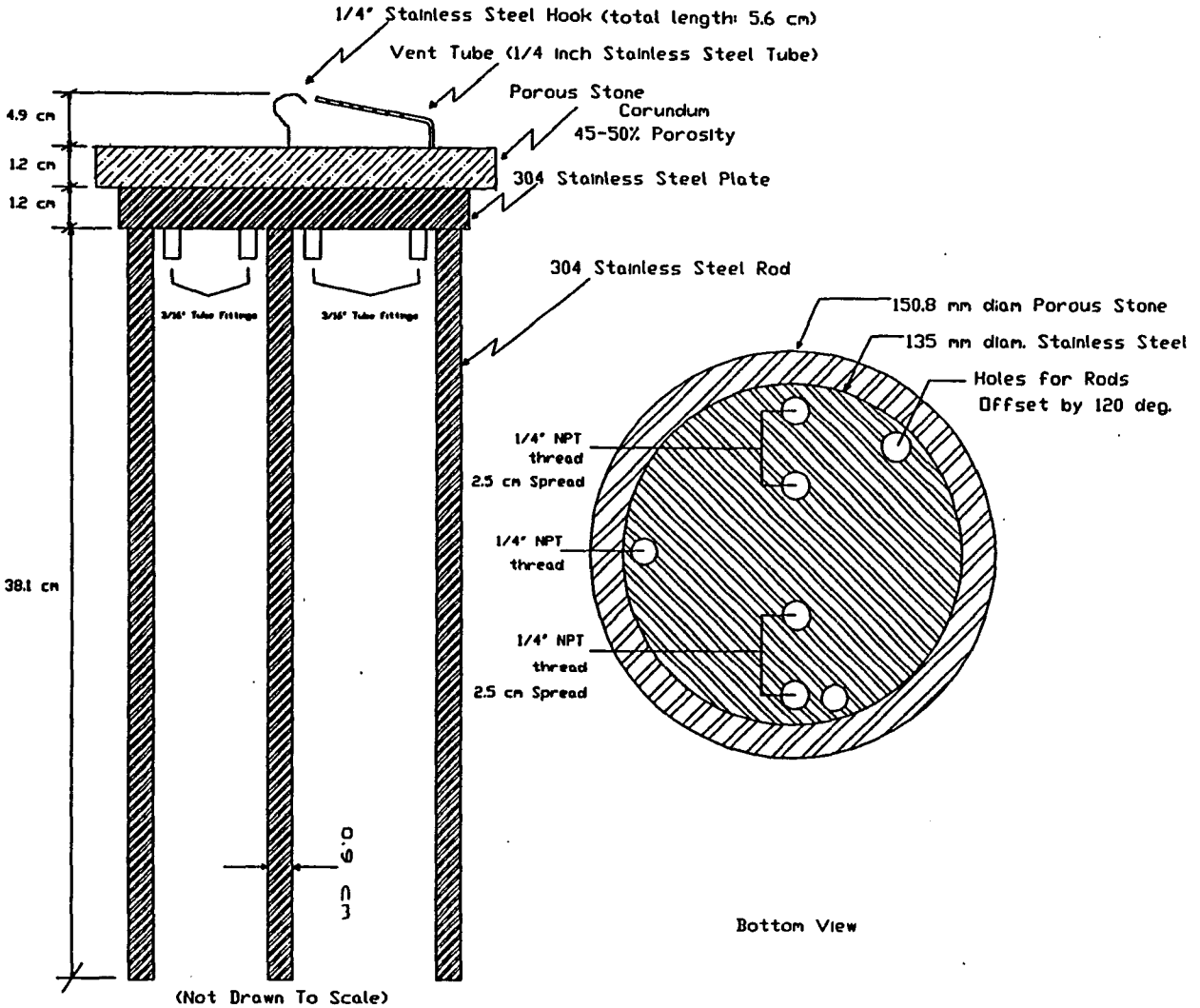

Figure 5.1 Injection stand installed at site C. The stand uses a porous stone on top to prevent sand particles from clogging the flush parts.

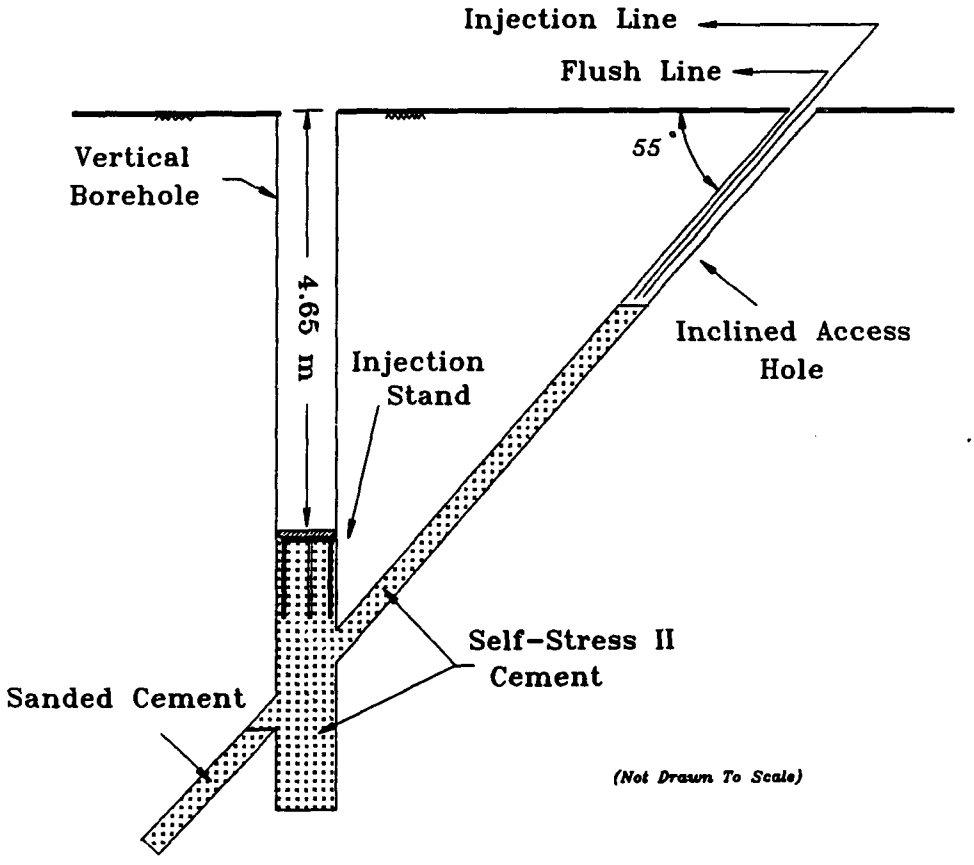

Figure 5.2 Injection stand installed at the bottom of the test zone. Self-Stress II Cement grout stabilizes the stand and seals the vertical hole and most of the inclined hole.

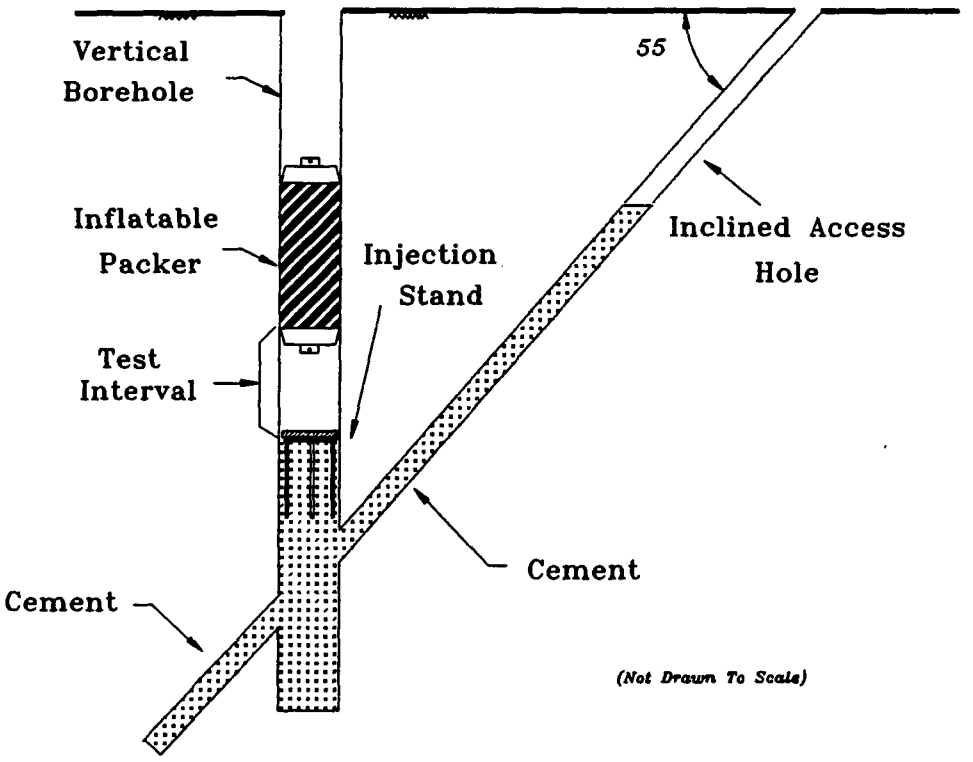

Figure 5.3 Configuration for steady-state flow testing of rock bottom borehole seal. Inflatable packer isolates the test interval.

calculated over 24 h span intervals. Figure 5.4 shows the flow rate as a function of time, calculated using 24 h span intervals. The 21-day test shows that the flow rate is approaching a stable non-decaying flow value. A power curve fit is used to describe the flow rate decay curve. The power curve does not, however, predict the eventual saturated steady-state flow rate (i.e. the curve approaches zero at time infinity). An empirical equation is derived using a least squares empirical fit applied to the power equation to predict the saturated steady-state flow as the asymptote of the curve. This derived flow value from the curve is 0.0576 cc/h. The empirical equation describing the flow decay curve is:

$$F = 0.183x(t^{(-0.59)}) + 1.59x10^{-5} \qquad (5.1)$$

where :

t = time (hours)

F = flow rate (cc/hr)

By assuming that the bottom seal is impermeable the hydraulic conductivity of the rock calculated from the derived flow rate value is 3.6 x 10^{-11} cm/s, assuming prolate and ellipsoidal flow, and 3.5 x 10^{-11} cm/s assuming radial flow with radius of influence of 718 mm (equal to the injection interval length). Because both calculated permeability values

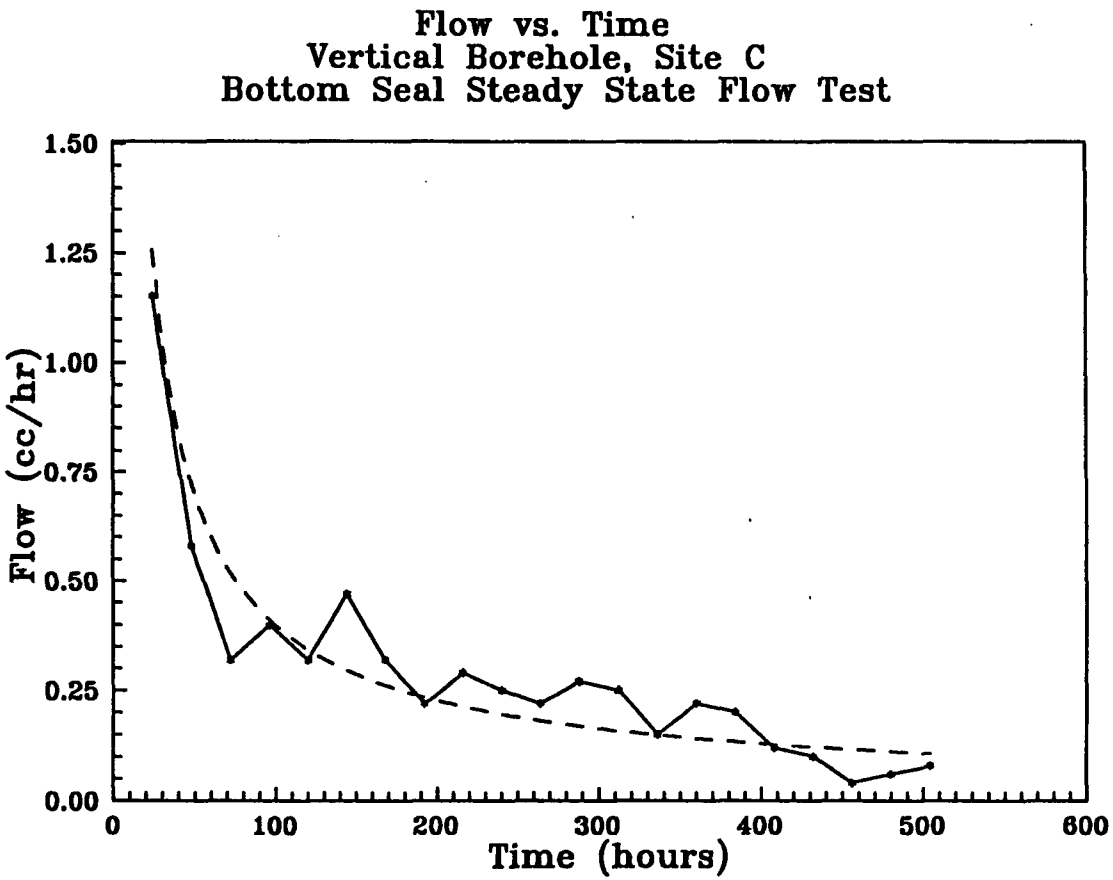

Figure 5.4 Flow rates as a function of time: results of bottom hole flow test. Curve fit (dash line) and experimental results.

assume the bottom seal to be impermeable, the hydraulic conductivity of the rock calculated above overestimates the rock permeability due to the influence of the permeability of the cement bottom seal.

5.4 Installation of Cement Borehole Plug

On September 9, 1989, a cementitious borehole plug has been installed in vertical hole C. The configuration of the installed plug is given in Figure 5.5. The plug is comprised of the same material used for the bottom borehole seal. The cement plug material is "Self-Stress II" provided by the Dowell Schlumberger Company. Volume of the plug is approximately 3900 cc, comprised of 6.5 (600 cc) mixes made within a time period of 18 min. at an ambient temperature of 24 °C. The plug has been poured at one time with a bailer.

The plug was allowed to cure for nine days with approximately 3000 cc of distilled water on top to prevent drying. After the curing period, injection tests could be initiated.

5.5 Steady-State Flow Tests

Steady-state flow tests were begun on Sept. 18, 1989 at site C and were performed with a water injection beneath the plug of 0.26 MPa - 0.28 MPa. Injection beneath the plug was performed without interruption

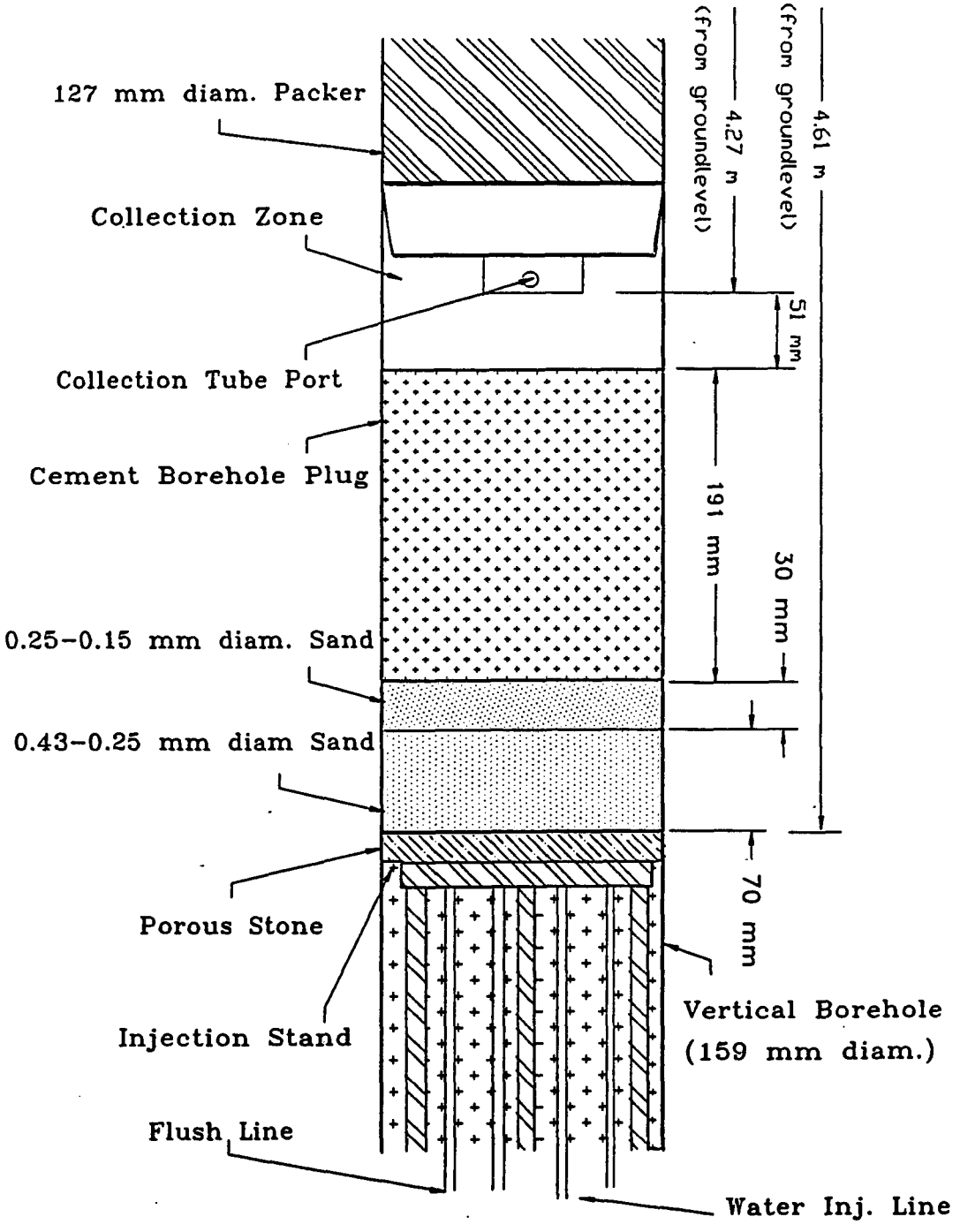

Figure 5.5 Schematic of cement plug installed at site C.

for 102 days for the first trial, 54 days for the second trial and 162 days for the third trial. Water flow in this steady-state test can be visualized by referring to Figure 2.4 and Table 2.1. The constant head test is the easiest and usually most reliable of the hydraulic tests. In addition, it allows saturation of the plug and surrounding test zone permitting transient tests to be performed after the steady-state test. Once steady out flow is collected from the top of the plug, the test is terminated or modified.

5.5.1 Trial 1

Figure 5.6a shows the injection flow rate, Q_{in} as a function of time. The flow rate is calculated using a moving average over a 24 h span interval. From the beginning of the test to time 850 h the flow rate is erratic, partially due to a faulty wiring of a sensor. For 2.5 days data was not recorded while the problem was corrected. Thereafter, the sensor reported data more reliably. A best fit line of the data from 950-1450 h shows that the injection flow rate is relatively steady. The flow rate calculated from the linear best fit is 0.0643 cc/h. Figure 5.6b shows the cumulative change of the fluid volume injected beneath the plug as a function of time. Erratic sensor readings are recognized as variations in the cumulative volume (y-axis) from 250 - 850 hours. The cumulative injected volume is calculated starting at 250

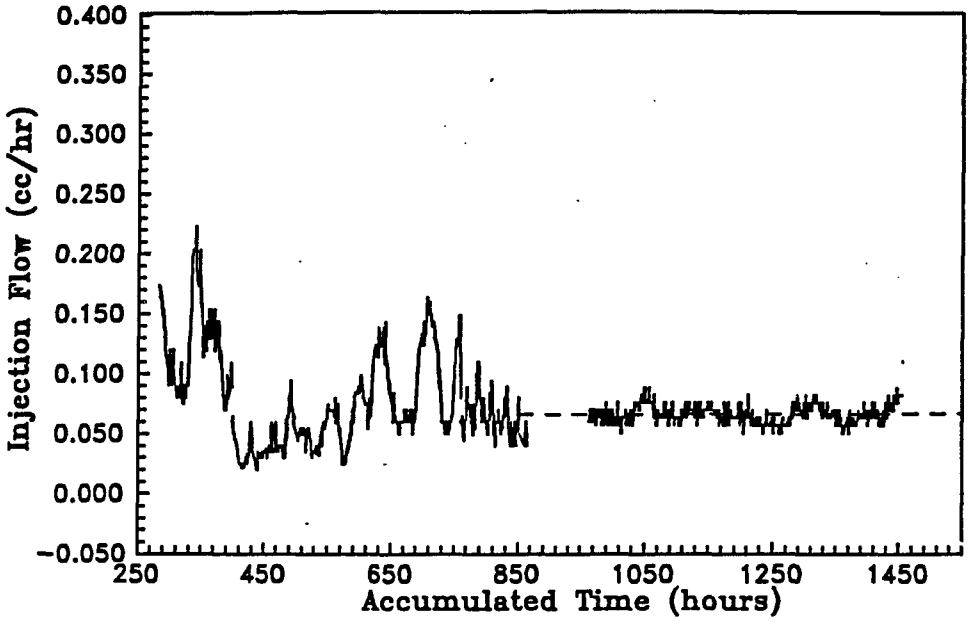

Figure 5.6 a) Injection flow rate Q_i as a function of time for the first steady-state test trial.

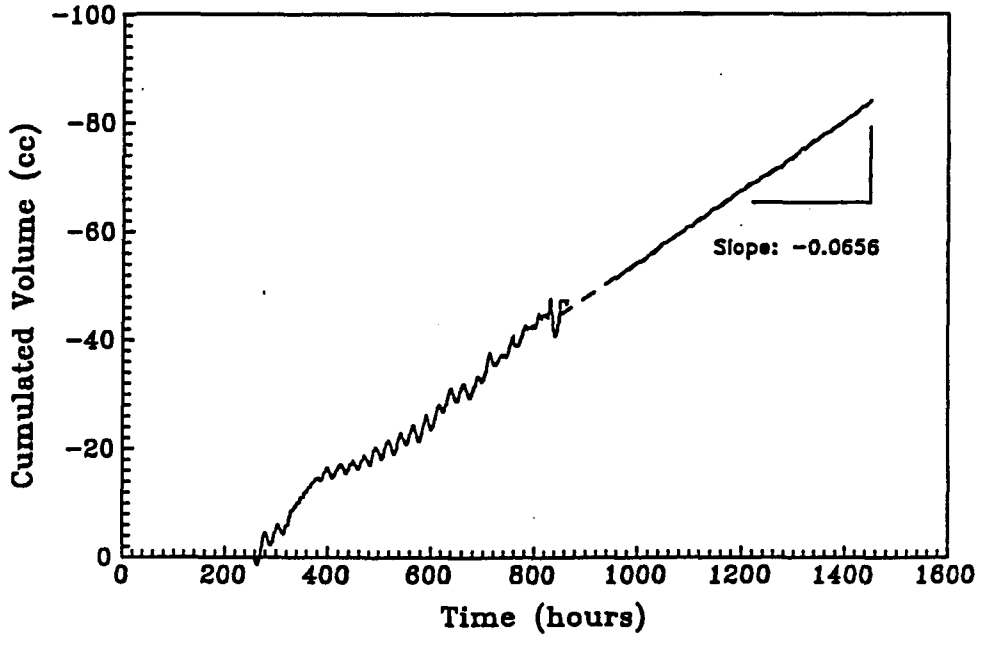

b) Cumulative change of fluid volume injected beneath the borehole plug as a function of time.

hours after the steady state test was initiated. This corresponds to the collection data described later in this section. The values are negative because the injected water flows from the pump into the injection zone. This sign convention corresponds to the collection flow values. A linear best fit of the cumulative injected volume taken from a period between 950 to 1450 hours indicates that the injection flow rate is steady (correlation coefficient is 0.94). The slope of this line represents the average injected flow rate of 0.0656 cc/h. This value is nearly equal to the injection flow value derived from Figure 5.6a. The hydraulic conductivity of the rock around the injection zone based on the dimensions given in Figure 5.5 is $k = 2.10 \times 10^{-11}$ cm/s assuming radial flow, and 5.4×10^{-11} cm/s assuming ellipsoidal and prolate flow.

Figure 5.7a shows the collection flow rate, Q_c as a function of time. The flow rate values are calculated using a moving average of the flow values over a 24 hr. span interval. Faulty wiring allowed only intermittent recording of collection data over the period of 0-280 hours. Analog readings (measured from the scale on the tube) of the collection tube during this period showed water being collected at an average rate of -0.012 cc/h. Electronic readings of the sensors are made every 40 minutes. From 280 to 600 hours, the data indicates that water flows into the collection zone. Such data is recorded as negative flow values. From approximately 600 to 1150 hours the flow reverses

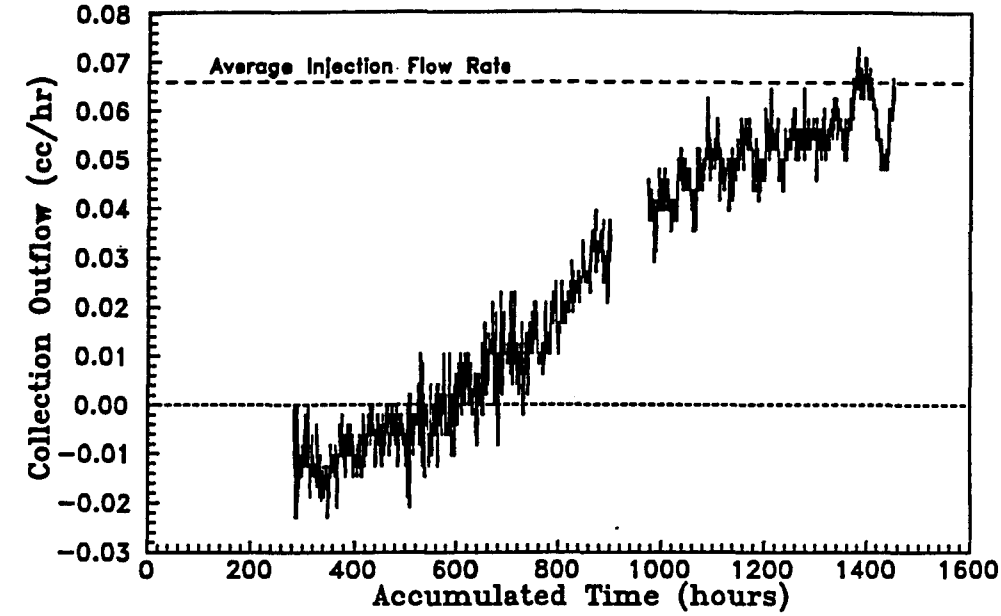

Figure 5.7 a) Collection outflow rate, Q_C, as a function of time for the first steady-state injection trial.

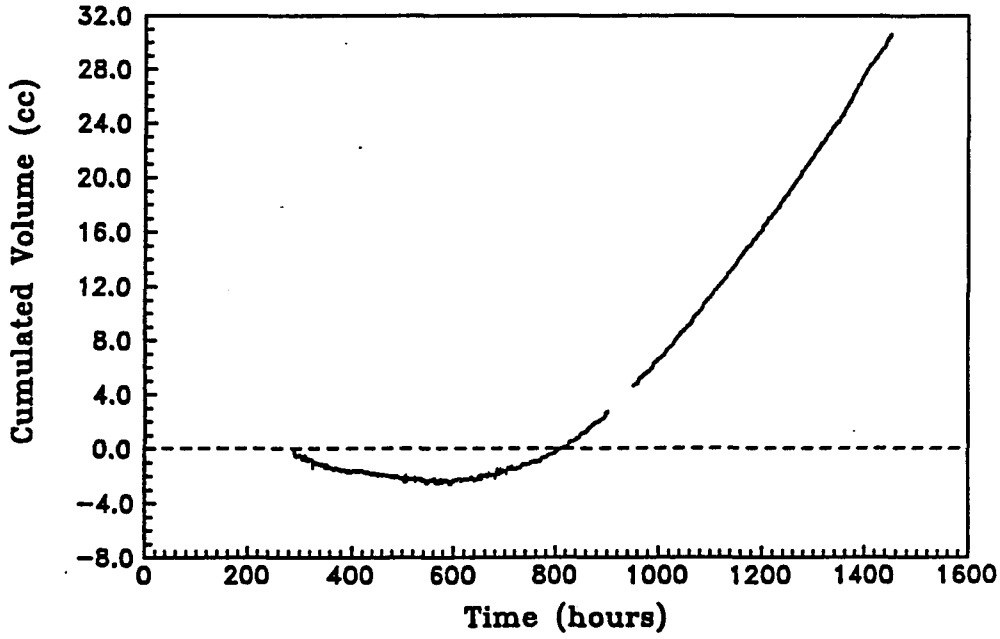

b) Cumulative change in collection fluid volume.

direction and is recorded as positive (out of the collection zone). The flow rate steadily increases during this time. At approximately 1150 hours the flow rate shows signs of equilibrating to an average outflow rate of 0.0521 cc/h. This flow rate is obtained from the slope of the cumulative volume in the collection zone between the hours 1200 and 1450. Figure 5.7b gives the cumulative fluid volume in the collection zone as a function of time. The cumulative volume is calculated beginning at 280 hours, not at time 0 hour, because of the faulty wiring of the sensor during the earlier measurement period. The flow rate of 0.0521 cc/hr corresponds to a hydraulic conductivity of the cement plug of 6.08×10^{-10} cm/s. The calculation assumes that the flow is one dimensional, that Darcy's law is valid and that the rock is an impermeable boundary. This assumption overestimates the permeability of the cement plug. To determine the extent of this overestimation, the permeability of the host rock must be known. This can be determined by injection from the top of the plug and collecting outflow from beneath the plug. Through injection from the top, injection interval lengths can be incrementally increased. The resulting change in fluid flow would be due to the increasing exposure of the rock mass. From this analysis, the permeability of the surrounding rock mass could be determined and compared to the permeability of the plug.

Figure 5.8 shows the injection and collection flow rates together

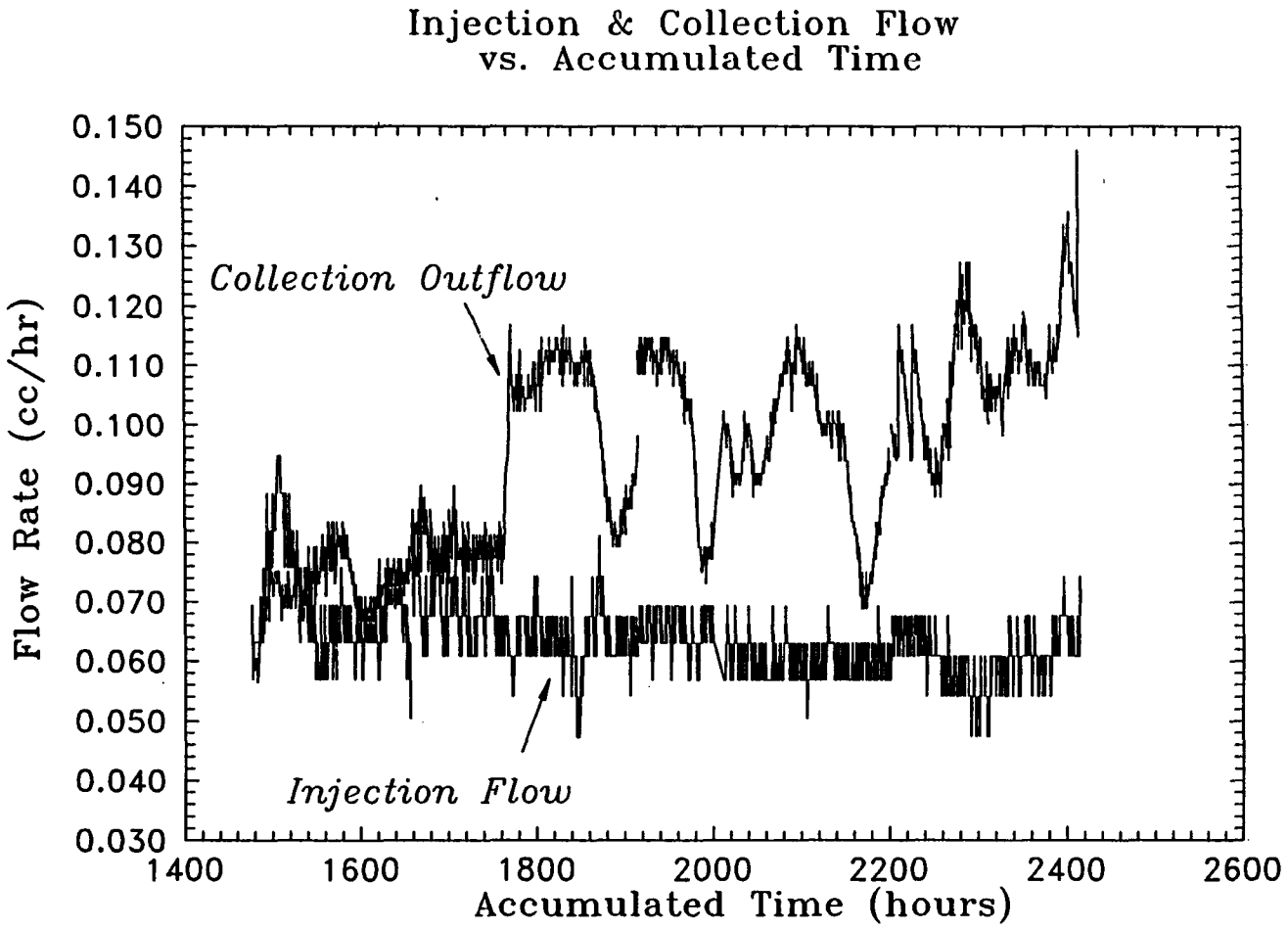

Figure 5.8 Injection & collection flow rates. Collection flow rate, Q_C, overtakes Qi at approximately 1600 hours after the start of the test.

as a function of time from 1450 through 2450 hours after plug emplacement. The injection flow rate, Q_i, is relatively stable over the tested period. The collection outflow rate, Q_c, increases with respect to time and overtakes the injection flow rate at approximately 1600 hours. Because $Q_c > Q_i$, this violates the continuity of the steady state test system described in Chapter 2. Possible causes of $Q_c > Q_i$ are described in Table 5.1.

Table 5.1 Potential Causes for Excessive Outflow

1) Pneumatic packer leaking N_2 into the collection zone, which in turn drives the collection outflow.
2) Leaking injection pump, causing abnormally low injection flow rates.
3) Electrical abnormalities of the electronic sensors (LVDT, pressure transducers).
4) Higher than normal formation head, H_{fc}, due to water seepage from the ground surface or groundwater infiltration.

All the electronic sensors have been checked for abnormalities and recalibrated. None of the sensors have shown any signs of deteriorating signals. The recalibration of the sensors indicates only a less than 2% deviation from the original calibration made 4 months previously. Groundwater levels at the site are well below the test zone (Chap. 3) and are not a contributing factor to H_{fc}. In addition, the test zone is approximately 5 meters below ground level and is placed in intact rock, making water infiltration from runoff or groundwater seepage an unlikely contributor to H_{fc}. The injection pump used to maintain H_i and for

measuring Q_i has been tested at half of its capacity (1.72 MPa, 6 x normal injection pressure) for 24 hours. The pump has been found to be without leaks, and exhibited negligible stick slip. The packer has been tested by shutting out its N_2 source and monitoring for any pressure drops. This test has been conducted for 4 days with a drop in packer pressure of 24 kPa, a drop of 3%. A second test has been made by reducing H_i beneath the cement plug to atmospheric pressure. The collection outflow and packer inflation pressure have been monitored for 150 hours (6 1/4 days). The results of this test, given in Figure 5.9, indicate that an inverse relationship between packer pressure and collection outlfow rates may exist. Statistical analysis does not indicate this however.

Collection outflow is most likely being driven by gas leakage from the packer. At the termination of this test, the submerged packer was deflated. A considerable amount of gas could be seen escaping from the collection zone, indicating leakage of N_2 from the pneumatic packer. In addition, some days later, after removal of the packer from the vertical hole at site C, a gas pocket developed between the outer and inner layers of the rubber gland. Problems of packer leakage and its effects on flow testing are discussed in Greer and Daemen (1991). For long term testing, N_2 leakage from the packer is judged unacceptable. For short flow term tests (2-3 weeks), and flow tests in more permeable media, the amount of leakage is acceptable due to its small quantity and delayed

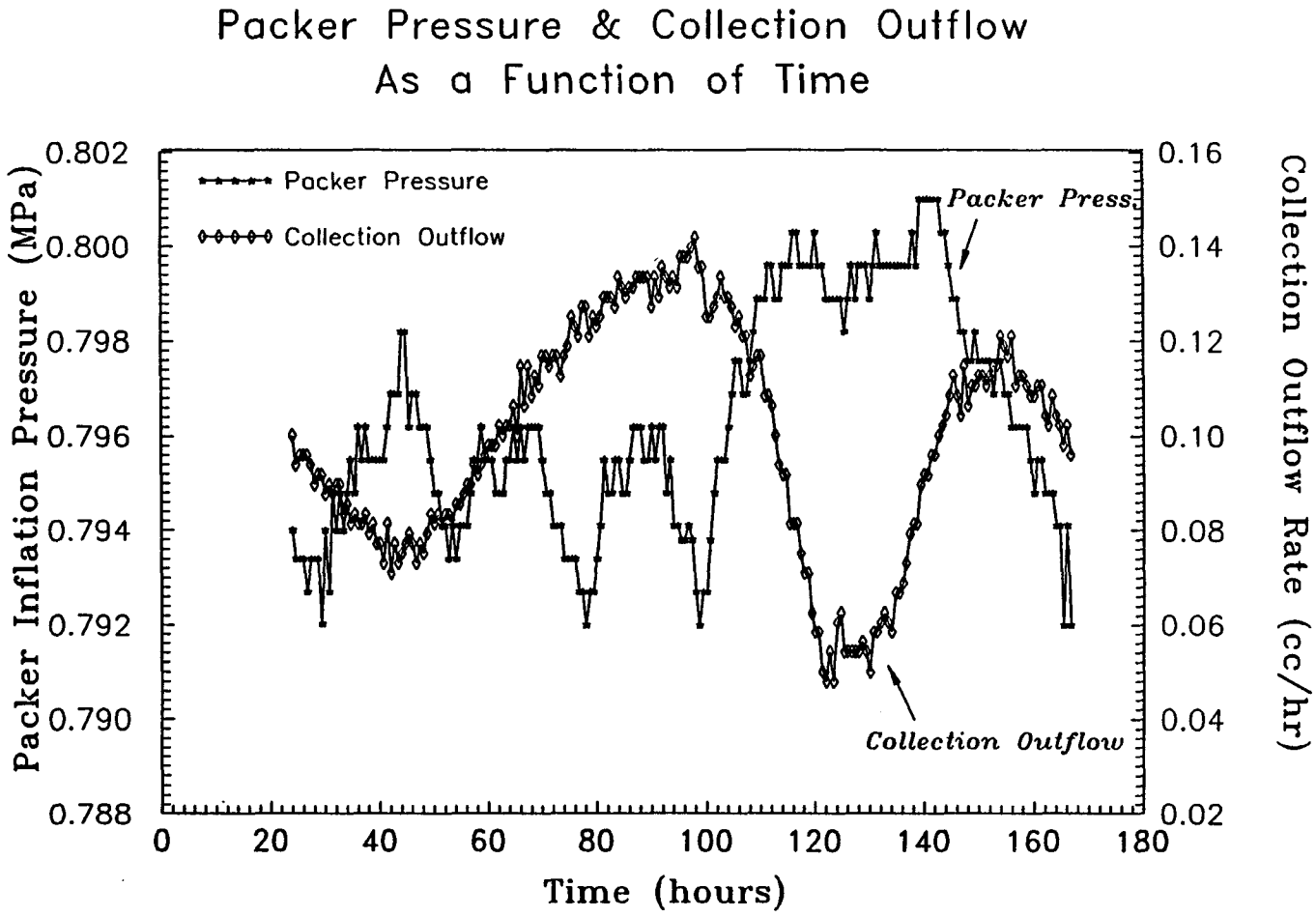

Figure 5.9 Packer and collection outflow. Injection pressure and flow = 0. Collection outflow entirely driven by packer inflation media leakage.

effect.

5.5.2 Trial 2

On January 9, 1990, the steady-state flow test at site C was restarted with a water injection pressure beneath the plug of 0.28 MPa. The purpose of this test was to reevaluate the earlier test results of trial 1 and begin the resaturating process of the test zone and plug.

A new packer, identical in design to the previous one was installed in the vertical hole of site C. This packer was partially filled with water, with the remaining inflation medium being N_2. It was hoped that the water would have a limited tendency to migrate through the natural rubber gland and escape into the collection zone.

Figure 5.10 shows the collection outflow rate and injection inflow rate as a function of time. After approximately 1060 hours, collection outflow again overtook the injection inflow rate due to gas diffusing through the gland of the new packer. Figure 5.11 gives the cumulative fluid volume in the collection zone as a function of time. Based upon the relatively constant collection flow between the hours 940 and 1080, the slope of the curve during the same hours in Figure 5.11 (a) indicates an average collection flow of 0.054 cc/h. This flow rate corresponds to a hydraulic conductivity of the plug of 6.3×10^{-10} cm/s based upon the assumptions that the flow is one dimensional through the plug,

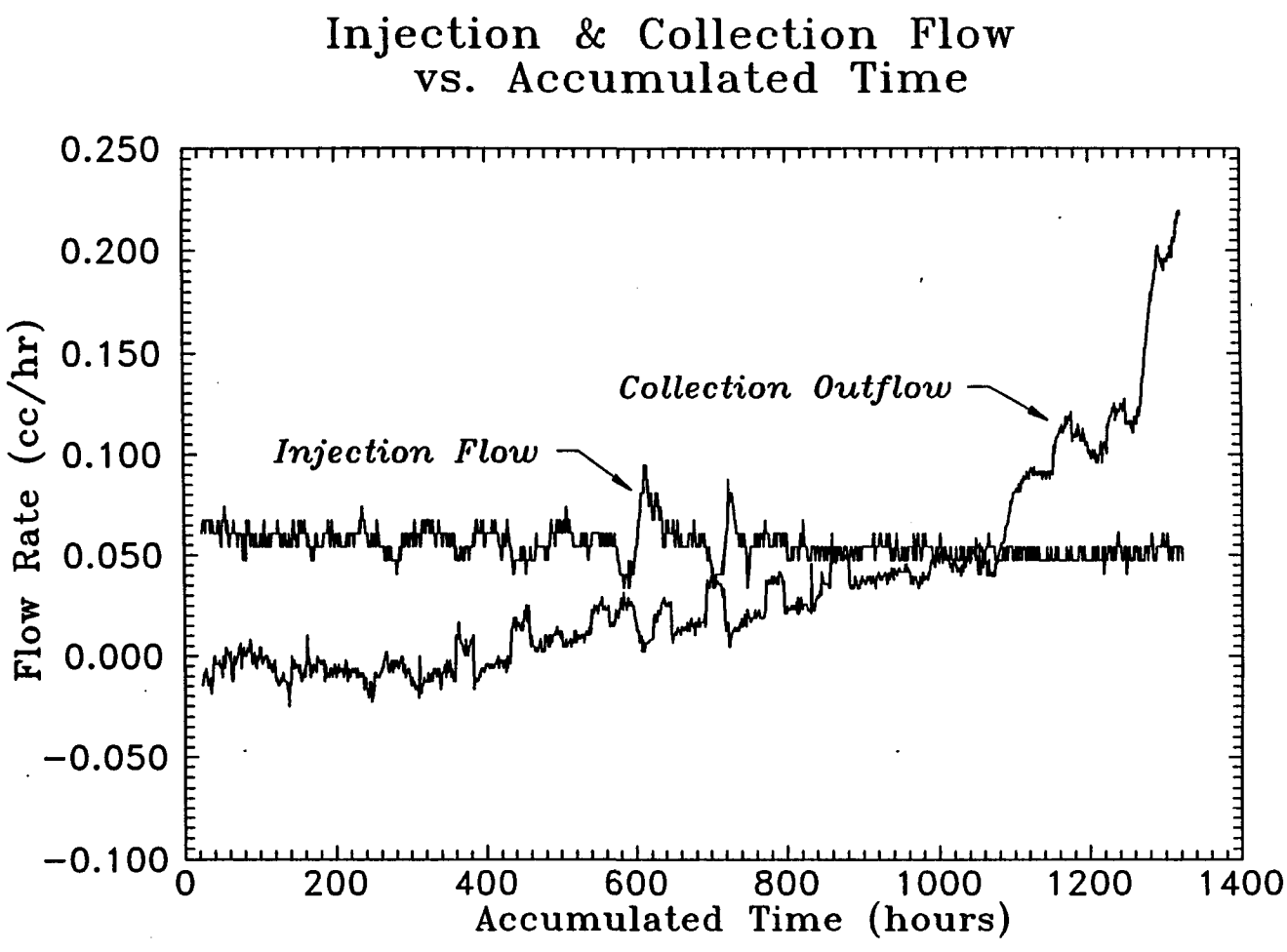

Figure 5.10 Injection and collection flow rates as a function of time for trial 2.

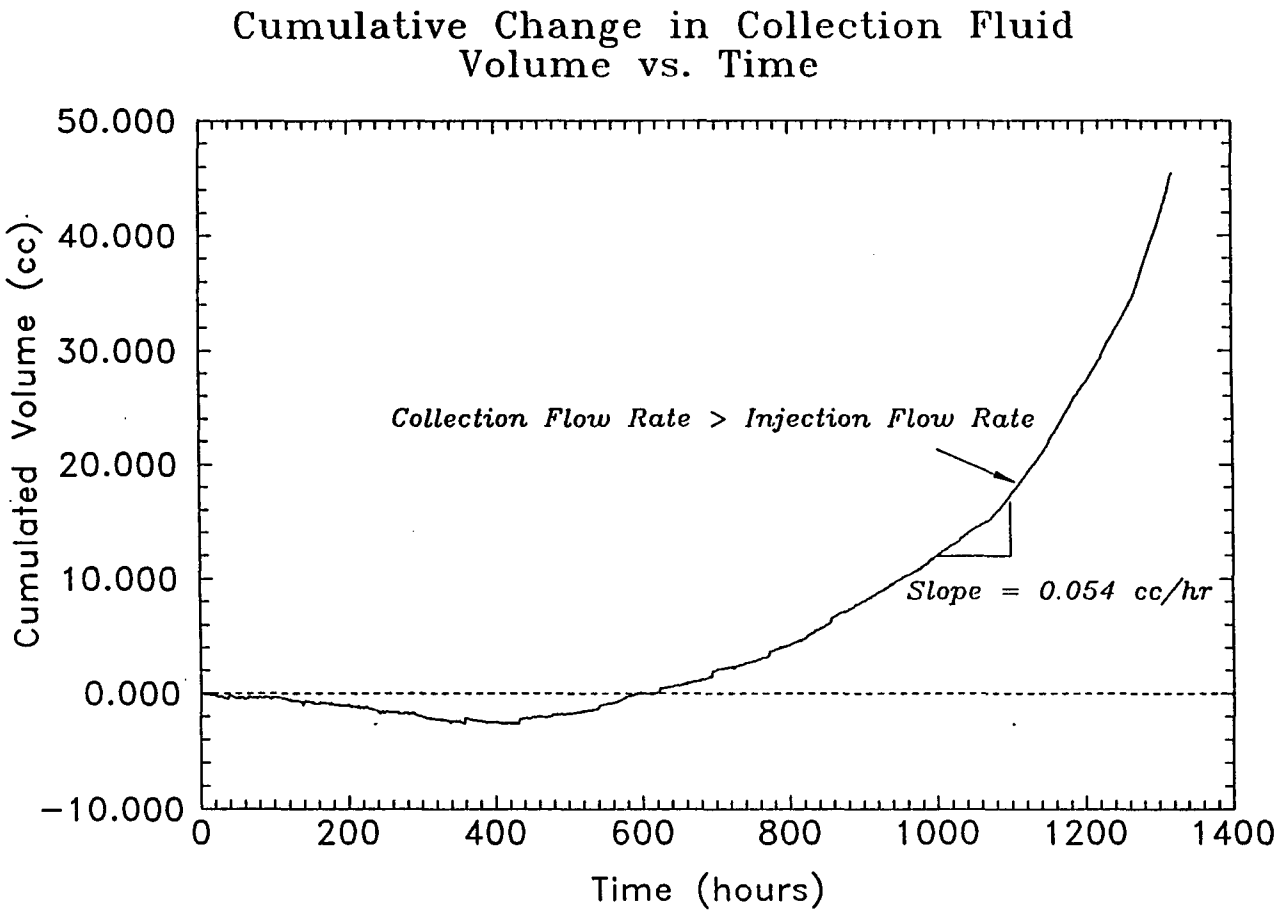

Figure 5.11 Cumulative change in fluid volumes, trial 2.
a) Cumulative collection, avg. flow rate 0.054 cc/hr.

that Darcy's law is valid and that the surrounding rock is an impermeable boundary.

Figure 5.12 shows the cumulative change of the fluid volume injected beneath the borehole plug as a function of time. The values are negative because the injected water flows from the pump into the injection zone. This sign convention corresponds to the collection flow values, which are positive. The slope of the curve in Figure 5.12 (b) between the hours of 940 and 1080 indicates an average injected flow rate of 0.0608 cc/hr. The hydraulic conductivity of rock around the injection zone is $k = 2.0 \times 10^{-11}$ cm/s assuming radial flow, and is 5.2×10^{-11} cm/s assuming ellipsoidal and prolate flow.

5.5.3 Trial 3

On April 2, 1990, steady-state testing with injection beneath the plug was initiated for a third time. The purpose of this test was to more accurately verify the results of earlier steady-state tests. Problems involving the pneumatic packer, used to isolate the collection zone, leaking N_2 into the collection zone made the results of earlier tests difficult to evaluate. In the third trial, the packer was inflated for a much shorter period of time to avoid the effects of gas leakage from the packer. The effects of packer leakage on seal permeability testing are discussed in Greer and Daemen (1991).

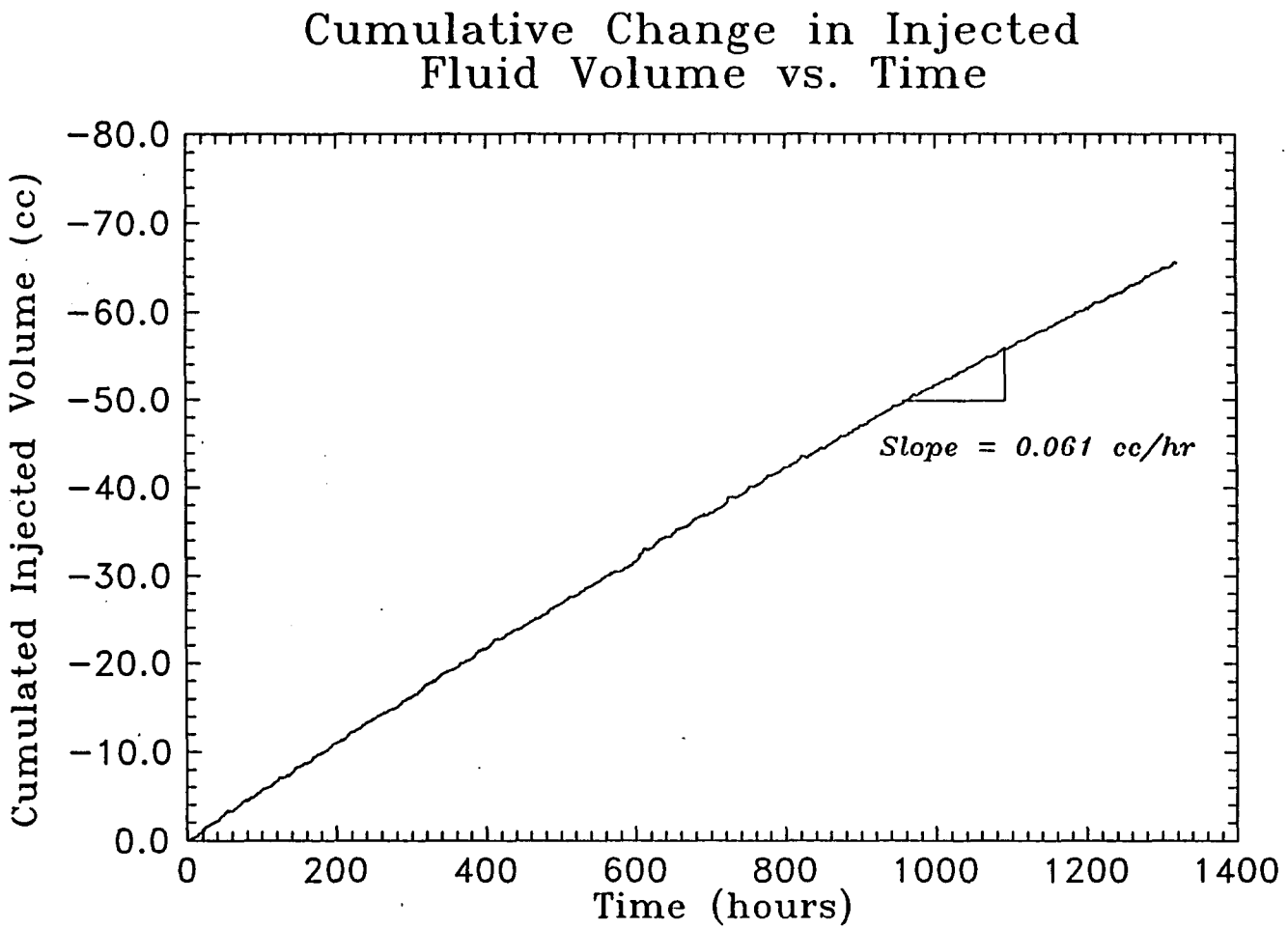

Figure 5.12 Cumulative change in fluid volumes, trial 2.
b) Cumulative injection, avg. flow rate 0.061 cc/hr.

After a period of steady-state injection behind the cement plug had been performed continuously for nearly 8 months, a pneumatic packer was set in position just above the plug and inflated, developing the closed off collection zone. Monitoring of the outflow, Q_o has been performed for a period of 14 days in the third trial with an injection pressure beneath the plug of 0.28 MPa. Figure 5.13 shows the injection and collection flow rates as a function of time for the third trial. With the packer inflated for a relatively short period of time (2-3 weeks) gas leakage from the packer was not evident.

The average measured injection inflow, Q_i, for the test period is 0.0587 cc/h. This flow rate corresponds to a hydraulic conductivity of the rock around the injection zone of $k = 1.8 \times 10^{-11}$ cm/s assuming radial flow and $k = 5.0 \times 10^{-11}$ cm/s assuming ellipsoidal and prolate flow. The average collection outflow, Q_o for the test period is 0.0521 cc/h. This flow rate corresponds to a hydraulic conductivity of the cement plug of 5.9×10^{-10} cm/s.

5.5.4 Summary of Steady-State Injection Beneath the Plug

Table 5.2 summarizes the three steady-state injection tests of the cement plug at site C. All the hydraulic conductivity values calculated for the plug and the injection zone are very alike, well within the same order of magnitude. The flow values indicate, however, a reduction in

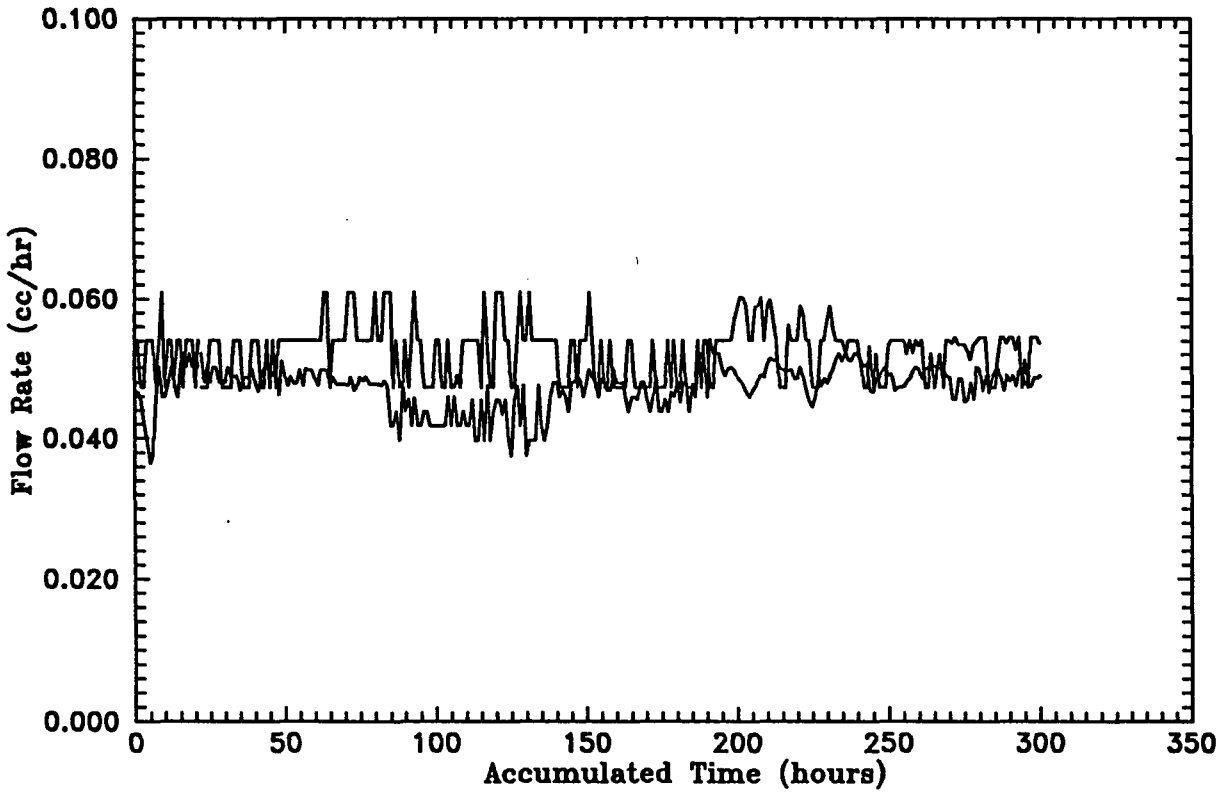

Figure 5.13 Injection and collection flow rates as a function of time for the third trial.
(Bottom is collection, top injection.)
Collection is approximately 15% < injection.

the permeability of the injection zone and of the plug. The injection pressure for trial two is slightly greater than that of trial one and the measured flow rates for both injection and collection are correspondingly higher. The third trial has the same injection pressure as trial two, yet the injection and collection flow rates have dropped, most significantly the injection flow rate. This would indicate that the bottom seal and the surrounding rock mass have not fully saturated. Likewise, the collection outflow rate for the plug has also reduced between trials two and three. This reduction in outflow from the plug may also indicate that the plug and surrounding rock mass have not yet fully saturated. However, the variation in collection outflow from the plug may be due in part to propagation of error caused by physical and electronic uncertainties. The maximum uncertainty in the collection outflow rate, Q_o, has been determined to be ±0.02 cc/h. This uncertainty may account for the variations between trials 1 - 3. The maximum uncertainty in injection outflow, Q_i, has been determined to be ± 0.002 cc/h, one order of magnitude less than that of the collection flow rate measurement. The variations in the injection flow rates described in Table 5.2 are far greater than the uncertainty. Although the propagation of error due to physical and electronic uncertainties may account for a significant amount of variation in the measured flow rates, the trends indicate that the rock and the cement, (both the plug and the bottom seal), may not be fully saturated.

Table 5.2 Summary of Trials 1-3 of Steady-State Injection Tests

Trial #	Avg. H_i (m)	Avg. Q_i cc/h	Avg. Q_c cc/h	K_i radial flow (cm/s) x 10^{-11}	K_i ellipsoidal prolate flow (cm/s) x 10^{-11}	K_p (cm/s) x 10^{-10}	Test Period (Days)
1	26	0.0643	0.0521	2.1	5.4	5.9	102
2	28.6	0.0608	0.0540	2.0	5.2	6.3	54
3	28.6	0.0587	0.0521	1.8	5.0	5.9	162

5.6 Head Buildup Test (recovery variation)

A head-buildup test, first recovery variation, was performed on the seal at site C during the period June 24, 1990 to July 31, 1990. The test was performed after a long period of constant head testing with injection from below the seal.

5.6.1 Results of Test

On June 24, 1990, a head buildup test had been started by shutting out the collection zone above the borehole plug, and monitoring the pressure buildup with a submersible pressure transducer mounted inside the mandrel of the pneumatic packer. Figure 2.6 gives a general schematic of the test. Appendix J describes the procedures for the head buildup test and the measurement of the storage coefficient S_c. Data was recorded on an hourly basis until July 31, 1990 when the site was

vandalized. Enough data was collected however for proper curve matching. Figure 5.14 shows the build-up of pressure head, H_c, in the collection reservoir. Upon deflation of the pneumatic packer, no gas was seen escaping from the collection zone, indicating that the packer did not leak N_2 into the collection reservoir.

5.6.2 Analysis

The experimental data (Figure 5.14) was found to closely fit the dimensionless curve for $\xi = 0.1$ (Figure 2.7). Table 5.3 describes the calculations made for the head build-up test. The specific storage and hydraulic conductivity value obtained in the this test are upper limit values since inflow from the surrounding formation to the collection zone has been neglected in the analysis.

The resulting hydraulic conductivity obtained from the head build-up test is slightly lower than that measure through the three consecutive steady-state tests. These hydraulic conductivity values are upper limit values for the plug since inflow from the surrounding formation to the collection zone has been neglected in the 1-D analysis.

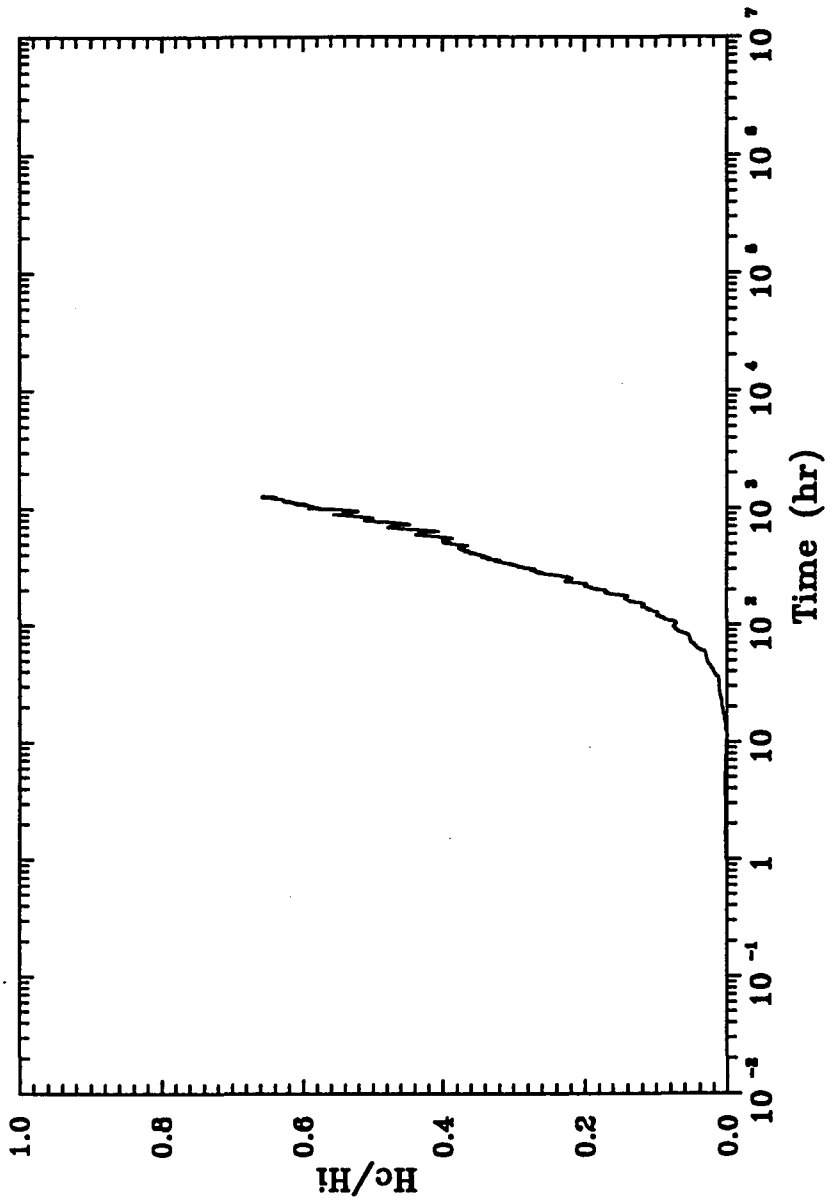

Figure 5.14 Results of head-buildup test, site C.

Table 5.3 Hydraulic Conductivity and Specific Storage for Site C Based on Results of Head Build-up Test

Measured Quantity	Value
ξ	0.1
$\alpha\xi^2$	10^{-2}
α	1
A (Area)	197.9 cm^2
L (Plug Length)	19.1 cm
S_C	0.0102 cm^2
S_S	2.6981×10^{-7}
t, at match point	102 hours
Hydraulic Conductivity, K	2.73×10^{-10} cm/s

5.7 Transient Constant Head Test

A transient constant-head test was performed on the neat cement plug at site C during October 1990 after steady-state injection beneath the plug for 10 months. The transient constant head test is described in Chapter 2, Section 2.3.3. This test is similar to tests described by Greer and Daemen (1991). A generalized schematic of the test geometry is shown in Figure 2.8. Results of the transient flow test yield the hydraulic diffusivity, (K_s/S_{ss}), of the seal. With K_s, seal hydraulic conductivity, determined from steady-state tests, S_{ss}, specific storage of the seal, can be obtained from the hydraulic diffusivity.

5.7.1 Results of the Test

The transient constant head test was begun by reducing the injection pressure beneath the borehole plug at site C from 0.27 MPa to 0.19 MPa. Injection and collection flow rates were monitored on 10-minute intervals for 5 days. Collection outflow reduced from 0.0521 cc/h to 0.0365 cc/h. The test results are plotted in Figure 5.14 as a semilog plot of the collection outflow. A smooth transition was difficult to measure due to the accuracy of the collection flow measuring system and the relativily minor change in injection pressure.

5.7.2 Analysis

The test results plotted in Figure 5.14 are superimposed upon the type curve in Figure 2.9. This yields a match point of:

$$t_d^* = 1.12, \quad t=2.6 \text{ hours}$$

where t_d^* is a dimensionless expression for time in terms of the hydraulic properties and the length of the seal (L_s). The hydraulic conductivity determined from the reduced outflow, Q_w is 4.7 x 10^{-10} cm/s. Subsituting K_s = 4.7 x 10^{-10} cm/s, the length of the seal, (L_s = 19.1 cm), and the determined match points into Eq. 2.34, yields a specific storage of the seal of S_{ss} = 1.1 x 10^{-8} cm^{-1}.

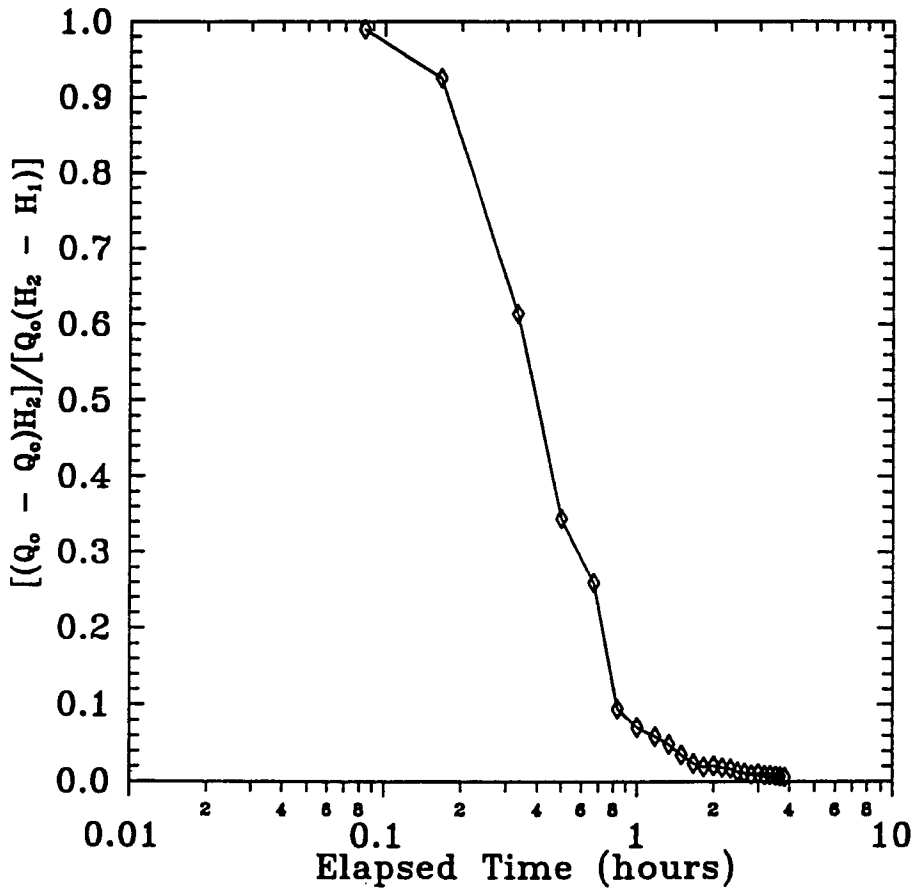

Figure 5.15 Results of transient-constant head test.

The resulting hydraulic conductivity measured from the transient constant head test compares closely to values obtained from the head buildup test and the steady-state tests. Like the previous tests, the transient constant head test is a one-dimensional test. The values for the hydraulic conductivity of the plug and the specific storage of the seal are considered only upper limit values since inflow from the surrounding formation to the collection zone has been neglected in the analysis.

CHAPTER SIX

FIELD TESTING OF CRUSHED TUFF/BENTONITE PLUG

6.1 Introduction

This chapter presents the hydraulic evaluation of a crushed tuff/bentonite mixture borehole plug. Initial hydraulic evaluation of the site through packer tests, described in Chapter 3, Sec. 3.9.3, indicated a fractured rock mass throughout the test borehole length. To properly evaluate the seal, the permeability of the rock mass had to be reduced. A series of pressurized grouting applications, described in Appendix B, were completed to reduce the overall permeability of the rock mass. After the grouting applications were performed, a suitable test interval was selected for installation of a plug. The portion of the borehole below the test interval had to be sealed and equipment permanently installed for flow tests. After the installation of the bottom seal and equipment, single packer tests were performed to determine the permeability of the bottom seal before installation of a test plug.

Once the testing of the bottom borehole seal had been completed, a crushed tuff/bentonite mixture plug was installed in the vertical borehole. The configuration of the test system, similar to site C, (Chap. 5), allows access to both top and bottom of the seal without penetrating it.

6.2 Preparation of Site A for Crushed Tuff/Bentonite Plug Tests

Based upon packer tests, (Chapter 3, Figure 3.12), and core and videologs, the vertical borehole of site A contains fractures throughout its length. To properly evaluate the sealing characteristics of a borehole plug, it is desirable to install it in a rock mass having a lower permeability than the plug itself. This allows both inflow and outflow rates to be accurately monitored, and allows the use of the one-dimensional flow models described in Chapter 2. To reduce the overall permeability of the vertical hole, a series of pressurized grout applications is performed. The procedures and the results are described in Appendix B. Overall the pressurized grouting applications have reduced the permeability of the hole by three orders of magnitude. The permeability of the vertical test hole after grouting approaches the permeability of the cement grout injected into the fractures, (10^{-9} cm/s).

6.2.1 Instrumentation Configuration

Figure 6.1 shows a general schematic of the vertical and intersecting boreholes of site A with the installed instrumentation at the bottom of the vertical hole. A stainless steel injection stand identical to one installed at site C, (Chapter 5, Figure 5.1), is cemented in place 6.2 m below ground level in the vertical hole of site A. Two 4.8 mm

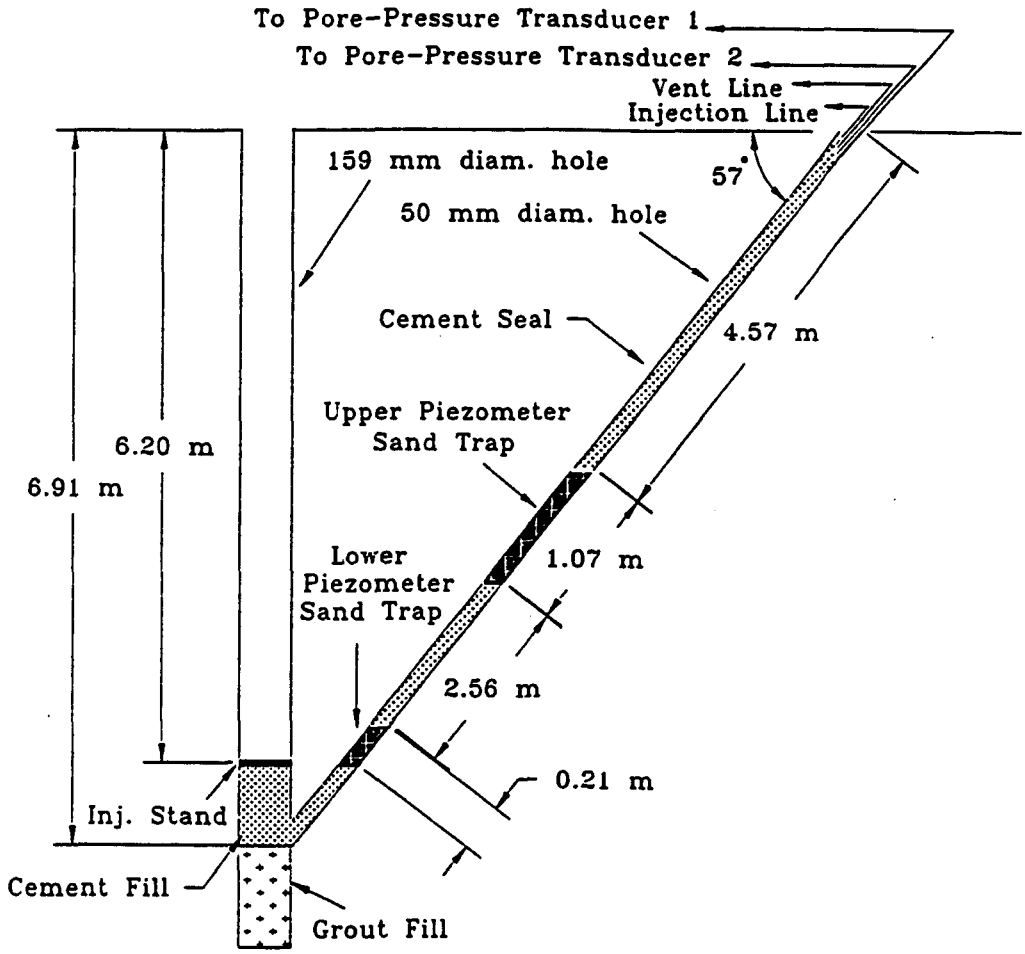

Figure 6.1 General schematic of the vertical and intersecting inclined borehole of site A.

(3/16 inch) nylon lines connected to the injection stand allow water injection, venting of trapped air and circulation of fluids beneath the installed plug. Type II portland cement with a 1:1 water/cement ratio (by weight) was used to seal the stand in place.

Two piezometers have been installed in the inclined hole. The lower piezometer (Figure 6.1), is used to monitor the buildup of injection head at a location approximately 0.29 m horizontally from the center of the injection zone. The second piezometer is located 4.28 m vertically below groundlevel, 1.92 m vertically above the center of the injection zone. This piezometer is used to measure the influence of surface water seepage. Both piezometers consist of a 140 micron stainless steel filter tip attached to the end of a 4.8 mm nylon line. The filter tip prevents the clogging of the nylon line. The line is connected to an Omega PX-236, 0-0.21 MPa (0-30 psig) pressure transducer located just below ground surface, (Figure 6.2). Cement seals separate both piezometers and the upper piezometer from the ground surface through the inclined hole. The cement consists of a Self-Stress II expansive formula with the expansive agent reduced by approximately one half to reduce the risk of opening new or existing fractures and of increasing the permeability of the inclined hole.

On the ground surface, an instrument shelter has been constructed to house lifting equipment for the vertical hole, data logger, injection/collection panel and controlling equipment for a pneumatic packer, (Figure 6.3). The shelter, unlike the one at site C, does not cover the

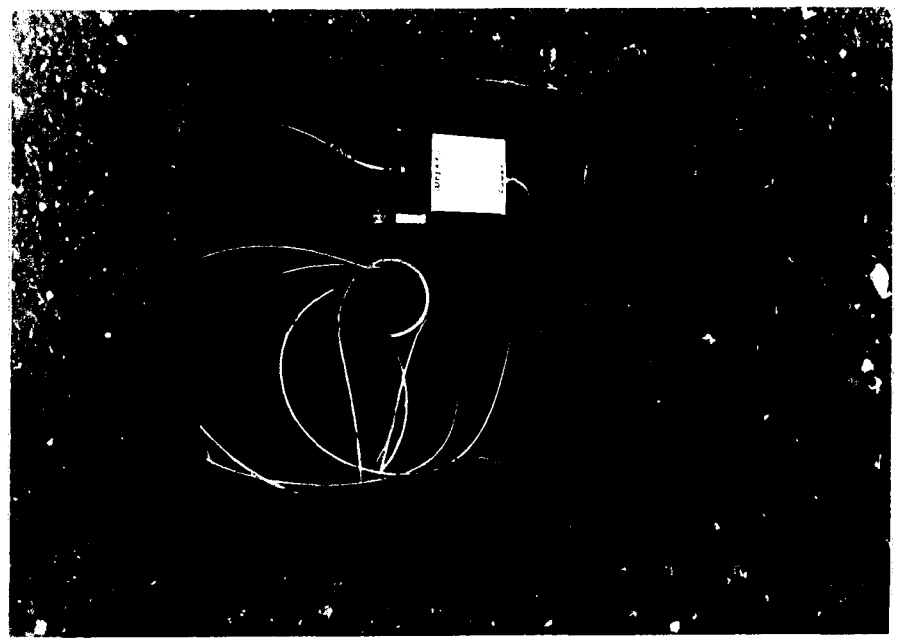

Figure 6.2 Inclined hole access with two pressure transducers to measure piezometric head in the inclined borehole.

Figure 6.3 Instrumentation shelter for site A

vertical or inclined holes. All electrical and gas/water lines are buried beneath the shelter and connect to the vertical and inclined holes through covered trenches.

6.2.2 Hydraulic Characterization of Rock and Bottom Seal

Steady-state flow testing of the grouted rock mass and bottom borehole seal after the installation of the injection stand hydraulically characterizes the bottom borehole seal. Chapter 2, Sec. 2.2.2 describes the arrangement for this characterization method using a single pneumatic packer. This procedure will allow the amount of injected flow beneath the plug to be corrected for flow into the bottom cement seal and into the grouted rock mass. Figure 6.4 shows the results of two flow tests. The first test was performed with an injection interval length of 356 mm and an average applied head of 7.2 m. The average measured flow rate for the first test is Q_1 = 1.04 cc/h. The second test was performed with the packer raised 266 mm with an injection interval length of 622 mm and an average applied head of 7.2 m. The average measured flow rate for this test is Q_2 = 1.67 cc/h. Because the injection pressures are the same for both tests, the flow rate through the rock for the first test can be calculated from Eq. 2.4:

$$Q_R = \frac{(Q_2 - Q_1)}{\left(\frac{L_2}{L_1} - 1\right)} \qquad (2.4)$$

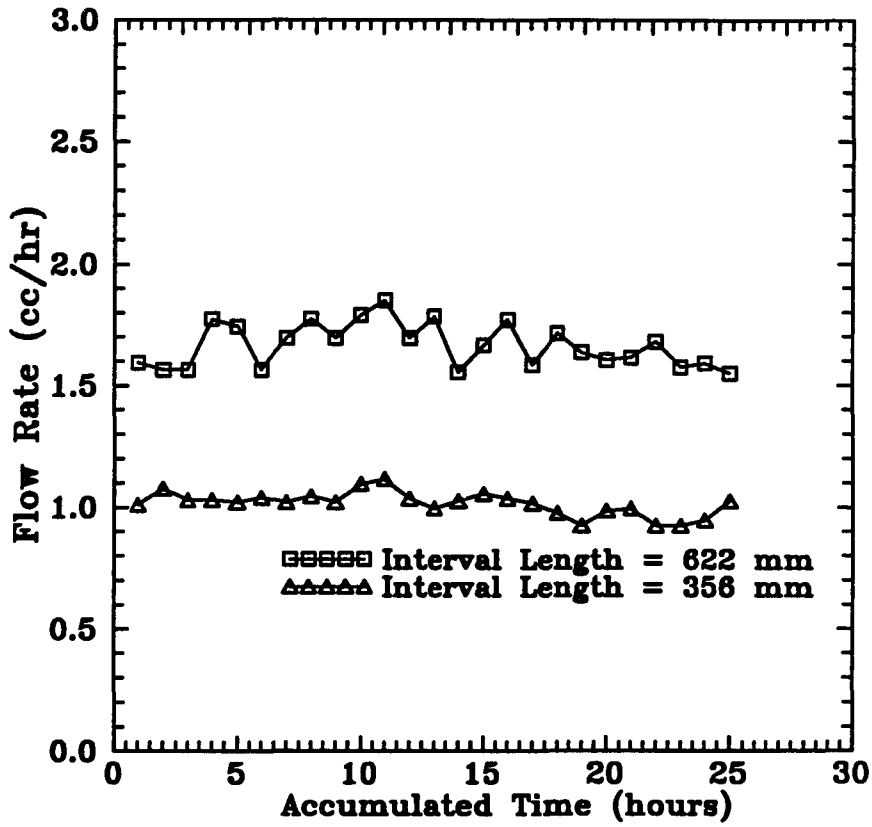

Figure 6.4 Results of injection flow tests to characterize both the host grouted rock mass, and bottom borehole seal.

where: Q_1, Q_2 = flow rate of tests 1 and 2 [L^3/T]
L_1, L_2 = length of injection zones of tests 1 and 2 [L]
Q_R = flow rate through the grouted rock mass for test 1 [L^3/T]

The flow rate through the bottom seal of the vertical hole for the first test can be obtained from Eq. 2.5:

$$Q_{BS} = Q_1 - Q_R \tag{2.5}$$

where: Q_{BS} = rate of longitudinal flow through the bottom seal

From the two flow tests, Q_R = 0.87 cc/h and Q_{BS} = 0.16 cc/h for an injection length of 356 mm with an injection head of 7.2 m. After installation of the borehole plug, these values will allow the flow into the rock and bottom seal to be separated from the measured injection flow rate beneath the seal. This will yield an estimate of the flow through the plug, and in turn will allow determination of the permeability of the seal assuming one-dimensional flow through the seal.

6.3 Installation of Crushed Tuff/Bentonite Plug

The crushed tuff/bentonite seal was installed at site A on November 22, 1990. Figure 6.5 shows a schematic of the installed seal in the vertical test hole. The plug was constructed of four layers, has a dry bulk density of 1.72 g/cm^3 and a length to diameter ratio of 1.49. The

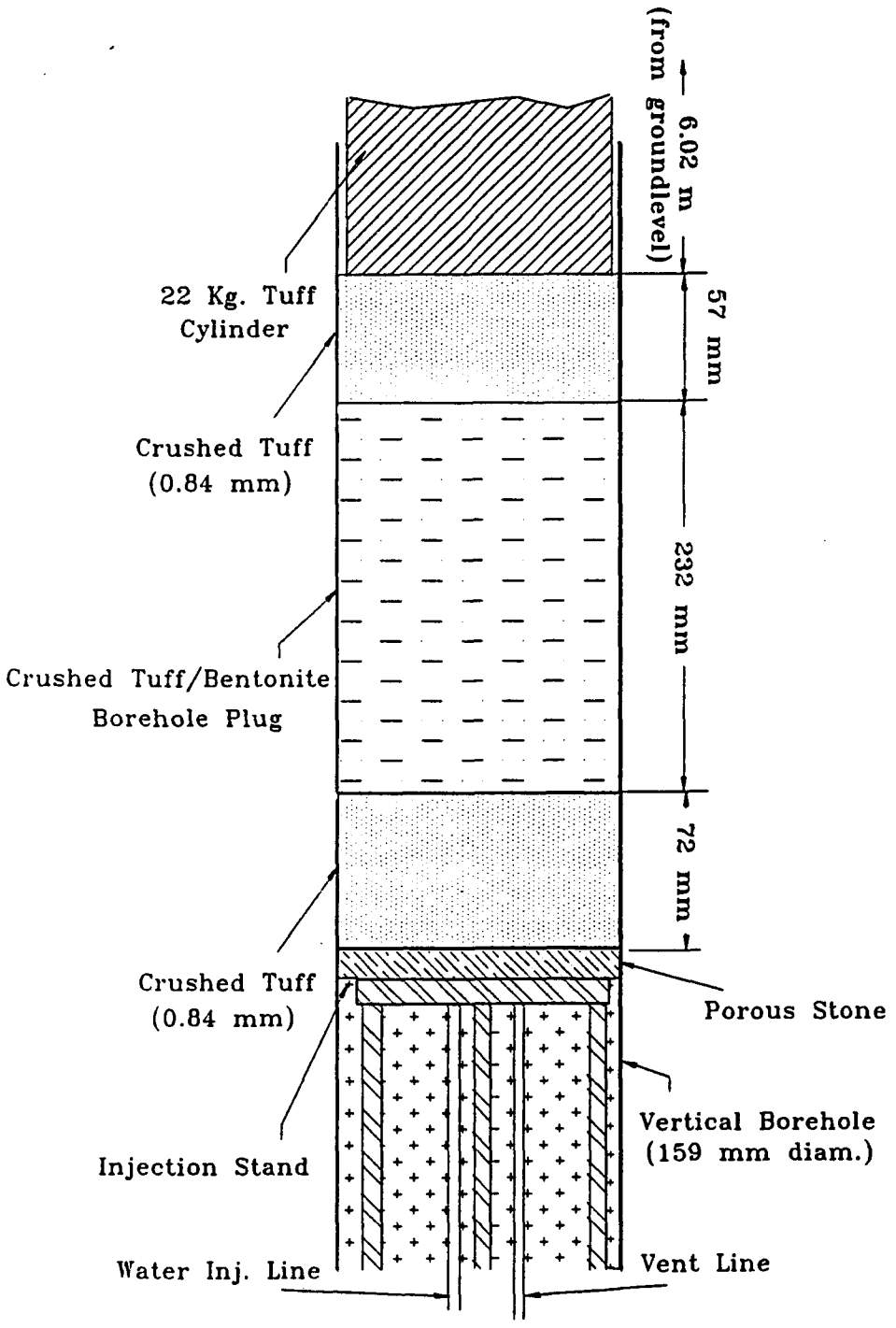

Figure 6.5 Schematic of the installed crushed tuff/bentonite plug in the vertical hole of site A.

seal consists of 35% C/S granular bentonite and 65% crushed tuff with a type A gradation. The materials and ratios of materials used for this plug are identical to the mixture plugs tested in the laboratory (Chapter 4). A 22 kg. tuff cylinder, 0.32 cm smaller in diameter than the borehole, is placed on top for confinement of the plug, with a pneumatic packer inflated and touching the top of the cylinder. As the seal absorbs water, the bentonite will tend to swell, reducing the overall bulk density of the installed seal. Confinement on top of the seal will reduce the swelling, and will aid in maintaining the physical integrity of the seal during flow tests. The packer will close the zone above the seal which can be used for monitoring injection or collection flow through the seal.

6.4 Flow Tests of Crushed Tuff/Bentonite Plug

A falling head injection flow test was performed on the crushed tuff/bentonite plug for a period of 89 days. Water was injected from below the plug with an average injection head of 6.4 m. Figure 6.6 shows the results of the test. The injected flow has stabilized to an value of 0.51 cc/h. Compensating for flow into the grouted rock mass surrounding the injection zone and through the bottom seal, the estimated flow into the seal is 0.18 cc/h. The equivalent hydraulic conductivity of the seal assuming that the estimated flow into the seal is one-dimensional is 2×10^{-9} cm/s. This value should be considered upper

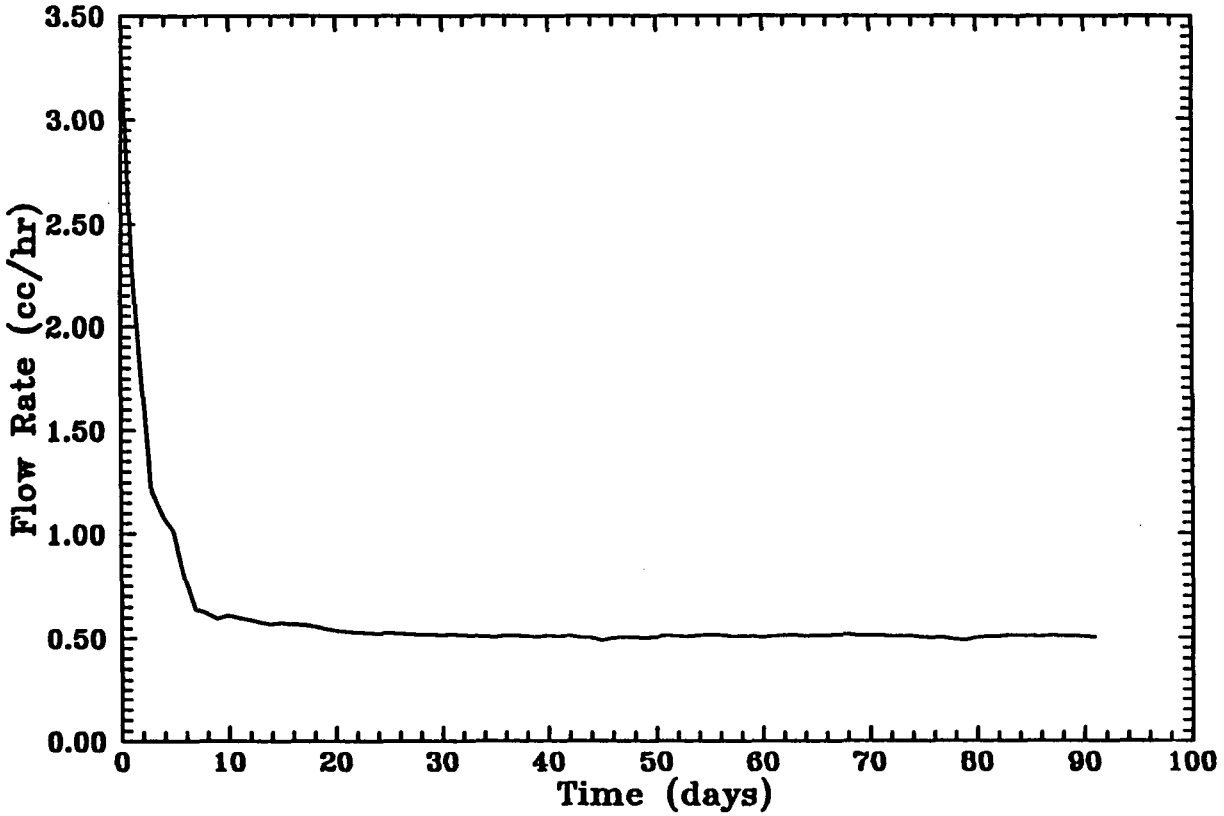

Figure 6.6 Results of the falling head flow test on the crushed tuff/bentonite plug of site A. Injection is from below the plug with an average head of 6.4 m.

limit due to the fact that flow takes place into the rock immediately adjacent to the plug. Outflow from the seal was not achieved due to the relatively long length of the collection zone, allowing flow into the surrounding grouted rock mass to dominate. The injection zone has a length of approximately 7.2 cm. The length of the collection zone is 99 cm. This is due to the configuration of the packer, the 22 kg tuff cylinder used for confinement and the sand layer on top of the seal (Figure 6.5). Because of the excessive length of the collection zone, flow into the grouted rock mass far exceeds flow through the seal. Since the grouted rock mass and the seal have approximately the same estimated hydraulic conductivity, (10^{-9} cm/s), an accurate outflow measurement cannot be made with this excessively long collection zone. To establish an accurate outflow rate, injection should be performed from above the plug with collection from below. Outflow through the seal can be measured more effectively and accurately with a collection zone of minimum length. In addition, injection from the top of the seal would allow a higher injection head than the applied 6.4 m.

The piezometers installed in the inclined hole were used to study the influence surface water may have on the flow tests of the plug. The reason for this concern is the fact that the grouting at site A was not performed in the uppermost 2.5 m of the vertical borehole, and that the seal was installed at a relatively shallow depth of 6.2 m.

Figure 6.7 shows the buildup of head at the level of the lower piezometer, radially adjacent to the injection zone beneath the mixture

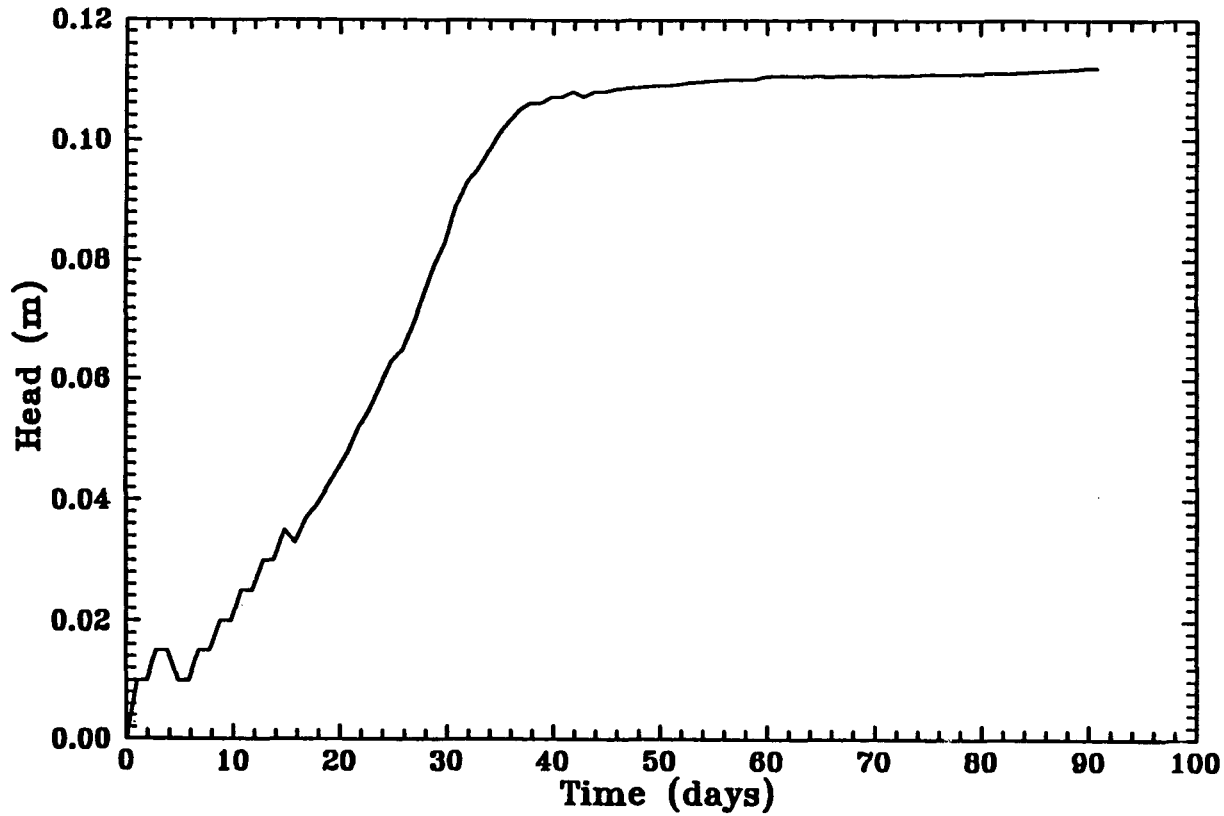

Figure 6.7 Readings of the lower piezometer during the flow test period.

plug. The head in the sand trap of the lower piezometer is stabilizing to approximately 0.17 m, (2.7 % of the injection head). The injection zone, located 0.29 m horizontally from the low piezometer, has an average injection head of 6.4 m. No influence from ground surface seepage is recognized in the data. The amount of head buildup in the lower piezometer is a function of the permeability of the lower sand trap and the amount of applied head in the injection zone. The lower piezometer is closed off both above and below by cement.

The upper piezometer is located 4.19 m below ground level in the incline borehole, (Figure 6.1). Figure 6.8 shows the output of the upper piezometer. The upper piezometer is located in a section of the inclined borehole which is not grouted and where fractures intersect as determined in the packer tests described in Chapter 3, Sec 3.9.3, 3.8.2. In addition the upper piezometer sand trap is 5 times longer than the lower piezometer sand trap. Rainfall events are represented by the vertical numbers in Figure 6.8, in inches during a 24 h period. The events are recorded from a raingage located 0.8 miles from the site. The rainfall events are short yet intense which is typical for the area. Peak piezometer readings are recognized usually 3-5 days after a rainfall event. It should be noted that the ground surface at the field site is not entirely natural. An asphalt surface, approximately 4 cm thick, covers half the site surface, acting as a shield and as a conduit for water flow along the road surface. Beneath the asphalt surface is approximately 30 cm of soil and gravel fill with fractured rock below.

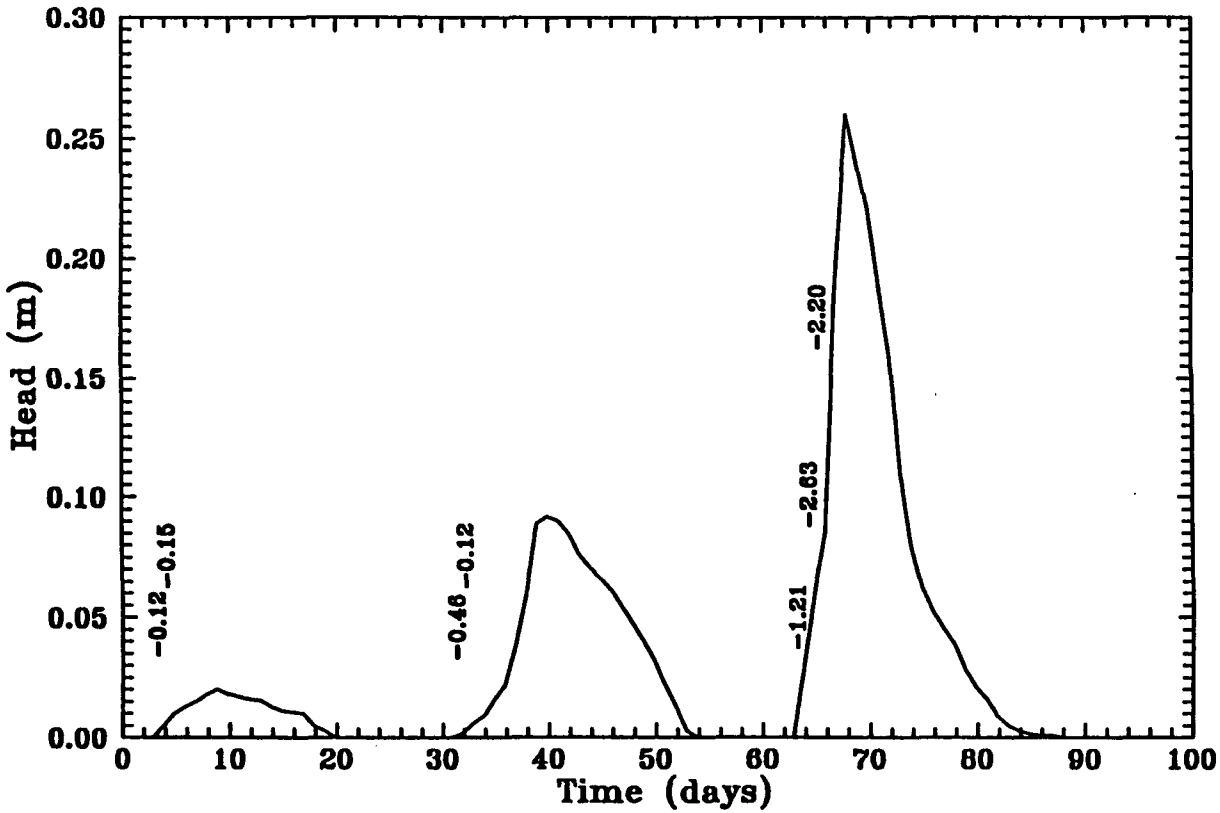

Figure 6.8 Readings of the upper piezometer taken during the flow test period. Vertical numbers indicate amount of rainfall near the site in inches over a 24 hr. period.

The asphalt and fill retard flow into the fractured rock mass below. In addition, seepage through fractures along the road cut at site A will influence the piezometer readings. The significant factor is the recognizable influence the rainfall events have at the depth of the upper piezometer and the absence of influence at the depth of the lower piezometer.

CHAPTER SEVEN

SUMMARY, CONCLUSIONS AND RECOMMENDATIONS FOR FURTHER RESEARCH

7.1 Summary

7.1.1 Objectives

An experimental assessment of the sealing performance of expansive neat cement plugs and of a crushed tuff/bentonite mixture plug in uncased boreholes is made through flow tests. The study provides a valuable data base on the sealing effectiveness of the plug materials. In addition, information regarding the impact of installation methods on the hydraulic performance of the seals is discussed as well as the methods of performance monitoring of borehole plugs.

7.1.2 Approach of Study

Two sites out of three were selected to receive borehole plugs for analysis based upon a series of preliminary surveys. All sites are in the brown unit of the Apache Leap tuff near Superior Arizona. The criteria for selecting seal locations at each site include an absence of hydraulically significant fractures; maximum depth below ground level; and an overall low effective hydraulic conductivity for the selected

test interval. The preliminary surveys consisted of analysis of core logs, downhole videologging, and constant-head and falling-head injection tests using a straddle-packer system (Chapter 3). Each site consists of a 50 mm diameter access hole drilled at an incline of approximately 60° below ground level. A 150 mm diameter hole is drilled vertically to intersect the inclined borehole at depth. This configuration allows the inclined hole to be used for access below the installed seal. Access to the top of the seal is from the vertical hole.

The installation procedures of the plug materials are developed through a series of laboratory models using field installation methods. Flow analysis has been performed on laboratory models of the crushed tuff/bentonite plug to assess the installation procedures used in the field and to compare to the insitu plug installed in the field.

Analysis of the in-situ flow tests performed on the plugs is based upon models of one-dimensional axial flow through the plug. The models assume that the seals are a homogeneous and isotropic porous medium. The analytical solutions for the models are presented in Chapter Two. Procedures are given for determining hydraulic properties from test results. Estimates of the hydraulic conductivity of the seals, K_s, from the flow models are upper limits due to the fact that flow through the host rock mass surrounding the seal is ignored.

7.1.3 Expansive Cement Plug, Site C

On September 9, 1989, a cementitious borehole plug was installed in the vertical hole of site C. With access to both ends of the seal, tests using a two-side configuration were performed over a 1 3/4-year period from September, 1989 to May, 1991.

7.1.3.1 Steady-State Constant Head Test

The primary flow test performed on the expansive cement plug was the steady-state constant head test, described in Chapter 2, Sec. 2.2. Three trials were performed, with injection of water beneath the seal. Injection head ranged from 26 m, (trial 1), to 28.6 m, (trials 2 & 3). The hydraulic conductivity of the seal was determined from the measured outflow of fluid collected on top of the seal. For the first two trials, the collection outflow eventually overtook the flow rate of the water injected below. This phenomena was due to the pneumatic packer, used to isolate the collection zone, leaking N_2 into the collection zone and driving the fluid at an accelerated rate. The hydraulic conductivity of the seal was determined from outflow rates before they exceeded the injection inflow. The problems encountered with the packer appear to be delayed, starting 3-4 weeks after it was installed. For the third steady-state trial, the packer was installed for only 2 weeks, to avoid erroneous outflow values. Injection had been continued prior for a

period of 8 months and during the third steady-state test without interuption.

The hydraulic conductivity of the plug based upon the three steady-state tests ranged from 5.9 $x10^{-10}$ cm/s to 6.3 x 10^{-10} cm/s. These values are based upon a one-dimensional analysis, assuming flow does not occur through the rock.

The injection inflow rate yielded the hydraulic conductivity of the intact rock surrounding the injection zone beneath the plug. Values for these flow values were not affected by the packer. Two assumptions were made concerning the hydraulic conductivity analysis of the injection inflow values. The first is that the injected flow is into the rock only and not into the plug above or bottom cement seal below, (i.e. impermeable boundaries). The second is that the flow is either ellipsoidal prolate in geometry away from the center line of the injection zone and through the rock or that it travels radially and horizontally away from the center of the injection zone. For the radial flow assumption, a radius of influence must also be assumed. For all calculated results it is ten times the injection zone length.

Hydraulic conductivity values for the rock surrounding the injection zone range from 5.4 x 10^{-11} cm/s to 5.0 x 10^{-11} cm/s. The hydraulic conductivity of the rock is determined from injection flow values taken at the same time as the collection outflow values for all three trials. The calculated conductivities generally decline gradually from the first trial through the third trial.

7.1.3.2 Head-Buildup Test

A head-buildup test (first recovery variation), was performed on the cement seal after the three steady-state trials were completed. The injection beneath the plug was continued from the steady-state tests without interruption. From this test, both the hydraulic conductivity and the specific storage are obtained. The collection zone above the plug is closed off, and the buildup of pressure is monitored. Like all of the tests performed, this test utilizes a one-dimensional analysis.

The resulting hydraulic conductivity of the plug from this test is 2.73×10^{-10} cm/s. The specific storage of the plug, S_s, is 2.7×10^{-7} cm^{-1}. Evidence of packer leakage into the collection zone was not discovered. The test however was prematurely stopped due to vandalism of the instrumentation. Overall the hydraulic conductivity of the plug measured through the head-buildup test is approximately half of the values determined in the steady-state test, yet well within the same order of magnitude.

7.1.3.3 Transient Constant-Head Test

A transient constant-head test was performed on the cement seal after the head-buildup test. Injection from below the plug was maintained, yet rapidly reduced from 0.27 MPa to 0.19 MPa with the resulting change in collection outflow monitored. From this test, both the

specific storage and hydraulic conductivity of the seal are obtained. The hydraulic conductivity of the plug is determined from the reduced collection outflow.

Assuming that the steady collection outflow at the end of the test is one-dimensional flow through the seal, the hydraulic conductivity is calculated as 4.7×10^{-10} cm/s. Using this conductivity, a specific storage for the seal of 1.1×10^{-8} cm^{-1} is obtained. The conductivity value for the plug compares reasonably well with values obtained from the earlier tests. The specific storage varies by slightly more than one order of magnitude from the value obtained in the head buildup test.

7.1.4 Crushed Tuff/Bentonite Mixture Plug, Site A

The crushed tuff/bentonite seal was installed at site A on November 22, 1990. Geometry of the test arrangement with two boreholes, and an injection stand is very similar to the one used for testing of the expansive cement plug. Tests using the two-side configuration were performed over a 7 month period from November, 1990 to May 1991.

7.1.4.1 Falling Head Injection Flow Test

A falling head test was performed with injection below the plug. The purpose of this test is to saturate the mixture plug and evaluate

the hydraulic performance of the seal. Collection outflow was monitored, yet not achieved due to the large volume of the collection zone above the plug. All hydraulic conductivity values of the plug are based upon injection flow measurements. Based upon earlier tests prior to installation of the plug, flow into the rock and bottom borehole seal is subtracted from the injection flow measurements to yield an estimated one dimensional flow into the plug.

The estimated hydraulic conductivity of the plug determined from this test is 2×10^{-9} cm/s under an average injection head of 6.4 m. This value should be considered an upper limit conductivity value for the plug. Because the hydraulic conductivity of the grouted rock mass surrounding the plug approaches that of the plug, a significant amount of flow may be traveling into the rock mass immediately adjacent to the plug. The hydraulic conductivity of the plug determined in the field compares well with hydraulic conductivity values measured from a laboratory plug of similar size yet slightly lower in bulk density. Both values are within the same order of magnitude.

7.2 Conclusions

7.2.1 Characterization of the field sites prior to plug installation

Straddle packer and single packer injection flow tests were the most significant tool for chosing the interval for installing the seals.

During development of the field sites, injection tests in the inclined holes aided in locating the vertical test hole. Injection tests in the vertical holes allowed determination of the hydraulic properties of the rock and of the bottom seals of the test holes for later use in the seal-test analysis. In addition, the injection tests allowed performance evaluation of grouting applications at site A. Long term injection tests to characterize the intact rock, fractured rock, and the grouted rock mass with test periods equivalent to the seal test period should be performed. Long term tests would be useful in the seal analysis, and evaluation of the grout performance.

7.2.2 Expansive Cement Seal Installation

Installation of cement seals with standing water present can cause a significant amount of piping in the plug. This was clearly demonstrated by the laboratory trials using a bailer (Chapter 4, Sec. 4.2). Piping channels were recognized as dark vertical streaks along the tube and plug interface. The channels create pathways for preferential flow along the interface. The piping effect was recognized for seals installed with any level of standing water in the pipe. When a plug was installed without standing water, the piping effect was not visibly recognized along the tube and plug interface. The piping effect in cement seals installed with a bailer has also been recognized by Daemen et. al., (p. 71, 1983). Cross-sections of the plugs after curing revealed

the dark streaks as open channels.

In addition to the piping effects noticed during installation of cement seals underwater, severe mixing of the cement with the water was evident. This mixing can significantly reduce the hydraulic and mechanical qualities of the plug. This effect was particularly noticeable with a high amount of standing water present during installation in which the upper 1/4 - 1/8 of the plug turned a light grey, indicating mixing of the cement with water. This end effect can be very significant for short plugs, and cam significantly reduce the sealing quality of the plug.

Based upon the information determined from the laboratory trials of the cement plug installation, the plug in the field was installed under dry hole conditions. Prior to installation of the seal all water was pumped out. Any residual water in the hole was sponged out. Sand was then installed to develop an injection zone beneath the plug and to provide a dry surface to pour the plug. Any air trapped beneath the plug was removed using a vent tube in the injection stand.

7.2.3 Crushed Tuff/Bentonite Mixture Plug Installation

Three trials were performed in the laboratory to develop and evaluate installation procedures. After installation of the seal, flow tests with injection from below the plug were performed. Based upon

information from these tests, four critical factors for proper installation of this plug type became apparent. Homogeneity of the plug material, uniformity of compaction, bulk density and confinement of the plug, and particle size of the crushed tuff aggregate play significant roles in the sealing performance of this material.

Separation of the tuff aggregate into regions of fine material and coarse material create an inhomogeneous plug mass which aggravates the effect of channeling and piping during flow tests. The separation of materials during installation is primarily due to the bailer used to lower the plug material in place. Redesign of the bailer and increasing the number of layers to construct the plug reduced and averaged out any inhomogeneity effect of the materials. Further changes to the bailer should be considered to reduce separation of the plug material during installation.

Particle size and distribution of the crushed tuff must be tailored for a given borehole diameter. For the 150 mm diameter boreholes, the laboratory model indicated that even with a high degree of compaction and minimal separation of materials, voids of significant volume are still present. Thus to assure proper sealing, maximum particle size must be determined for a given borehole size to avoid development of large voids in the plug.

Low bulk densities due to poor compaction play a significant role in increasing the risk of channeling and piping in the plug. With low bulk densities and the inhomogeneity of the plug material, the bentonite

content may not be adequate to allow healing of voids and pockets. In the first two trials, piping occurred both along the plug/tube interface and internally in the plug. Increasing the bulk density through proper compaction reduces the void space in the material, and increases the amount of bentonite for a given plug volume. To maintain the compacted bulk density after installation, the plug must be properly confined so that the plug will maintain integrity during absorption of water. For field testing, the use of rock cylinders allowed open access to the top of the plug while providing a vertical confinement. In seal design, confinement should be provided by either a concrete or cement bulkhead. In addition to proper confinement and degree of compaction, the compaction of the plug must be uniform. This can easily achieved in the laboratory by moving the compaction hammer over the entire surface area of the top of the plug. In the field, control is more difficult, particularly for plugs installed in deep holes. To achieve a uniform compaction, surface area of the compaction hammer must be at least 50 % of the surface area of the plug.

7.2.4 Configuration

All of the test sites employed two-sided configurations. This allows use of one-dimensional flow analysis with a higher degree of accuracy than a one-side configuration. The two-sided configuration allows verification that test flow rates are not erroneous through a

mass balance check of the injection and collection flow rates. The ability to collect outflow through the seal yields a lower upper limit on the seal hydraulic conductivity than the injection flow from a one-side test. In addition, the two-sided configuration allows a one-dimensional analysis of the head buildup test to be performed. The configuration also allows any of the flow tests to be repeated and verified with flow originating from either direction of the seal.

7.2.5 Sealing Performance of Expansive Cement Plug

The hydraulic conductivity of the cement seal has been determined by three types of tests. All three yield a value in the order of magnitude of 10^{-10} cm/s. A slight indication was noticed that the seal hydraulic conductivity decreases over time. Due to the limited accuracy for measuring the outflow on which the conductivity is based, this may not be the case. Evidence for reduction of the conductivity of the rock during testing is solid. Injection flow decreased gradually over the test period of nearly two years.

Hydraulic conductivity of the plug determined through the one-dimensional head buildup test is approximately half of the value determined in the steady-state test, yet still within the same order of magnitude. The accuracy of the head buildup test is less than that of the steady-state test due to difficulty in verification of erroneous data. In addition, the head buildup test relies upon determination of

the compressive storage of the collection zone, which is a difficult value to determine accurately considering the packer being a major component of the collection zone.

The specific storage of the seal determined from the head buildup test is 2.7×10^{-7} cm^{-1}. This is a reasonable value for intact rock or for cement. From the transient constant head test, a specific storage of the seal is determined to be 1.1×10^{-8} cm^{-1}. Again this value although one order of magnitude lower than what was determined from the head buildup test is reasonable for intact rock or cement. Discrepancies between the two values are due to the sensitivity of the tests to accurate flow and pressure measurements and matching against a given type curve.

7.2.6 Sealing Performance of Crushed Tuff/Bentonite Plug

Hydraulic conductivity of the plug determined through falling head tests is in the order of magnitude of 10^{-9} cm/s, assuming one-dimensional flow through the plug. This is a significantly higher upper limit than the values determined for the cement plug. Without outflow from the plug, and a grouted rock mass with a similar conductivity to that of the plug, determination of hydraulic conductivity of the mixture plug is less accurate than that of the cement plug. The conductivity values compare favorably with laboratory tests on mixture plugs. Evaluation of the hydraulic performance of the mixture plug would be more

accurate if it were installed in a host rock mass with a lower hydraulic conductivity. Injection from the top of the seal should allow collection of fluid below the plug with a reasonable accuracy. This will yield a lower upper limit on the hydraulic conductivity of the plug.

7.2.7 Equipment Performance

Implementation of a remote data acquisition system at each site proved to be invaluable and highly reliable. The system at site C powered and recorded eight to ten sensors continuously for over two years at a rate of every 10 minutes to 60 minutes without a fault. One sensor was inaccurately connected, yielding flow data with amplified noise. The problem was corrected after a week. The system at site A is similar to the one at site C and has performed flawlessly. Accuracy for both flow measuring systems is a function of sensor accuracy and susceptibility to the changing environment, not the recording system.

A packer was used to isolate the collection zone above the cement plug. Leakage of packer-inflation gas into the collection zone was a significant problem in the testing of the cement seal. Typically after two weeks or more of continuous inflation, a mass balance of the flow rates (injection and collection), indicated that the collection flow exceed the injected flow. The cause was leakage of packer gas into the closed off collection zone. Trapped gas bubbling to the pool surface could be seen upon deflation of the submerged packer . All the packers

used in the field are checked in the lab for leaks during a 48 - 62 hr long test prior to their use in the field. The leaking effect is delayed, and appears to be a function of the permeability of the natural rubber gland and of packer construction and is not easily verified in the lab. The leaking is avoided by inflating the packer with pressurized water and by flushing the annulus between the packer gland and mandrel. With the packer inflated with water, no effect on flow rates at site C has been noticed for a period of over nine months of continuous packer inflation.

7.3 Recommendations

7.3.1 Cement Seal

Investigate the long term effects of flow testing to determine if the hydraulic conductivity of the expansive cement seal decreases or increases over time.

Perform steady-state tests with a significant range of injection pressures to determine if the hydraulic conductivity of the seal is sensitive to changes in head.

Perform an axisymmetric analysis of the steady-state, head buildup, and transient constant head test on the expansive cement seal. A comparison should be made to the one-dimensional tests to validate the one-dimensional analysis.

Perform flow tests in the opposition direction, (injection from top), determine if the hydraulic characteristics of the plug are the same in both directions.

Inject below the plug and overcore the seal to determine preferential flow paths around and through the plug. This can yield invaluable information pertaining to plug design and validity of the porous media assumption.

Perform push out tests to determine bond strength of the expansive cement seal.

Perform a tracer travel-time test to determine an upper limit to the minimum travel time for water to move from the injection to the collection side of the seal.

Examine the use of a constant-flow test rather than a constant-head test for low flow seals. This would overcome problems associated with measuring flow from a mechanical pump which causes mechanical noise in the data.

Develop a method to install cement seals underwater without piping effects or mixing with the water.

7.3.2 Crushed Tuff/Bentonite Seals

Dye injection and overcoring of the mixture plug can yield information pertaining to preferential flow paths around the seal. Dye however is adsorbed by the bentonite, masking any preferential flow paths in the

plug itself. Nevertheless, since the host rock at site A has a hydraulic conductivity nearly equal to that of the plug itself, determining preferential flow paths around the seal is crucial to understanding the flow regime in this complicated configuration.

Perform long term flow tests on the mixture plug to determine if the plug conductivity changes over extended periods of time.

Perform hydraulic tests wtih different water types, e.g. simulated groundwater chemistries.

Develop a collection zone on top of the seal with a minimum length, yet provide adequate confinement of the plug during flow testing. This may be best accomplished with either a mechanical plug or cement plug.

After leaving the plugs for many years, investigate plug rock interactions. This could involve coring out short sections along the interface once a year.

APPENDIX A

JOINT ORIENTATION MEASUREMENTS

Table A.1 Results of Joint Measurements of Survey Line No. 1. Number of measurements = 35, presented in quadrant system. Trend of survey line is N 7° E.

N16W, 44E	N76E, 89E	N66E, 85E	N15W, 32E	N89E, 87S
N5E, 71E	N87E, 87N	N10E, 32E	N5E, 32E	N11E, 32E
N66E, 90E	N5E, 90E	N40E, 60E	N40W, 80W	N85E, 88E
N86E, 88E	N53E, 72E	N10E, 74E	N13E, 69E	N18E, 74E
N19E, 79E	N21E, 85E	N23E, 85E	N25E, 79E	N88E, 87N
N34E, 32S	N86E, 88N	N26E, 27E	N32E, 28E	N33E, 31E
N28W, 67W	N24E, 27E	N43W, 89W	N88E, 87S	N22W, 46W

Table A.2 Results of Joint Measurements of Survey Line No. 2. Number of measurments = 72, presented in quadrant system. Trend of survey line is N 30° E.

N35W, 74W	N75W, 90E	N35W, 72W	N80W, 70W	N45W, 85W
N80W, 70W	N62W, 89S	N43E, 74E	N9W, 90W	N11W, 88W
N65W, 89S	N24W, 88W	N27W, 79W	N26W, 84W	N24W, 85W
N23W, 65W	N64E, 80N	N25W, 76W	N21W, 85N	N74E, 66S
N83E, 81S	N63W, 77S	N35W, 81W	N55W, 69N	N59W, 87S
N83E, 78N	N20E, 72S	N40W, 76W	N33W, 87N	N37W, 85N
N98E, 76S	N20E, 65W	N68W, 80S	N87W, 81S	N82E, 89N
N75W, 78S	N45W, 85W	N43W, 75W	N35W, 80W	N44W, 89W
N66W, 64W	N65W, 78W	N22E, 23E	N10W, 29E	N40E, 29E
N51E, 13E	N34E, 13E	N57E, 11E	N61E, 21E	N21E, 20E
N33E, 17E	N46E, 19E	N47E, 23E	N12E, 25E	N35E, 22E
N29E, 19E	N48E, 11E	N43E, 17E	N57E, 23E	N42E, 18E
N19E, 8E	N43E, 23E	N48E, 18E	N45E, 11E	N63W, 88S
N57W, 76S	N49W, 81S	N68W, 79S	N88W, 80S	N77W, 79S
N72W, 76S	N59W, 87S			

Table A.3 Results of Joint Measurements of Survey Line No. 3. Number of measurements = 15, presented in quadrant system. Trend of survey line is N 86° W.

N86E, 84S	N1W, 90W	N35W, 87W	N21W, 79E	S12E, 79W
N6E, 83W	N31W, 71W	N4W, 78W	N85E, 85S	N20W, 76E
N34W, 76E	N83E, 86E	N84E, 85E	N33W, 85E	N20W, 66E

Table A.4 Results of Joint Measurements of Survey Line No. 4. Number of measurements = 42, presented in quadrant system. Trend of survey line is N 50° W.

N21W, 89W	N67E, 79S	N2W, 84W	N87E, 72S	N69E, 82S
N72E, 72S	N67E, 78S	N82E, 75S	N80E, 82S	N67E, 83S
N84E, 87S	N58E, 89S	N85E, 80E	N65E, 77S	N65E, 77S
N69E, 81S	N65E, 74S	N85E, 80E	N85E, 83E	N50E, 80W
N75W, 75W	N85W, 78W	N50E, 75W	N58E, 85E	N58E, 85E
N59E, 84E	N52E, 84E	N75E, 79W	N65E, 78W	N65E, 78W
N6W, 80W	N36W, 82S	N33E, 80N	N81E, 87N	N38W, 77S
N60E, 89W	N12E, 78E	N8E, 88N	N50W, 89E	N33W, 76N
N32W, 72N	N35W, 77N			

Table A.5 Results of Joint Measurements of Survey Line No. 5. Number of measurements = 13, presented in quadrant system. Trend of survey line is N 75° E.

N46W, 90E	N5E, 80E	N18W, 16W	N30W, 62W	N5W, 35W
N27E, 87W	N32E, 76W	N15E, 88E	N32W, 70E	N34W, 39W
N32W, 70W	N35W, 45W	N32E, 74W		

Table A.6 Orientation and spacing of the four recognized joints in quadrant format

Joint Set # 1	Strike N30E	Dip 21SE	Avg Spacing: 0.37 m
Joint Set # 2	Strike N88E	Dip 74SE	Avg Spacing: 0.64 m
Joint Set # 3	Strike N12E	Dip 59SE	Avg Spacing: 0.49 m
Joint Set # 4	Strike N25W	Dip 63SW	Avg Spacing: 0.67 m

APPENDIX B

Pressurized Grouting of Site A

B.1 Introduction

In mining and civil engineering construction in rock, the presence of discontinuities is unavoidable. These discontinuities may have been caused by tectonic events, such as by faulting, folding, shearing or tension, or by the engineering excavation process itself. Discontinuities increase the hydraulic conductivity of the rock mass, causing a greater rate of groundwater flow.

In the context of ground engineering the term grouting is used for the process of pressure injection of setting fluids into the pores, cavities and fissures of a soil or rock mass. This process has been used successfully in the construction of dams, tunnels, and shafts for the purposes of reducing the rock mass permeability, to consolidate and improve the strength of the geological media, as well as to pre-stress the linings, of shafts and tunnels. Thus, the process of grouting can be considered to be both a preventive and a remedial measure in engineering construction.

Despite the fact that grouting has been used in engineering construction for over a century, the development of grouting and grout-

ing practices has been a relatively slow process. The literature on the subject is voluminous, with case histories being a common vehicle for the presentation of information.

B.2 Review of Current Practices

B.2.1 Development of Grouting Materials

Important developments in cement grouting are attributed to Francois, who in 1910 found that cement particles could be transported into fine rock fissures for considerable distance before settling out (Francois, 1914). This was achieved by using well-agitated dilute suspensions pumped continuously into the formation, frequently under high pressure. This technique is still widely used for rock grouting around shafts and tunnels and in dam foundations (Deere, 1982). With the advance of technology in mining and civil engineering, underground openings located several hundreds of meters below the ground surface are not uncommon. Consequently, the voids or fissures that have to be sealed with the grout material have tended to become smaller. Caron (1963), summarizing data from a Russian paper, concludes that coarse sand (greater than 0.8 mm) can be injected by suspensions containing particles of up to 0.50 microns. Caron (1963) states that a grout containing even a small proportion of coarse particles can form a filter cake in the soil near the injection source. In additions cement suspensions

with particles as large as 100 microns will form filter cakes in soils with permeabilities as high as 0.05 mm/s. Although the preceding studies were not conducted on rock fissures, it is apparent that there exists a limiting size at which the injection of a cement grout into a rock formation is impossible.

Because of these limitations, the use of solution grouts which gel after the injection process have been emerged. These grouts, which are commonly referred to as chemical grouts and as resin grouts, perform as well as cement grouts and can frequently penetrate finer apertures in soils and rocks (Lau and Crawford, 1986).

The evolution of chemical grouts began towards the end of the 1800s. By 1910 Francois refers to grouts based on sodium silicate in combination with other reacting chemicals. Such materials were used as preliminary injections to improve the penetration of subsequently injected cement on other particulate grouts. The development of a two-shot process by Joosten in 1925, Joosten (1954), greatly advanced the application of grouting by allowing rapid set times.

The use of organic polymerising solutions, commonly known as resins, has gained wide acceptance in recent years. The penetrability of these resin grouts is extremely high (Deere and Lombardi, 1985). Recent studies indicates they can be injected into medium to fine silt that has permeability ranging from 1 cm/s to 0.01 cm/s (Houlsby, 1982b).

Despite the various advantages of chemical and resin grouts, the application of cement grouts has not been replaced. One of the main

reasons is due to the difficulties in controlling the gel time of chemical and resin grouts (Deere 1982). These difficulties arise primarily because of the influence of the ground temperature on the gel time of the grout (Houlsby, 1982a). In the case where the gel time is overestimated, the grout may gel prior to or during injection. If this happens, the gel may inhibit the grout from propagating to the anticipated extent requiring the use of secondary or tertiary grout holes.

Ultrafine or microfine cements are gaining wide acceptance because of their fine grain size distribution, which results in a higher penetrating capability of the injected grout. Microfine cement was developed in Japan because organic grouts were banned after a toxicity incident with acrylamide grout in 1970. Recent studies have shown that microfine cements can be injected into fine sands with permeabilities ranging from 0.01 cm/s to 0.001 cm/s (Shimoda & Ohmori 1982). The average particle size of microfine cements range from 4 micron (Japanese MC-500) to 3 micron (domestic MC100) compared with 15 micron for high early strength, Type III Portland cement and 20 micron for Type II Portland cement.

B.2.2 Overview of Field Procedures

The first requirement is the assessment of the subsurface geology. Through the use of boreholes, the nature of the rocks's discontinuities can be studied. The size and geometry of discontinuities in terms of

aperture, extent and orientation are all factors which must be known prior to any grouting application. Knowledge of the physical nature of the rocks's discontinuities ensures that a proper specification of grouting procedures is achieved. Based on the nature of the subsurface geology, some of the factors affecting a grouting program are (Houlsby, 1982, Deere and Lombardi 1985).

a) Spacing of joints. Close joint spacing often leads to surface leaks and uneven, uncontrollable grouting penetration. Wide spaced joints often make grouting easier.

b) Aperture of joints. Joints with large apertures may require a large grout volume. Joints with narrow apertures less than 500 μm may require very lean grouts at high pumping pressures.

c) Orientation of joints. The grouting of near vertical joints may require the use of inclined grouting holes. Radial penetration of grout in near vertical joints is more difficult than horizontal joints.

d) Strength and soundness of rock mass. A sound rock mass can withstand higher grouting pressures. If fracturing were to occur, new passages would be created for grout travel and this in turn would necessitate an increase in the grout take.

In practice, whether or not grout can be injected into the rock mass is frequently determined by a water pressure tests. Boreholes are drilled and water is pumped under pressure through the rock's discontinuities. A measure of the acceptance of grout is determined by the water take during pumping. The European practice describes that if the

flow of water is less than 1 liter/m/min at a pressure of 0.01 Pa, then the rock is considered watertight and grouting will be necessary only under very exceptional conditions (Mayer, 1963). The commonly accepted rule in North America indicates that grout injection is not necessary if the hole takes water at a rate less 57 liters/min (Minear, 1957).

Coupled with the water flow test, pressure washing of the joints to be grouted is usually undertaken. Pressure washing is accomplished by alternately pumping water and air under pressure through the joints and out to a receiving hole. The purpose of this operation is to clean the joint surfaces from clay and silt infillings since good grouting results are achieved only if the grout has consistent and continuous contact to the rock joint surfaces.

The importance of field control in a grouting program has been discussed in detail by Deere (1982). Deere emphasizes that field control and monitoring can be achieved using simple field instruments such as the Marsh Cone for measuring apparent viscosity, flow meters, pressure transducers, and data recorders. By continuous monitoring of the density, viscosity, injection pressure and the intake rate of the grout, better control of the grouting operation can be made.

B.2.3 Grout Injection Parameters

Apart from determining hole geometry, grouting depth, and equipment configuration, the grouting engineer must deal with the factors that influence the rate and extent of grout penetration. The most important factors are: (a) pumping pressure, (b) consistency of the

grout and (c) aperture of the rock joints (Deere & Lombardi, 1985).

B.2.3.1 Pumping Pressure

The selection of an appropriate maximum pumping pressure is an important factor in the design of a grouting program. The use of excess pressure may cause hydraulic fracturing of the rock mass. The effects of hydraulic fracturing of the rock mass translate into a larger volume of grout to be injected, which in turn may mean that the time and the cost of the grouting job increases. Extensive rock fracturing would also create a weakening of, as well as an increase in the hydraulic conductivity of the rock mass. However, it is a common practice to keep the pumping pressure high so as to minimize the time to perform the grouting operation as well as to obtain greater penetrability of the grout (Morgenstern and Vaughan, 1963). Wong and Farmer (1973) discuss the conditions for hydrofracture initiation for both vertical and horizontal fractures intersecting a borehole based upon grout pressure, tensile strength of the rock and overburden pressures.

In most practices, the common rule of thumb for estimating the grouting pressure is 1 psi per foot of depth. This rule is quite conservative when sound rock conditions are present. The Army Corps. Of Engineers uses the rule that the maximum allowable pressure, in psi at the collar of the borehole should not exceed the depth of the overlying rock, in feet, plug 0.5 the depth, in feet, of any overburden material above the rock. Houlsby (1982) gives the recommended maximum grout pressures based upon the soundness of the rock and depth below surface.

B.2.3.2 Grout Consistency

The consistency of the grout is defined by the water:cement ratio, is the most significant variable that affects both the penetration and the durability of the grout (Deere & Lombardi 1985, Lau & Crawford 1986). Grout mixtures with low water:cement ratios provide a very durable barrier but due to their high viscosity, their penetration is limited primarily by the allowable pumping pressure and secondarily by the aperture of the rock joints. Lean grout mixtures give the grout mobility (Deere & Lombardi 1985) but the water, if in excess, may create problems such as reduced strength, durability and stability. In addition, water, due to differences in specific weight with respect to the grout, tends to rise out of the mix by the process of bleeding. Bleed water creates pockets and paths that may eventually delineate weak spots to the grouts permeability

Grout consistency, in practice, varies from a water:cement ratio (by weight) of approximately 0.6:1 to 12:1 depending upon the ground conditions as determined by geological investigations and pumping or packer tests (Harris, 1983). The initial grout injected has a very high water:cement ratio (by volume usually near 8:1 to 12:1 (Houlsby, 1982b). This is done in order to allow the grout to penetrate the finer fissures of the rock. The grout is then progressively thickened to a point at which premature filter blockage of the fissure is suspected. Grouting is continued by diluting the mix and increasing the pressure to permit the flow of grout through the existing grout. Once this is accomplished, the thickening of the grout mix is repeated until filter block-

age occurs. This condition is referred to as refusal.

Refusal is usually defined as a condition at which the thickest possible grout is pumped at a prescribed maximum allowable pressure. In the field the volume flow of grout or the pump's speed is monitored. When a reduction in the volume flow of grout is noticed, with a corresponding build-up pressure, the grout is at refusal.

A review conducted by Houlsby (1982b) of British field practices with respect to the optimum water:cement ratios for rock grouting. Produced the following conclusions:

a) A water:cement ratio equal to 2:1 (by volume) is regarded as the optimum basic mix.

b) The optimum mix should be increased to a ratio of 3:1 (by volume) if grouting fissures 750 μm or finer. If grouting fissures larger than 1.5 mm the ratio should be decreased to 1:1.

c) Grout mixtures with values of water:cement ratio greater than 5:1 by volume have been proven to produce non-durable grouts.

d) After preforming a grout application, benefits can be obtained by thickening the mix during the course of the injection.

United States Army Corps of Engineers experience in grouting fine fissures indicates the desirability of thick grouts with water:cement ratios down to 1:1 by volume for reasons of durability and reductions of bleedwater (Albritton, 1982). Moller, Minch and Welsh (1983) outlines their grouting experience on the injection of ultrafine cement grout into granite joints. They conclude that water:cement ratio of 1:1 by weight appears to be optimum. They point out that increasing the amount

of water slows down the setting time and decreases the compressive strength of the grout. Based on their successful experiences in various dam construction projects as well as from laboratory testing, Deer and Lombardi (1985) indicate that a water:cement ratio of 1:1 by weight (1.5:1 by volume) appears to be optimum.

B.2.3.3 Aperture of Rock Joints

The aperture of the rock joints is a variable that cannot be controlled in the process of grouting. It is also the variable on which the least reliable information is available. As mentioned previously, detailed geological investigations are frequently conducted prior to grout injection. Nevertheless a complete description on the nature and geometry of the discontinuities cannot always be obtained.

Pressure build-up at a particular grouting stage is often the result of the presence of constrictions and of branching of the joint aperture. In such cases, two methods are traditionally available to improve grout penetration: a) increase pumping pressure, or b) reduce grout consistency (increase water:cement ratio or use dispersents). If the maximum specified pumping pressure is not to be exceeded, the grout consistency must be reduced.

An alternative method, outlined by Mayer (1963) may be used to facilitate the injection of grout into a fissured rock mass. This consists of an initial injection of diluted sodium silicate solution which coats the joint surfaces with a thin film of silca gel, lubricating the joint surfaces and easing the grout's penetration.

The relationship between the aperture of the rock fissure and size of the grout particles is also important. Mitchell (1970) defines the groutability ratio for particulate grouts pumped into soils as ratio of D_{15} (diameter at 15 percent finer) of the size to D_{85} (diameter at 85 percent finer) of the grout, stating that successful grouting requires this ratio to be greater than 25. In the case of rock grouting, the groutability ratio refers to the ratio of the joint aperture to the maximum particle size of the grout (D_{100}). Mitchell (1970) and Crawford and Groskopf (1984) indicate that a minimum ratio of 3 should be attained for successful grouting. Karol (1985), refers to this process of the blockage of open passages as "blinding" in which cement particles attempt to enter a void simultaneously, thereby blocking the joint opening. Other researchers (Mayer, 1963) believe that groutability is not a property that can be measured or established by a number or a formula. The same cement grout under different injection pressures, having different consistencies and with different additives will respond differently to filter blockage.

B.3 Pressurized Grouting of Site A, Superior Arizona

B.3.1 Objective

The purpose of this test is to reduce the overall permeability of a borehole. The procedure described here is for 150 mm diameter boreholes. The hole depth is approximately 10 m. The inclination of the

intersecting 57 mm diameter hole is greater than 60 deg. Pneumatic packers and a compressed air driven single component grout plant is used for the experiment.

B.3.2 Apparatus

- 1 50 mm diameter, 100 cm long fixed head Baski pneumatic packer (for sealing a 57 mm diam. borehole while providing inlet for grout)
- 1 127 mm diameter, 208.3 cm long fixed head pneumatic packer (for sealing a 150 mm diam. borehole)
- 1 Grout plant (Chem Grout model CG-550A) with a minimum capacity of 23 l/min, pump pressure capacity of at least 1.4 MPa and mixer capacity of 113.6 liters.
- 2 N_2 gas cylinders with pressure regulators
- 20 m of nylon high pressure tubing (4.8 mm O.D., 17.2 MPa capacity).
- 1 stainless steel bulk head.
- 13 m of 38 mm I.D. rubber grout line with a 2 MPa capacity
- 1 gas powered water pump
- 1 spool of hose, 25 mm I.D., 10 m in length
- 2 three way valves
- 1 pressure gage 2.1 MPa capacity, 0.07 MPa resolution
- 1 wire brush, 17 mm diam. with attaching flexible rod, 10 m total length
- 1 Marsh Funnel for apparent viscosity measurements

B.3.3 Test Method

Figure B.1 describes the general arrangement of the grout application. The hole length is grouted at one time rather than is sections.

1. For the first grout application only, flush the hole with 1500 to 2000 liters of water under low pressure (< 345 kPa).
2. Remove any standing water in the borehole with the water pump until the hole is dry.
3. Both the grout line and packer inflation line are attached to the 50 mm diameter packer and secured together so that the lines do not tangle.
4. The 50 mm diameter packer and attached lines are set in position with the front of the packer just visible at the intersection of the two boreholes. Connect the packer to the three - way valve and regulator and inflate to a pressure of at least 700 kPa greater than the applied grout pressure.
5. Attach the stainless steel bulkhead to the end of the 127 mm diam. packer with the threads sealed with Teflon paste and connect the packer to its N_2 source. Lower the packer in the vertical borehole so that the bulkhead is at a depth of 4.5 m. The top of the pressurized grout zone will be at 3.9 m. Leave the packer deflated.
6. Attach the grout line to the grout pump with the 2.1 MPa capacity gage just after the outlet of the pump. Attach the compressed air line to the grout pump.

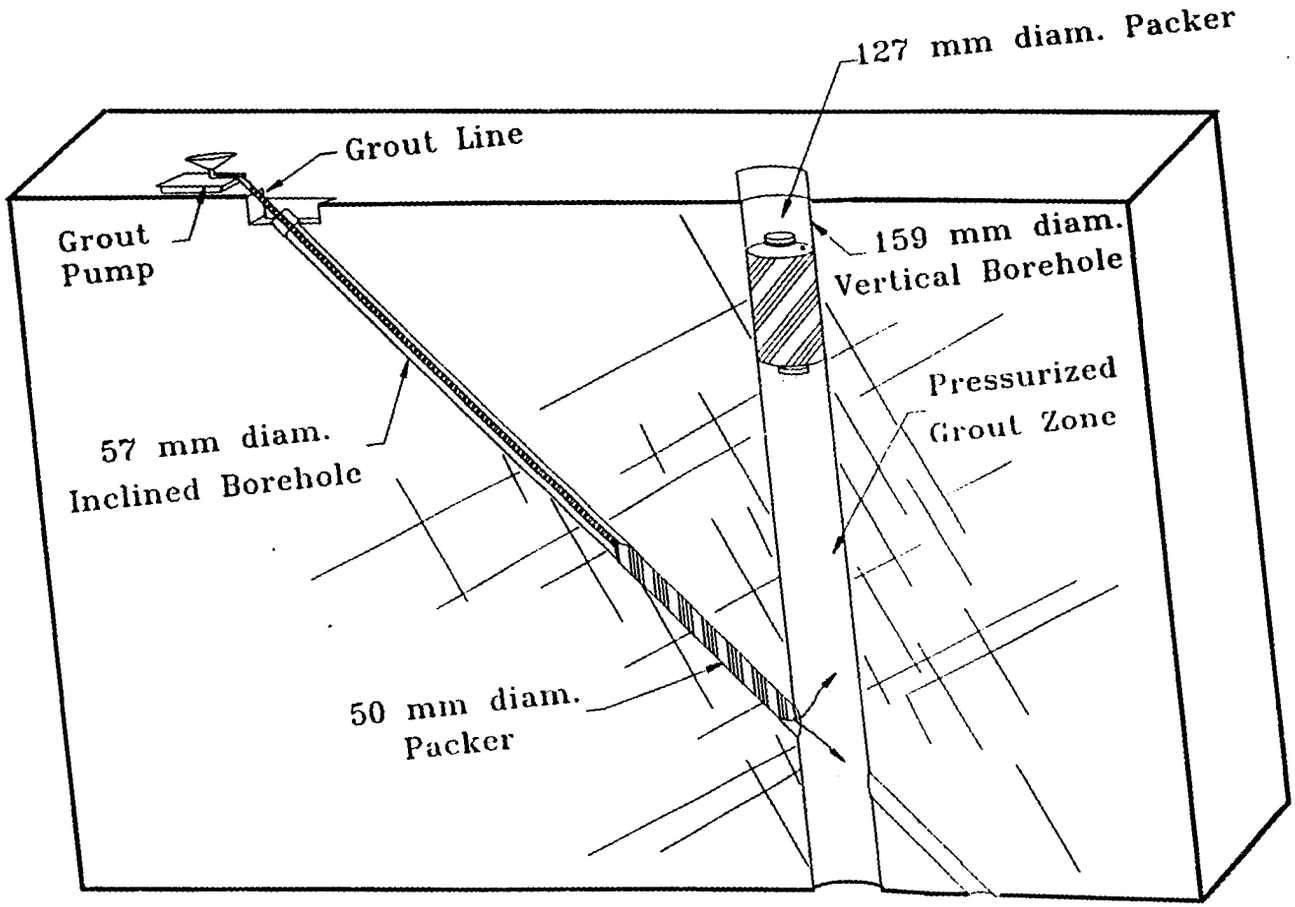

(Not Drawn To Scale)

Figure B.1 Arrangement of the pressurized grouting system used for site A. Two pneumatic packers are used to isolate the pressurized grout zone.

7. Load approximately 90% of the water anticipated for the size batch to be mixed and with the mixer running. The amount of water depends upon the desired water:cement ratio (w/c) and the amount and type of additives used.

8. Add any necessary additives to the water at this time. Allow sufficient time for the ingredients to mix.

9. Slowly add the required amount of cement. Allowing sufficient time for the slurry to mix, slowly add any sand if it is part of the formulation. Add the remaining amount of water.

10. After allowing the slurry to mix (3-4 minutes), fill the hopper of the pump to 3/4 level and simultaneously start the pump. Maintain the level in the hopper throughout the application.

11. Drain 15 liters of the grout into a pail to monitor set time, and amount of bleed water development. From the 15 liters, drain 1.5 liters for apparent viscosity measurements by using a Marsh Funnel.

12. With the pumping started, monitor the vertical hole for rising grout. As soon as the grout is visible and begins to submerge the packer, quickly inflate it to an inflation pressure of at least 700 kPa greater than the applied grout pressure. Monitor the vertical hole for any continued grout rise. Once the packer has set in position, the grout should stop rising. Take any cable tension off the packer. This process allows any buildup of air or water to be discharged from the pressurized grout zone.

13. As the grout zone pressurizes, allow the pressure to rise to the desired level and maintain it with as little fluctuation as possible by balancing the pump speed and bleeding excess grout with an over-flow tube.

14. Maintain the grout pressure for the desired period. The length of time for the pressure application depends upon the set time of the grout, the amount of grout necessary to build pressure and the pumping capacity. The optimum application period is the time it takes for the grout to begin to set. Setting is monitored on the 15 liters of grout drained at the beginning of the application, and taking into account the knowledge of the set time for the particular formulation used.

15. After the application is complete, deflate and remove the 127 mm diameter packer from the borehole. Immediately rinse off all cement.

16. Drain the grout pump of any remaining grout and fill the mixer with water. Under low outlet pressure (<275 kPa), flush the hole with water by pumping it with the grout pump. Simultaneously pump the slurry out of the vertical hole by using the water pump. If the slurry is too thick, allow the injected water to dilute it first.

17. After approximately 300 liters of water have been pumped by the grout pump, use the wire brush to ream the borehole walls. At the same time continue to pump an additional 300 - 600 liters of water or until the water coming out of the borehole begins to clear.

18. Deflate and remove the 50 mm diameter packer from the inclined hole.

19. Pump all the water out of the hole and replace it with clean water. The water will allow the grout to properly cure, and keep it from drying out. Record the depth of the borehole. Allow the grout to cure for at least 7 days before performing flow tests.

B.3.4 Results

Three applications of pressurized grouting have been performed at site A. Flow tests after each application assess the effectiveness of the grouting. Table B.1 describes the grout formulations and pumping parameters used for each of the three applications. Figure B.2 shows the results of the flow tests performed after each application. All the flow tests are performed with an average head of water of 159 kPa. The average flow rate before the first grout application is 1.25 cc/s based upon initial flow tests described in chapter 3, section 3.9.3. The primary factors affecting the selection of grout formulations and parameters at site A include the spacing of the joints, aperture of the joints, measured permeability of the hole, orientation of the joints and strength of the rock mass. These factors were evaluated through borehole videologging, corelogs of the vertical and inclined borehole, material characterization of the rock (Fuenkajorn and Daemen 1990), results of laboratory fracture grouting (Sharpe and Daemen 1990), and flow tests.

The first grout application using Type II Portland Cement, 10% by weight, 0.84 mm diam. sand and 2% by weight C/S Granular Bentonite,

Appli-cation	Cement Type	Water/ Cement (by vol-ume)	Additives (by weight)	Length of Grouted Hole (m)	Average Injection Pressure (kPa)	Set Time (hrs)	Duration of Grout Applica-tion (min)	Average Flow-rate after Grout Applica-tion (cc/s)
1	Type II Portland Cement	2:1	2% C/S Granular Bentonite 10% 0.841 mm ϕ Sand	4.9	862	2	30	0.068
2	Microfine Cement (MC500)	2:1	1% (by vol) NS-200 Dispersant	4.5	1000	2	30	0.045
3	Microfine Cement (MC500)	1:1	1% (by vol) NS-200 Dispersant	4.1	724	1	60	0.0034

Table B.1 Grout formulations and pumping parameters used for the grout applications at site A.

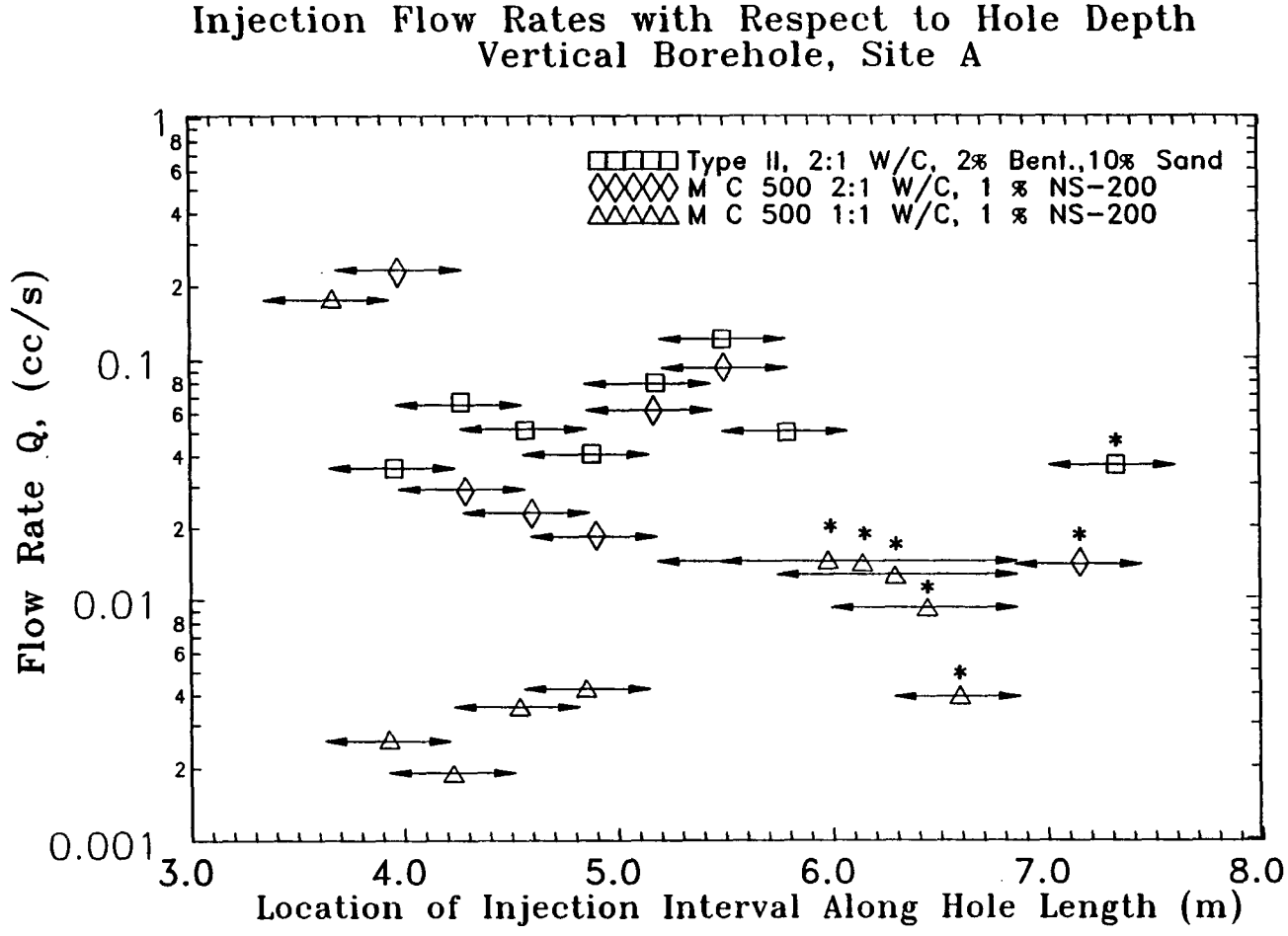

Figure B.2 Results of the flow tests performed after each application. * denotes single packer tests. All other tests are straddle packer tests. Centered symbol represents center of injection zone. All flow tests are performed with an average water pressure of 159 kPa.

reduced water flow in the fracture rock mass by 1.5 order of magnitude. Average joint spacing for the vertical joint sets is 0.58 m, and 0.37 m for the near horizontal joint set which intersects vertical hole A (Chap. 3). Most of the sand settled out of suspension and sank to the bottom of the borehole due to the high w/c ration and relatively large grain size. A smaller grain size of 0.4-0.2 mm (#40-#60 mesh) may have stayed in suspension longer, yet may not have adequately filled the voids in the rock mass. A larger sand particle size (>0.8 mm diam.) would not be pumpable with the grout pump used based on observations during testing of the pump in the lab. The bentonite was added to increase fluidity and stability of the grout.

The second and third application utilized MC500 Microfine Cement. MC500 was chosen because of its fine grain size distribution (50% grain size = 0.004 mm), which results in a higher penetration capability. Information pertaining to its properties and applications is found in Sharpe and Daemen (1990), and Shimoda and Ohmari (1982), Moller et al., (1983), Clarke (1984), and Nagoao (1985). A water-reducing agent, naphthalene sulphonate (NS-200) is used to decrease the interparticle attractive forces so that full wetting and mixing results, thus providing a better mix with respect to fluidity, workability, and stability (Lau and Crawford, 1986). The second grout application, with a 2:1 w/c ratio, of MC500 did not significantly improve the results of the first grout application. In practice, a 2:1 (by volume) w/c ratio is regarded as an optimum basic mix for cement grouts (Houlsby 1982b) and for the MC500 cement (Shimoda and Ohmari 1982), (Clarke 1986). Lau and Crawford (1986), and Deere and Lombardi (1985) however conclude that the

ultrafine cement with a 1:1 w/c ratio by volume is optimum because it produces a stronger and more durable barrier and that dispersents and bentonite can be used to control sedimentation, viscosity, grout density, set time, and strength. Increasing the amount of water beyond a w/c ratio of 1:1 slows down the setting time, decreases the compressive strength of the grout, decreases durability and increases the amount of bleedwater (Deere and Lombardi, 1985). It is felt that for these reasons, the second grout application, particularly with near vertical joints, did not perform well. In addition, since the second application lasted for 1 hr. (30 min pressurized, 30 min standing), and the set time of the MC500 is 2 hours with a w/c ratio of 2:1, flushing of the hole after the grout application most likely washed a great deal fo the grout from the joints before it had time to properly set.

The third grout application, which used MC500 with a w/c ratio of 1:1 by volume reduced water flow by greater than one order of magnitude, as seen in Figure B.2. The grout was pressurized for 1 hr., which is the set time of the MC500 with a w/c of 1:1. Once the grout began to set, the impact of flushing the hole is significantly reduced. With a w/c of 1:1, the cement is just pumpable unless an increased amount of the dispersent NS-200 is added to compensate for the increased viscosity of the cement (Lau and Crawford, 1986).

Overall the pressurized grouting applications have reduce water flow in hole A by three orders of magnitude. The permeability of the fractures approaches the permeability of the microfine cement (1×10^{-9} cm/s) assuming the rock is impermeable, and that no more than two fractures intersect a given test interval.

REFERENCES

Albritton, J.A., 1982, "Cement Grouting Practices U.S. Army Corps of Engineers". Proceedings of the Conference on Grouting in Geotechnical Engineering, New Orleans, Louisiana, pp. 264-278.

Bartholomew, C.L., And M.L., Haverland, 1987, Concrete Dam Instrumentation Manual, United States Department of the Interior, Bureau of Reclamation.

Bear, J., 1979, Hydraulics of Groundwater, McGraw-Hill, New York.

Call, R.D., Savely, J.P., Nicholas, D.E., 1976, "Estimation of Joint Set Characteristics From Surface Mapping Data", 17th U.S. Symposium on Rock Mechanics, Snowbird Utah, Society of Mining Engineers of AIME, 1977, New York.

Caron, C., 1963, "Grouts and Drilling Muds in Engineering Practice", Institution of Civil Engineers, Butterworth, England, pp. 98 - 103.

Cherry, J.A., And P.E. Johnson, 1982, "A Multilevel Device for Monitoring in Fractured Rock," Ground Water Monitoring Rev., Vol. 2, No. 3, Summer, pp.41-44.

Christensen, C.L., C.W. Gulick, and S.J. Lambert, 1982, "Sealing Concepts for the Waste Isolation Pilot Plant (WIPP) Site," SAND81-2195, Sandia National Laboratories Albuquerque, NM.

Christensen, C.L., and E.W. Peterson, 1982, "The Bell Canyon Test Summary Report," SAND80-1375, Sandia National Laboratories, Albuquerque, NM.

Crawford, A.M., Groskopf, G., 1984, "Groutability Ratio for Filter Blocking of Joints in Rock". Proceedings of the Twenty-Fifith Symposium on Rock Mechanics, Evanston, Illinois, pp. 899-906.

Creasey, S.C., and R.W. Kistler, "Age of some copper-bearing porphyries and other igneous rocks in Southern Arizona", U.S.G.S. Prog. Paper 524-F, p. F1-F47, 1966.

Daemen, J.J.K., et. al., 1983, "Rock Mass Sealing-Experimental Assessment of Borehole Plug Performance," Annual Report, NUREG/CR-3473,

prepared for the the U.S. Nuclear Regulatory Commission, by the Department of Mining and Geological Engineering, University of Arizona, Tucson.

Daemen, J.J.K., W.B. Greer, K. Fuenkajorn, A. Yazdandoost, H. Akgun, A. Schaffer, A.F. Kimbrell, T.S. Avery, J.R. Williams, B. Kousari, and R.O. Roko, 1986, "Experimental Assessment of Borehole Plug Performance, Rock Mass Sealing Annual Report June 1, 1984 - May 31, 1985", NUREG/CR-4642, prepared for Division of Radiation Programs and Earth Sciences, Office of Nuclear Regualrtory Research, U.S. Nuclear Regulatory Commission, by the Department of Mining and Geological Engineering, University of Arizona, Tucson, Arizona.

Darton Software, 1987, "SPLOT - for the Analysis of Structural Data," Rapid City, SD.

Deere, D.U., 1982, "Cement-Bentonite Grouting for Dams". Proceedings of the Conference on Grouting in Geotechnical Engineering, New Orleans, Louisiana, pp. 279-300, American Society of Civil Engineers, New York.

Deere, D., & Lombardi, G., 1985. "Grout SLurries-Thick or Thin?". Proceedings of the Session Sponsored by the ASCE Geotechincical Engineering Division on "Issues in Dam Grouting". Denver Colorado, pp. 154-162, American Society of Civil Engineers, New York.

Dunnicliff, J., 1988, Geotechnical Instrumentation For Monitoring Field Performance, John Wiley & Sons, New York.

Eilers, L.H., 1974, "Sealing AEC #1 Well, Lyons, Kansas - Final Report," Report ORNL/SUB/33542-74/1, Union Carbide Corporation, Oak Ridge, Tennessee, Nuclear Division.

Environmental Protection Agency, 1975, Manual of Well Construction Practices, EPA-570/9-75-001.

Evans, D.D., 1983, "Welded Tuff Characteristics at the Nevada Test Site and Near Superior, Arizona," Technical Report prepared for U.S. Nuclear Regulatory Commission, Division of Health, Siting and Waste Management, Office of Research, by Department of Hydrology and Water Resources, University of Arizona, Tucson.

Filho, P.R., 1976, "Laboratory Tests on a New Borehole Seal for Piezometers," Ground Eng., Vol. 9, No. 1, Jan., pp. 16-18.

Francois, A., 1914, "New or Improved method for Making Water-bearing Strata Watertight, British Patent #8482.

Freeze, R.A. and J.A. Cherry, 1979, Groundwater, Prentice-Hall, Englewood Cliffs, New Jersey.

Fuenkajorn, K. and J.J.K. Daemen, 1991, "Mechanical Characterization of Densely Welded Apache Leap Tuff," Technical Report, NUREG/CR-4641, prepared for the U.S. Nuclear Regulatory Commission, by the Department of Mining and Geological Engineering, University of Arizona, Tucson, Arizona.

Goodman, R.E., 1980, *Introduction to Rock Mechanics*, John Wiley & Sons, New York, p. 149.

Greer, W.B. and J.J.K. Daemen, 1991, "In-situ Tests of the Hydraulic Performance of Grout Borehole Seals," Technical Report, NUREG/CR-5684, prepared for the U.S. Nuclear Regulatory Commission, by the Department of Mining and Geological Engineering, University of Arizona, Tucson, Arizona.

Gulick, C.W. Jr., D.M. Walley , and A.D. Buck, 1980, "Borehole Plugging Materials, Development-Report 2," SAND79-1514, Albuquerque, NM, Sandia National Laboratories, Febuary 1980.

Harris, Frank 1983, "Ground Engineering Equipment and Methods." Mc Graw Hill, London, England, pp. 123-150.

Holcomb, D.J., And D.W. Hannum, 1982, "Consolidation of Crushed Salt Backfill Under Conditions Appropriate to the WIPP Facility, SAND82-0630, Albuquerque, NM; Sandia National Laboratories, April 1982.

Houlsby, A.C., 1982a, "Cement Grouting for Dams", Proceedings of the Conference on Grouting in Geotechnical Engineering, New Orleans, Louisiana, pp. 1-34, American Society of Civil Engineers, New York.

Houlsby, A.C., 1982b, "Optimum Water-Cement Ratios for Rock Grouting Proceedings of the Conference on Grouting in Geotechnical Eng., New Orleans, Louisiana, pp. 319-321, American Society of Civil Engineers, New York.

Hvorslev, M.J., 1951, "Time lag and Soil Permeability in Ground-Water Observations," Bulletin No. 36, April, Waterways Experiment Station, U.S. Army Corps. of Engineers, Vicksburg, Mississippi.

Joosten, H.J., 1954, "Joosten Process For Chemical Soil Solidification and sealing and its development from 1925 to date. N.V. Amsterdamishe Ballast Maatschappini, p. 46.

Karol, R.H. 1985, "Grout Penetrability." Proceedings of the Session Sponsored by the Geotechnical Engineering Division of the ASCE, Denver, Colorado, pp. 27-33, American Society of Civil Engineers, New York.

Kimbrell, A.F., T.S. Avery, and J.J.K. Daemen, 1987, "Field Testing of Bentonite and Cement Borehole Plugs in Granite," NUREG/CR-4919, Technical Report, prepared for Division of Engineering Safety, Office of Nuclear Regulatory Research, U.S. Nuclear Regulatory Commission, by Department of Mining and Geological Engineering , University of Arizona, Tucson, Arizona.

Lau, D., Crawford, A., 1986, "Grouting For the Underground Containment of Radioactive Waste." Technical Report prepared for the Atomic Energy of Canada Limited, by the Dept. of Civil Eng. University of Toronto, Toronto, Ontario.

Lingle, R., K.L., Stanford, P.E. Peterson, and S.F. Woodhead, 1981, "Wellbore Damage Zone Experimental Determination, ONWI-349, prepared for ONWI, Battelle Memorial Institute, Columbus, OH, by Terra Tek.

Marinelli, F., 1984, "Analysis of Constant Head Injection Tests in Single, Partially penetrating Boreholes," MS thesis, Department of Hydrology and Water Resources, University of Arizona, Tucson, Arizona.

Mayer, A. 1963, "Modern Grouting Techniques". Proceedings of the Symposium on Grouts and Drilling Muds in Engineering Practice, Institution of Civil Engineers, Butterworth, London, England, pp. 7-10.

Minear, V.L., 1957, "General Aspects of Cement Grouting of Rock", A.S.C.E. Journal of Soil Mechanics and Foundation Division, 83, pp. 1145(1)-1145(11), American Society of Civil Engineers, New York.

Mitchell, J.K., 1970, "In-Place Treatment of Foundation Soils", Journal of Soil Mechanics and Foundation Division, ASCE, New York, pp. 73-100.

Moller, D.W., Minch, H.L., And Welsh, J.P., 1983. "Ultrafine Cement Pressure Grouting to Control Water in Fracture Granite Rock." A.C.I. (American Concrete Institute) Report SP83-8, American Concrete Institute, Detroit, Michigan.

Morgenstern, N.R., And Vaughan, P.R., 1963. "Some Observations on Allowable Grouting Pressures", Proceedings on Grout and Drilling Muds in Engineering Practice, Institution of Civil Engineers, Butterworth, London England, pp. 36-42.

Ouyang, S. And J.J.K. Daemen, 1991, "Sealing Performance of Bentonite and Bentonite/Crushed Tuff Borehole Plugs," Technical Report, NUREG/CR-5685, prepared for the U.S. Nuclear Regulatory Commission, by the Department of Mining and Geological Engineering, University of Arizona, Tucson.

Peterson, D.W., 1961, "Dacitic ash-flow sheet near Superior and Globe, Arizona", Stanford Univ., Stanford, California, Ph.D., Thesis, U.S.G.S. Prof Paper 424-D, p. 82-84.

Pusch, R. And L. Borgesson, 1989, "Bentonite Sealing of Rock Excavations," paper presented at Sealing of Radioactive Waste Repositories, Braunschweig, Federal Republic of Germany, May 22-25, a workshop organized by OECD Nuclear Energy Agency and Commission of the European Communities.

Roy, D.M., M.W. Grutzeck, and L.D. Wakeley, 1985, "Salt Repository Seal Materials: A Synopsis of Early Cementitious Materials Development," Technical Report BMI/ONWI-536, prepared by Materials Research Laboratory, The Pennsylvania State University for the Office of Nuclear Waste Isolation, Battelle Memorial Institute, Columbus, Ohio.

Senger, J.A., And W.M. Perpich, 1983, "An Alternative Well Seal in Highly Mineralized Ground Water," in Proceedings of the 3rd National Symposium on Aquifer Restoration and Ground-Water Monitoring, Columbus, OH, D.M. Nielsen (Ed.), published by National Water Well Association, Worthington, OH.

Sharpe, C.J. And Daemen, J.J.K., 1990, "Fracture Grouting in Densely Welded Tuff," Technical Report, NUREG/CR-5683, prepared for Division of Engineering Safety, Office of Nuclear Regulatory Research, U.S. Nuclear Regulatory Commission, by Department of Mining and Geological Engineering, University of Arizona, Tucson.

Shimoda, M. & Ohmori, H. 1982. "Ultra Fine Grouting Material." Proceedings of the Conference on Grouting in Geotechnical Eng., New Orleans, Louisiana, pp. 77-91, American Society of Civil Engineers, New York.

Smith, D.K., 1976, Cementing, Monograph Volume 4, Henry L. Doherty Series, Society of Petroleum Engineers of AIME, New York.

South, D.L. And J.J.K. Daemen, 1986, "Permeameter Studies of Water Flow Through Cement and Clay Borehole Seals in Granite, Basalt, and Tuff," NUREG/CR-4748, Technical Report, prepared for Division of Engineering Safety, Office of Nuclear Regulatory Research, U.S. Nuclear Regulatory Commission by Department of Mining and Geological Engineering, University of Arizona, Tucson, Arizona.

Sternberg, B.K., J.M. Ryan, J.W. McGill, and M.E. Breitrick, 1988, "The San Xavier Geophysics and Tunnel-Detection Test Site," LASI-88-2, Mining and Geological Engineering Department, University of Arizona, Tucson.

Stormont, J.C., 1984, "Plugging and Sealing Program for the Waste Isolation Pilot Plant," SAND84-1057, Sandia National Laboratories, Albuquerque, NM.

Stormont, J.C., 1986, "Development and Implementation: Test Series A of the Small-Scale Seal Performance Tests," SAND85-2602, Sandia National Laboratories, Albuquerque, NM.

Sutherland, H.J., and S.P. Cave, 1984, "Gas Permeability of SENM Rock Salt, SAND78-2287, Albuquerque, NM; Sandia National Laboratories, January 1984.

Todd, D.K., 1980, Groundwater Hydrology, Wiley, New York

U.S. Nuclear Regulatory Commission, 1981, "Disposal of High-Level Radioactive Wastes in Geologic Repositories," Proposed Rule 10 CFR 60, Federal Register, Vol. 46, No. 130, p. 35281.

Warner, D.L. And J.H. Lehr, An Introduction to the Technology of Subsurface Wastewater Injection, 1977, U.S. Environmental Protection Agency, EPA-600/2-77-240.

Wong, H.Y., And Farmer, I.W., 1973, "Hydrofracture Mechanisms in Rock During Pressure Grouting", Rock Mechanics Vol.5, pp. 21-41, Springer-Verlag, Austria.

Zeigler, T.W., 1976, "Determination of Rock Mass Permeability", Technical Report S-76-2, U.S. Army Corps of Engineers Waterways Experiment Station, Vicksburg, Mississippi.